Co-processing Bio-crude at Petroleum Refineries

Fractional Distillation and Deoxygenation of HTL Bio-crude to Evaluate the Potential as Co-processing Feed

Master Thesis
Group TEPE4-1002
Department Of Energy Technology
Aalborg University
June 3rd 2014

AALBORG UNIVERSITY
STUDENT REPORT

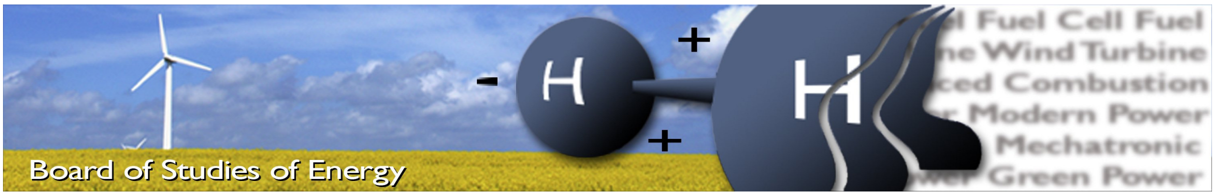

Title: Co-processing Bio-crude at Petroleum Refineries
Semester: 10^{th}
Semester theme: Master's Thesis
Project period: 01.02.14 to 03.06.14
ECTS: 30
Supervisor: Jessica Hoffmann and Lasse Aistrup Rosendahl
Project group: TEPE4-1002

Co-processing enables a gradual phase-in of HTL bio-crude, where feasibility of co-processing and availability of both bio- and petroleum crude oil can be balanced. To evaluate the potential of HTL bio-crude as a co-processing feedstock, 15 theoretical plate fractional distillation of HTL bio-crude is done to analyse elemental composition, HHV and FT-IR as function of TBP. 6 wt.% gasoline, 26 wt.% jet-fuel, 22 wt.% diesel and below 30 wt.% residue equivalent is determined for the HTL bio-crude. In order to enable co-processing it is an issue that the distribution of oxygen, nitrogen and sulphur is concluded to be different from that characteristic of petroleum crude oil. An experimental deoxygenation set-up is successfully designed and tested. Catalyst crushing is found to affect repeatability. Mild deoxygenation (330°C, 95 bar, 2h, 2:1 H_2:oil molar ratio) using $NiMo/Al_2O_3$ reduced O and S to 2.38 wt.% and 0.04 wt.% respectively. The deoxygenation product is characterised by a HHV of 44.3 kJ/g and FT-IR similar to petroleum crude. Remaining oxygenates are expected to be of cyclic and polycyclic nature and located in the residue fraction. As a conclusion, a mild deoxygenation step is considered to be sufficient to enable the synergy of co-processing without the need for major refinery modifications.

Claus Uhrenholt Jensen

Kristine Møllenbach Rasmussen

Copies: 5
Pages, total: 106
Appendix: A-E
Supplements: CD

By signing this document, each member of the group confirms that all participated in the project work and thereby all members are collectively liable for the content of the report.

Preface

This Master's Thesis report was carried out by group TEPE4-1002 on 10th semester, at Department of Energy Technology, Aalborg University.

The potential in co-processing HTL bio-crude in existing petroleum crude oil refineries is investigated. Fractional distillation of HTL bio-crude is used to analyse the heteroatom distribution and thereby the need for upgrading in order to fulfil specifications and become a drop-in biofuel.

The project consists of a main report and appendices. The report is divided into seven chapters comprising an introduction to co-processing, theory regarding fractional distillation, results of distillation and analysis of HTL bio-crude, theory on upgrading, upgrading solution and results, and finally a discussion and a conclusion. The chapters are arranged numerically while appendices are sorted alphabetically and can be found at the end of the report.

The Harvard author-date referencing system has been used throughout the report. A report nomenclature list can be found after the preface. The report includes a CD with data from the experimental results obtained in the study. Furthermore, an electronic version of the report is included.

Nomenclature

Acronym	**Description**
ADU	Atmospheric Distillation Unit
AET	Atmospheric Equivalent Temperature
BDE	Bond Dissosiation Enthalpy
BPD	Barrels Per Day
CBS	Continuous Bench Scale
CKU	Upgrading Experiments
$FAME$	Fatty Acid Methyl Ether
FCC	Fluid Catalytic Cracking
$FT-IR$	Fourier Transform Infrared Spectroscopy
HDN	Hydrodenitrogenation
HDO	Hydrodeoxygenation
HDS	Hydrodesulphurisation
HTL	Hydrothermal Liquifaction
LSR	Light Straight Run
MON	Motor Octane Number
RON	Research Octane Number
TBP	True Boiling Point
TGA	Thermogravimetric Analysis
VDU	Vacuum Distillation Unit

Symbol	**Description**	**Unit**
HHV	Higher Heating Value	kJ/g
P	Pressure	$torr$
P_i	Purge, maximum, model and final pressure	bar
T	Temperature	°C
T_{cold}	Temperature of the cold reactor volume	°C
TAN	Total Acid Number	$mgKOH/g$
V_{cold}	Volume of the cold reactor above the sandbath	ml
$\widetilde{v}$	Wavenumber	cm^{-1}
λ	Wavelength	cm
	Density	g/ml

Contents

1 A Co-processing Path from HTL Bio-crude to Drop-in

Global energy demand in the transportation sector is increasing due to emerging markets and global growth (EIA, 2014*a*). The energy supply is however limited by depleting petroleum resources and decreasing resource quality (EIA, 2014*b*). Environmental concerns necessitate increasing efforts in mitigating greenhouse gas (GHG) emissions. To relief the mismatch between a growing energy demand, depleting resources and increasing environmental concerns, the global dependence on fossil resources must be replaced by a renewable feedstock that encloses the CO_2 cycle (EG FTF, 2011). Pyrolysis and hydrothermal liquefaction (HTL) are thermochemical processes capable of converting biomass into liquid energy carriers (Toor et al., 2011). In particular, HTL enables a feedstock-flexible conversion of non-food biomass to a liquid bio-crude with a higher heating value (HHV) around 35-40 $^{MJ}/_{kg}$. HTL bio-crudes possess higher quality than pyrolysis bio-oils as intermediate for biofuel production, due to oxygen contents around 5-10 wt.%, lower contents of corrosive carboxylic acids, and lower water content around 2 wt.%. These characteristic values are based on experience from the laboratory at Aalborg University. Though, with the above mentioned characteristics, the HTL bio-crude is still an intermediate that needs further upgrading to be classified as compatible with existing transportation infrastructure (Hoffmann, 2013). Figure 1.1 illustrates the HTL path from feedstock to direct drop-in biofuel or bio-crude compatible for co-processing at an existing refinery.

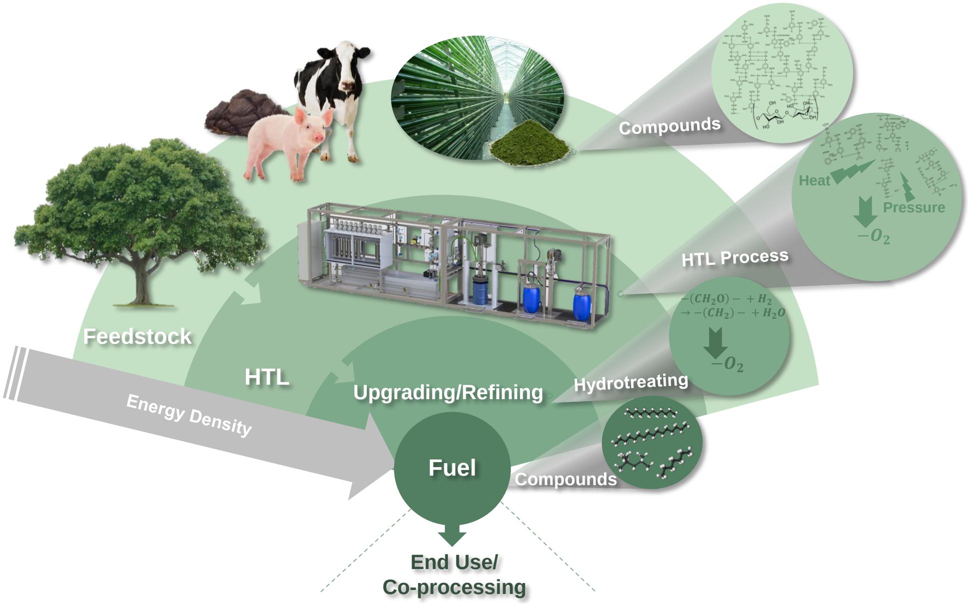

Figure 1.1. HTL conversion of biomass to bio-crude, and subsequent upgrading/refining of the intermediate into drop-in biofuel. (Hoffmann, 2013)

1.1 Scope of the Report

At present, the HTL bio-crude production in hot compressed water (HCW) has been the major research focus. More specifically, the influence of process conditions and mix of biomass feedstock has been analysed (Toor et al., 2011), (Toor et al., 2012), (Toor et al., 2014). Though, it is the aim of the present study to contribute to the next level of research, where the HTL bio-crude is evaluated as a potential refinery co-processing feedstock. It seems appropriate to co-process the HTL bio-crude with petroleum crude at existing refinery facilities. The arguments for this statement are presented in the following Section 1.2. But what is the appropriate drop-in location? Should the blending of bio- and petroleum crude be done prior to entering the refinery? Or does the nature of the bio-crude imply that the synergy of co-processing is higher, if the bio-crude is fed to a specific unit within the refinery? Is the HTL bio-crude of sufficient quality to enable co-processing without the need for major refinery modifications? Or is it appropriate to pre-upgrade the bio-crude to remove oxygen? These considerations are addressed in the present project, where the scope is formulated as follows:

How is the heteroatom distribution in HTL bio-crude different from that characteristic for petroleum crude oil and how does it affect co-processing? Secondly, how can oxygen be removed to enable co-processing without the need for major refinery modifications?

Fractional distillation of the HTL bio-crude enables analysis of the heteroatom distribution and other quality parameters. The amount of gasoline, jet and diesel fuel equivalent can be defined. Likewise, the nature of the different fractions and how they differ can be analysed, where especially the functional groups containing oxygen are in focus. Such analysis provides knowledge of the intermediate upgrading that is required in order to enable co-processing at existing refinery utility. Fractional distillation is done in a 15 theoretical plate column, and elemental analysis, HHV, density and FT-IR will be evaluated and related to the boiling point distribution. The fractional distillation is described in Chapter 2 and the results are presented in Chapter 3.

It depends on the nature of the HTL bio-crude to what extent intermediate upgrading such as deoxygenation is required. Based on the distillation results and the subsequent analysis, pretreatment of the HTL bio-crude prior to co-processing will be proposed. An experimental deoxygenation set-up is designed and installed and deoxygenation through hydrotreating is initiated. Chapter 4 briefly describes the upgrading process, whereas Chapter 5 presents the upgrading set-up designed in present study along with the results of the deoxygenation experiments.

1.2 Co-processing of Bio-crude with Petroleum Crude Oil

Co-processing bio-crude with petroleum crude oil at existing facilities is considered a crucial method towards obtaining competitive production prices of drop-in biofuels (Furimsky, 2013), (Chen et al., 2013), (Speight, 2011). Arguments for this statement will be presented in this section. The discussion includes both the perspective of the bio-crude producer, as well as the refinery incentives.

Figure 1.2 illustrates the concept of co-processing petroleum and bio-crude oil. For illustrative purposes, the drop-in location is chosen prior to the distillation column in this specific example. The drop-in percentage of liquid biofuels into conventional liquid fuels is depicted with green in the different product circles. Given that the bio-oil has unlimited drop-in abilities, this drop-in percentage may be increased gradually along with an increase in the production capacity of the biofuel. A gradual increase of the drop-in percentage enables a smooth phase-in, where feasibility of co-processing and availability of both bio- and petroleum crude oil can be balanced.

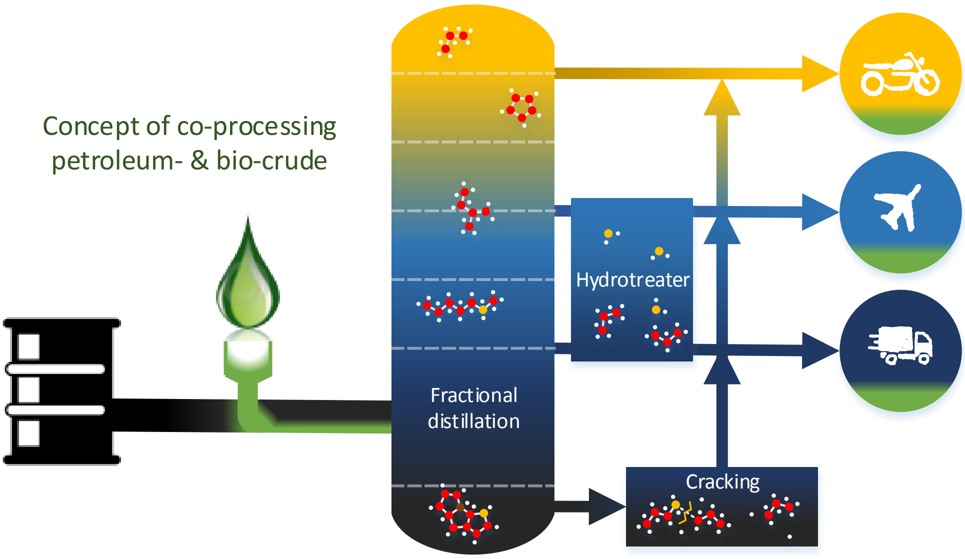

Figure 1.2. Co-processing enables a gradual phase-in of the use of biofuels in existing infrastructure.

The HTL bio-crude studied in this report has many similar properties to petroleum crude oil. A major similarity is the mix of hydrocarbons with different carbon numbers. This mix needs separation by fractional distillation in order to separate the oil into e.g. gasoline, kerosene and diesel boiling ranges. Figure 1.2 illustrates how distillation of the petroleum and biocrude may be combined in a co-process. Depending on the biomass feedstock, HTL bio-crude contains a similar amount of heteroatoms such as N and S when comparing to petroleum crude. These heteroatoms may be removed by co-processing the bio- and petroleum crude in for instance excisting hydrotreating units. Likewise, it is believed that any heavy residue in the bio-crude may be co-processed in the residue conversion units.

Refineries are extremely capital intensive due to the amount of different processing units required in order to meet fuel specifications. In fact, since 1977 there has not been built a new refinery in the US with an atmospheric distillation capacity above 100.000 barrels per day (EIA, 2013). This is remarkable, considering the increase in fuel demand during this period (EIA, 2014*a*). Instead the existing refineries are constantly extended and modified to meet changes in fuel regulations, such as low sulphur specifications. Refineries are also modified to handle crude oils that are generally heavier and of worse quality compared to the crudes that the refineries were once designed for (Speight, 2011). Figure 1.3 illustrates an example of how the crude oil quality in the US is generally decreasing (EIA, 2014*b*). The sulphur content of crude oils has almost doubled since 1985. At the same time, sulphur allowances in fuel products are becoming stricter. A recent EU directive reduces the allowed sulphur content in marine fuel from 3.5 % to 0.5 % by 2020 (EMSA, 2010). In addition, this EU directive reduces the allowances in marine fuels to 0.1 % by 2015 in particular 'Sulphur Emission Control Areas', which includes the North- and Baltic Sea (EMSA, 2010).

In addition to an increasing crude oil sulphur content, Figure 1.3 illustrates how the crude oils are also generally becoming heavier. Depleting resources and increasing energy demands lead to utilisation of extra heavy crude oils from e.g. Venezuela and Canada. Processing of heavier crude oils results in a larger residue fraction, which depending on the oil requires additional refining. It is a fact that the GHG emissions related to the additional refining of heavier crudes and bitumen is higher than the emissions related to refining of lighter crudes (Chen et al., 2013). Additional refining also increases the expenses related to producing on-specification fuel products. As a result, the environmental prospect and the economic margin left for looking at alternative crude oil resources, such as bio-crude, are increasing with the decrease in petroleum crude oil quality. (Gary et al., 2007) (Speight, 2011)

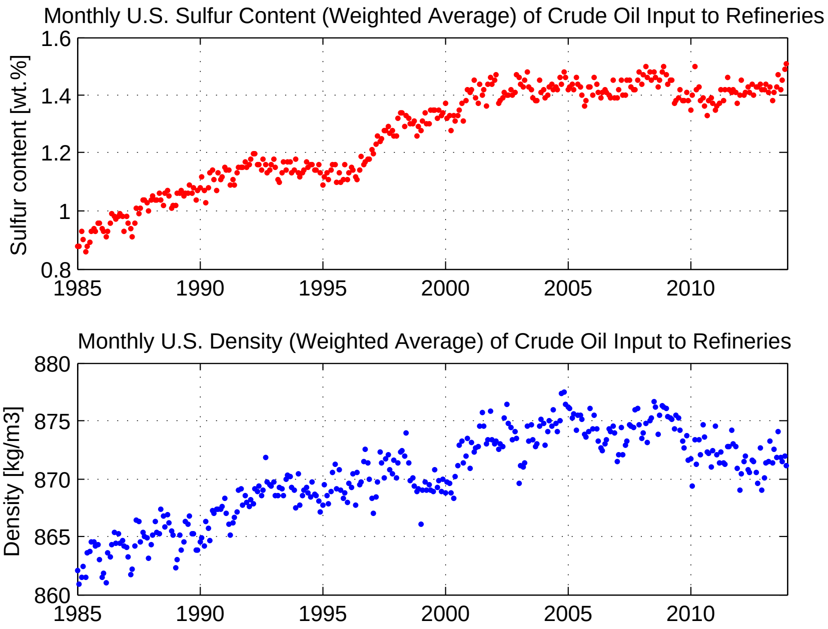

Figure 1.3. Petroleum crude oil feeding U.S. refineries are generally becoming heavier and contain more sulphur. (EIA, 2014*b*)

1.2.1 Different Perspectives on Co-processing

Bio-crudes that are possible alternatives for petroleum crude oil as refinery feedstock are sometimes included in the class of opportunity crudes (Speight, 2011). Characteristics that make opportunity crudes differ from the benchmark petroleum crude include a TAN above 1 mg of KOH/g oil and a higher overall density (> 0.9 g/mL) (Speight, 2011). An opportunity crude is not necessarily renewable, but the characteristics match those of the bio-crudes studied in this report. Corrosion issues in refinery units are increased by processing a high TAN feedstock. Likewise, fouling risks, cetane reduction and product stability are risks that arise with the processing of an opportunity crude (Speight, 2011). As a result, opportunity crudes are often sold at a discount compared to benchmark crude oils. This economic incentive is interesting for the refinery that may overcome the risks associated with opportunity crudes by effective refining technologies (Speight, 2011).

For the refinery, co-processing ensures full usage of the installed capacity on a long term basis. Secondly, bio-crude forms an alternative source of feedstock for the refinery. A feedstock that matches a demand for renewable fuel products that is likely to grow with global focus on sustainable energy resources (Speight, 2011). Additionally, a feedstock that forms an alternative, when expenses related to processing crude oil increases due to a decrease in crude oil quality (Speight, 2011). Finally, the refinery may obtain vital CO_2 credits by off-setting petroleum crude with renewable bio-crude. An analysis by *Milhench (2011)* concludes that European, in particular UK refineries, are forced to either shut down or relocate to locations with less carbon emission regulation. The floor of carbon credit costs is raised to a level in EU that violates the margin left for profit (Milhench, 2011). By processing renewables, the refinery costs associated with carbon emission can be reduced. This gives the bio-crude additional value relative to petroleum crude oil.

From the perspective of the bio-crude producer, the major benefit of co-processing is reduced investment costs related to refining. This might sound as a simple argument, but a potential bio-refinery requires a large amount of different processing units in order to produce on-specification fuel products. This is due to the heterogeneous nature of biomass that the bio-crude will be made from (Speight, 2011). One should expect the bio-crude to be of varying composition due to the varying composition of the biomass feedstock. Processing units that can handle a varying bio-crude composition are extremely expensive

(Gary et al., 2007), and thus the possibility of modifying existing refining capacity seems attractive for the bio-crude producer. Additionally, co-processing enables immediate introduction of the particular biofuel to the market. This will also reduce the capital required prior to market penetration.

As a conclusion, the synergy from co-processing of bio-crude with petroleum crude oil seems to favour both the bio-crude producer and the refinery. This supports the incentives for further evaluation.

1.2.2 Considerations on the Drop-in Location

What is the appropriate location of blending in the bio-crude in relation to co-processing with petroleum crude oil? Refineries are designed differently, due to the fact that crude oils have very different characteristics, depending on the origin. Some crudes are parafinnic, others aromatic and some are heavy, others light. As a result, the specific quality requirement to a bio-crude that must be met for possible co-processing, depends on the particular refinery that the co-processing is to be done at. Figure 1.4 illustrates an example of the possible units and how the major streams are distributed at a modern crude oil refinery designed for fuel production. Only some of the units will be present depending on the type of crude oil the particular refinery is designed for. (de Klerk, 2011), (Gary et al., 2007)

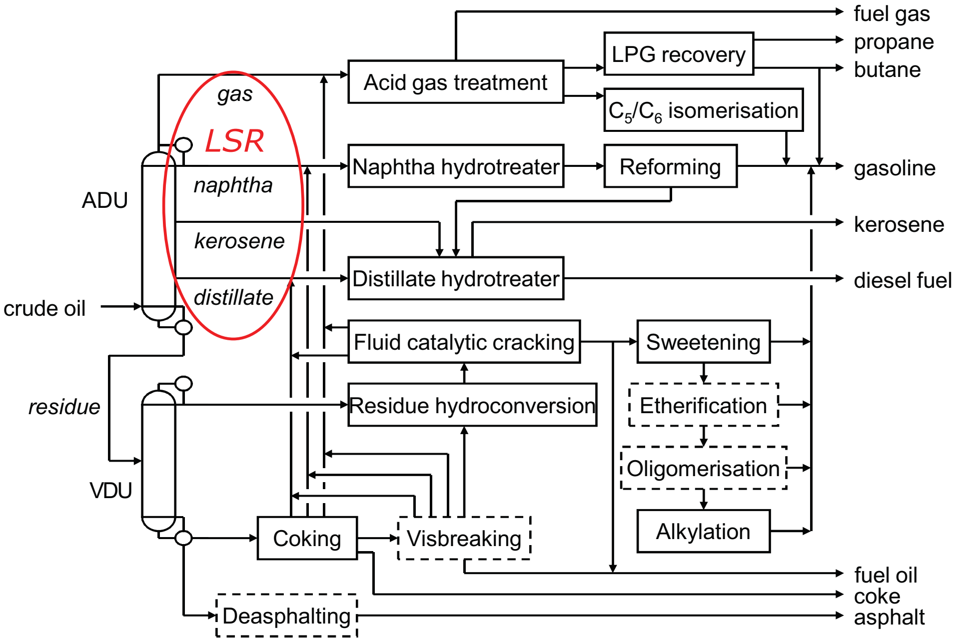

Figure 1.4. A general flow diagram of a modern petroleum crude oil refinery. Some units satisfy similar purposes and thus the units will not all appear in a certain refinery design simultaneously. (de Klerk, 2011)

The first major step of processing in a conventional refinery, after desalting, is distillation in the atmospheric distillation unit (ADU). This unit is usually running at temperatures approaching 400°C (Gary et al., 2007). Cracking may be observed when crude oil is exposed to higher temperatures. To avoid this, the residue from the ADU is fed to the vacuum distillation unit (VDU). Vacuum reduces the boiling point of a compound, and thus enables further distillation at lower temperatures (Gary et al., 2007). It will be described in Subsection 2.2.1, how a bio-crude is more prone to crack at elevated temperatures than conventional crude oil. This is due to a higher amount of oxygenates being present in bio-crude (de Klerk, 2011). To avoid cracking, it may then be appropriate to distil the bio-crude with the atmospheric residue in the VDU, rather than feeding it to the ADU as a first step. On the other hand, this might be inefficient, since the bio-crude light straight run (LSR) fractions boiling below 400°C, should be processed with the equivalent straight run fractions from the petroleum crude oil. These fractions are, as roughly illustrated with red in Figure 1.4, distilled off in the ADU. This means that the VDU is not designed for feeding any distillates to the streams leaving the ADU. Instead the distillate from the

VDU enters the residue hydroconversion, which is a catalytic hydrotreating unit suited for higher boiling components. This is illustrated in Figure 1.4. In other words, by feeding the entire bio-crude to the VDU, unnecessary processing of the LSR bio-fractions may be introduced. This should be avoided if possible, since additional processing is costly and energy consuming.

To enable atmospheric distillation of the bio-crude in a conventional refinery, deoxygenation may be required prior to blending with the petroleum crude. Considering the minor content of oxygenates in petroleum crude, a classic refinery is unlikely to have a large deoxygenation capacity. As a result, deoxygenation prior to blending may be advantageous in order to reduce the changes required in a refinery to enable processing of bio-crude. More on the deoxygenation step and nature of the oxygenates in Subsection 2.2.1.

Opposite what is expected, this study may reveal that any heteroatoms present in the bio-crude appear in the lighter fractions. It will be described in further details in relation with Figure 2.1 that the heteroatom content such as nitrogen and sulphur, increases with boiling point for petroleum crude oil. Does it however turn out that this distribution does not match with the heteroatom distribution in bio-crude, the refining path towards on-specification fuel for petroleum crude and bio-crude may be too different to justify co-processing. In this case, it may be appropriate to refine the bio-crude separately and instead blend the final products. This aspect underlines the relevance of fractional distillation and subsequent analysis.

1.2.3 Literature on Co-processing Bio-crudes with Petroleum Crudes

The present state-of-the-art study may conclude that heteroatoms such as oxygen, nitrogen and sulphur are present only in certain heavy fractions of the bio-crude. Thus, it would be convenient, as mentioned above, to distil the remaining straight run fractions with the petroleum crude to avoid unnecessary processing of these fractions. The larger volume that is processed, the larger energy requirement and the more costly the refining becomes. Despite this rather logic reasoning, no literature has been found on co-distillation of bio-crude and petroleum crude oil. The literature found on co-processing is based on feeding the entire bio-crude to a residue cracking or upgrading unit, without pre-distilling any straight run fractions. *Chen et al. (2013)* has published an extensive experimental study on co-processing canola oil and heavy vacuum gas oil (VGO) under typical hydroprocessing conditions using a NiMo/Al_2O_3 hydrotreating catalyst. VGO is the stream indicated in Figure 1.4 from the VDU to residue hydroconversion. *Chen et al. (2013)* concluded that co-processing the parafinnic canola vegetable oil (5-20 wt.%) with cyclic VGO (95-80 wt.%) for production of diesel range hydrocarbons, improved the product yield and product quality with respect to cetane number. This was also found by *Huber et al. (2007)*. It is not surprising that a parafinnic bio-oil with high H/C ratio improves the saturation of a heavy, low H/C ratio, aromatic gas oil. Though, *Chen et al. (2013)* also concluded that hydrodesulphurisation (HDS) and hydrodenitrogenation (HDN) conversions were not affected by the co-processing of canola oil compared to pure processing of VGO. At 395°C and 80-110 bar, the HDN and HDS conversions continued to be 96 % and 99 % respectively after including canola oil. This is interesting considering that the canola oil contained 8.3 % oxygen, which have inhibition effects on HDS and HDN in studies by *Mercader et al. (2007)*. *Mercader et al. (2007)* conducted co-processing of deoxygenated pyrolysis oils with LSR gas oil in FCC and hydrotreating units. Despite the difference in feed composition both results showed similar yields for the co-processing and the pure petroleum feed. It was observed that the inhibition effects HDO had on the HDN and HDS reactions did not permanently deactivate the catalysts. More details on the effect of oxygenates during hydrotreating is presented in Chapter 4.

Hydrodeoxygenated (HDO) pyrolysis oil (20 wt.%) was co-processed with VGO (80 wt.%) under fluid catalytic cracking (FCC) conditions by *Fogassy et al. (2010)*. An Y-zeolite FCC catalyst was used, and most of the oxygenates were removed as CO_2 and H_2O during co-processing. Though, phenolic compounds were not converted completely. Phenolic compounds are cyclic alcohols and these are known to be some of the more difficult oxygenates to convert to hydrocarbons (de Klerk, 2013). *Fogassy et al. (2010)* also concludes that the yield of gas and coke are higher under co-processing compared to processing pure

VGO. Though, the yield of liquid gasoline products were comparable. Finally, it is concluded that the deoxygenation consumes hydrogen from the feed, and thus the H/C ratio of the products are poor, containing more coke, aromatics and alkenes than without the pyrolysis-oil (Fogassy et al., 2010). FCC units (see Figure 1.4) are feed flexible units very popular for gasoline production at refineries. Generally, it is the main source of alkenes, which makes it an important unit (de Klerk, 2013). As a result, the conclusion of *Fogassy et al. (2010)*, having an increased amount of aromatics and alkenes is not necessarily bad, since these are high octane compounds. A higher coke yield is not desirable, but in relation to the HTL bio-crude subject to upgrading in this report, the increase in coke yield may not be as significant. This is considering a more parafinnic nature and a lower oxygen content (5-10 wt.%) of the HTL crude, where the deoxygenated pyrolysis oil studied in *Fogassy et al. (2010)* contained 21 wt.% oxygen.

No literature has been found on the co-processing of HTL crudes. But co-processing of heavy petroleum gas oil streams and both vegetable and deoxygenated pyrolysis oils have shown promising results. Table 1.1 lists the C, H and O composition of the oils mentioned above. Note how the HTL oil has a lower oxygen content compared to especially pyrolysis oils. Based on this and the above mentioned studies on co-processing, the incentive for investigating the outcome of co-processing HTL bio-crude with petroleum streams is even more inspiring.

	HTL oil CBS22-27	Pyrolysis oil (Deoxygenated)	Pyrolysis oil (Deoxygenated)	Vegetable oil
Ref.	CBS (2014)	Mercader et al. (2007)	Fogassy et al. (2010)	Chen et al. (2013)
Origin	Wood	Wood residue	Wood residue	Canola
C [wt.%]	82-84	74	69	77
H [wt.%]	10	10	10	11
O [wt.%]	5-7	16	21	8
$\frac{H}{C}$ molar ratio	1.44	1.61	1.73	1.70
$\frac{O}{C}$ molar ratio	0.05	0.16	0.23	0.08

Table 1.1. C, H and O composition of the bio-crudes mentioned in the literature-study on co-processing.

Whether the appropriate location of bio-crude drop-in is at the FCC, a hydrotreating unit or perhaps before entering the ADU, depends on the desired product. FCC's are suitable for gasoline production, whereas hydrotreating units are mostly used for distillate production (Gary et al., 2007). The appropriate fuel product plate depends on geographic location, but also on the nature of the crude oil. Additionally, the heteroatom distribution of the bio-crude may limit the drop-in location. Thus, the appropriate drop-in location will be left as a question open for further evaluation.

1.3 Current Regulation and Issues Related to the Drop-in Ability of Ethanol and Biodiesel

It is the aim to produce a liquid biofuel that is directly compatible with existing engines. So-called direct biofuels (Speight, 2011) avoid replacement of existing gasoline, diesel and jet engines in order to change from conventional to sustainable fuels. Consequently, the drop-in can be done gradually by balancing availability and feasibility of the biofuel production. Though, such compatibility requires a bio-crude with properties very similar to those of petroleum crude oil.

Not all liquid biofuels are characterised as direct biofuels with unlimited drop-in abilities. Ethanol and biodiesel are the most widely used drop-in biofuels, but both have limited drop-in abilities in existing infrastructure. These issues are discussed in the following.

Bio-ethanol has the advantage of being a renewable liquid fuel with high blending octane number of 114 (Gary et al., 2007). Though, due to the relatively heavy (16 $^{g}/_{mol}$) oxygen atom, bio-ethanol also has the disadvantage of a lower heating value, giving a mileage of 70 % compared to hydrocarbon gasoline (Gary et al., 2007). Furthermore, in the refinery, ethanol cannot be piped along with the hydrocarbon gasoline pool. This is because ethanol is more polar and thus more miscible with water than hydrocarbons. When water is present in the distribution system, two phases may form and the ethanol concentration of the gasoline is no longer known. As a result ethanol is stored and distributed separately and co-processing is not an option. Thus, so-called splash blending is required, where the ethanol is blended in right at the truck loading dock. (Gary et al., 2007)

The consumption of fuel ethanol and biodiesel are listed in Table 1.2 for U.S. and the European Union. The ethanol consumption in the U.S. has increased from roughly 1.3 vol.% in 2001 to 9.6 vol.% in 2011 (EIA, 2012). Table 1.2 however reveals how the increase in ethanol consumption has stagnated between 2009 and 2011. *EIA (2012)* states that the ethanol consumption face a blend-wall due to ethanols limited drop-in ability. 99 vol.% of the ethanol consumption in the U.S. in 2011 was through an E10 gasoline blend (EIA, 2012). E10 is a 10 vol% ethanol in gasoline blend. E15 blends are approved for cars and light trucks newer than model 2001 in the U.S. Though, *EIA (2012)* states that the E15 consumption will be limited to low volumes due to concerns related to auto-mobile warranties and misfueling with higher ethanol blends.

The European Union had a 2010 target saying that 5.75 % of the energy consumption in the transportation sector should be from renewable sources (EASAC, 2012). Table 1.2 indicates the lack of reaching this target by 2010. The present target set by the European Union, is for all the member states to have minimum 10 % renewables in the transportation sector by 2020. Of these 10 %, a maximum of 5 % is allowed from edible biomass resources (EASAC, 2012). To meet these targets by 2020, the increase in ethanol and biodiesel drop-in must continue with a higher pace, and no more than 5 % of the ethanol and biodiesel can be produced from edible biomass resources. Alternatively, there is a need for other biofuel production facilities. HTL is a prospective conversion platform in this respect, since it is feedstock-flexible and enables production of liquid bio-crude that is considered close to refinery compatible from non-food biomass.

	US					**EU-27**				
Fuel Ethanol Consumption	2001	2008	2009	2010	2011	2001	2008	2009	2010	2011
Volume in Thousand BPD	113	630	718	838	838	2.2	61	78	98	104
Vol% of Gasoline Consumption	1.3	7.0	8.0	9.3	9.6	0.1	2.7	3.5	4.6	NA
Biodiesel Consumption										
Volume in Thousand BPD	2.2	20.5	21.4	17.3	57.3	17	175	212	230	237
Vol% of Distillate Consumption	0.1	0.5	0.6	0.5	1.5	0.3	2.9	3.7	3.9	NA

Table 1.2. European and U.S. ethanol and biodiesel consumption 2008-2011. (EIA, 2014*a*)

Table 1.2 also lists the development in biodiesel consumption in Europe and the U.S. from 2001 to 2011. *EIA (2012)* states that the increasing use of biodiesel will continue with political impact on legislation favouring renewable fuels. Biodiesel or more accurately fatty acid methyl ether (FAME) is a renewable biodiesel that may be used as a diesel additive to improve lubricity and improve the cetane number of the diesel blend (NREL, 2009). Furthermore, biodiesel reduces tailpipe emissions such as CO, because the biodiesel contains 11 wt.% oxygen, which results in a cleaner combustion (NREL, 2009). On the downside, biodiesel contains 8 % less energy on a volume basis compared to hydrocarbon diesel (NREL, 2009). Additionally, FAME introduces issues related to cold flow properties and storage stability (NREL, 2009). More specifically, the storage stability is related to the oxygenates that over time tend to degrade and form acids, which will increase the TAN (NREL, 2009). For these reasons, the current diesel specifications have upper limits for the content of FAME. This will be described in relation to Table 1.4.

Instead of e.g. modifying the car fleet as in Brazil to accomodate E85 ethanol blends, or deal with issues on storage stability of FAME, it would be of great advantage to produce direct liquid biofuels with unlimited drop-in abilities. One of the major promising aspects, of the HTL bio-crude studied in this report, compared to other sustainable energy resources, is the prospect of an unlimited drop-in character. By producing a bio-crude with similar characteristics as conventional petroleum crude oil, the infrastructure of the transportation sector does not need major changes. More specifically, it is believed that the bio-crude can be co-processed with petroleum crude at existing refineries at the expense of minor refinery modifications (Speight, 2011).

1.4 Fuel Specifications

Fuel specifications are the constraining barrier that needs to be overcome in order to phase in drop-in biofuels from hydrothermal conversion processes of biomass in the transportation sector. The specifications are highly dependent on the application of the fuel, due to the significant differences in engine technology. The following lists of specifications for gasoline, kerosene, diesel and marine fuel will form the basis for discussing the required processing of the bio-crude. Though, first a very brief introduction to the origin of the differences in fuel specifications.

Considering its age and origin, it is obvious that petroleum crude oil was discovered before the different types of engines were invented. In fact the different engines were more or less invented to utilise as much of the petroleum crude oil as possible. Figure 1.5 illustrates how the different fuels cover most of a typical petroleum crude oil boiling range. Presented very roughly, the first cut of crude oil that was utilised on large scale was the jet-fuel fraction. This fraction was used as lamp oil (1854), and the remaining part of the barrel was thrown away. Later the gasoline (1872) and diesel (1893) engines were invented in a way that utilised more of the crude oil. Likewise, the fuel oil was used as an alternative to coal. The break through of electricity removed the need for lamp oil, but this fraction was later found to be utilised as jet-fuel in turbine engines (1939). (de Klerk, 2013)

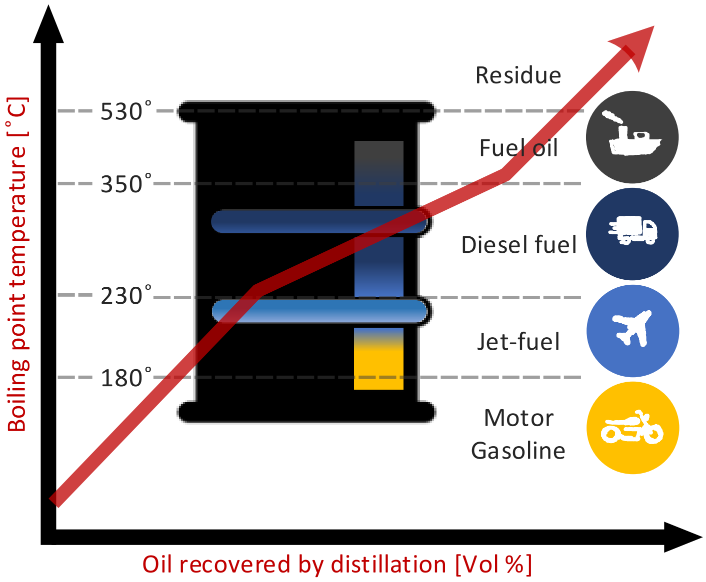

Figure 1.5. Illustrative distillation profile to show how the different fuels cover the different boiling fractions of a typical petroleum crude oil. The temperature cuts are indicative values. (de Klerk, 2011)

The above very brief introduction is given to underline the fact that the different fuels have specific boiling ranges. Thus, by fractional distillation it is possible to separate and investigate the different boiling ranges suitable for particular fuel types. The specifications that these fractions must fulfil are given in the following.

1.4.1 Gasoline Specifications

Gasoline is used in spark-ignition engines, where the point of ignition is crucial. To prevent so-called knocking, the gasoline must resist the temperature and pressure increase due to compression without igniting. The octane number quantifies this property to prevent auto-ignition or anti-knocking. The anti-knocking characteristics of a gasoline fuel depend on the engine operation. The research octane number (RON) relates to the antiknock behaviour at low and medium engine speeds, whereas the motor octane number relates to higher engine loads and speeds. The indicative octane number given at tank stations in Europe is the RON, whereas it is the mean of RON and MON in North America (de Klerk, 2013). The higher the octane number for a fuel, the higher a compression ratio is allowed in the engine without facilitating knocking. Table 1.3 lists the major fuel specifications for unleaded gasoline. (de Klerk, 2011) (ACEA et al., 2013)

Aromatic hydrocarbons have high octane numbers. Additionally, olefins have higher octane numbers than alkanes with the same carbon number. The octane number of linear hydrocarbons increase with branching and a decreasing carbon number. Note how there are upper limits for the high octane number compounds (Olefins, aromatic and benzene) in Table 1.3, but none for the lower octane alkanes. In relation to analysis of the prospects in producing fuel from bio-crude, it should be noted that oxygenates like alcohols also have high octane numbers. Thus, these are well suited for gasoline. On the other hand, aldehydes should be avoided because they facilitate wax formation. Based on this it is interesting to analyse in what kind of functional groups the oxygenates are present in the bio-crude. Note how, there is an upper limit for the amount of oxygenates allowed in a gasoline blend. Bioethanol is a renewable biofuel containing oxygenates, so the drop-in ability of ethanol is limited by the oxygenate specification. The blend-wall and the consumption of bioethanol was discussed in more details in Section 1.3. (de Klerk, 2011), (ACEA et al., 2013)

Gasoline			
RON, Research octane number		min	95.0
MON, Motor octane number		min	85.0
Density @ 15°C	$^{kg}/_{m^3}$		720 - 775
Vapor Pressure	kPa	max	65-80
T10 boiling point	°C	max	55
T90 boiling point	°C	max	130-175
Olefin content	$Vol\%$	max	10.0
Aromatic content	$Vol\%$	max	35.0
Benzene content	$Vol\%$	max	1.0
Oxygenate content	$wt\%$	max	2.7
Sulphur content	ppm	max	10

Table 1.3. Unleaded gasoline specifications for a market with highly advanced requirements for emission control and fuel efficiency. (ACEA et al., 2013)

To avoid inhalation of volatile vapours when refuelling with gasoline, there is an upper limit for the vapour pressure of a gasoline blend. This limit is season and region specific, depending on the climate. In addition, sulphur content is regulated to maximum 10 ppm and there is an upper (T90) and lower (T10) limit of the distillation profile. T10 reflects the temperature at which 10 vol% of the blend has vaporised and likewise for the T90 specification. (de Klerk, 2011)

1.4.2 Diesel Specifications

Diesel engines are compression ignition engines that are based on auto-ignition of the diesel fuel. So opposite the gasoline used in spark-ignition engines, diesel should be a low octane blend or in other words have a high cetane number. The cetane index is a measure of the ignition delay, and it is high for a fuel that easily oxidises with air. In Table 1.4 the minimum cetane specification for diesel blends is given along with other major diesel specifications. (de Klerk, 2011) (ACEA et al., 2013)

Low octane compounds are generally high cetane compounds. Thus, suitable diesel compounds when looking at the cetane specification are linear parafinnic hydrocarbons with little branching. However, to meet the cold flow properties, some branching is required. (de Klerk, 2011)

Diesel			
Cetane number		min	55.0
Density @ 15°C	$^{kg}/_{m^3}$		820 - 840
Viscosity @ 40°C	cSt		2.0-4.0
T90 boiling point	°C	max	320
Final boiling point	°C	max	350
Flash point	°C	min	55
Total aromatic content	$\% \ m/m$	max	15.0
Polycyclic aromatic content	$\% \ m/m$	max	2.0
Sulphur content	ppm	max	10
Water content	ppm	max	200
TAN	$mg\frac{KOH}{g}$	max	0.08
FAME^a	$\% \ v/v$	max	5

^{a} Only allowed in specific geografic locations

Table 1.4. Diesel specifications for a market with highly advanced requirements for emission control and fuel efficiency. (ACEA et al., 2013)

The diesel density is also specified in a particular range. This is due to the way the air-fuel ratio is practically applied in the engine. The air-fuel ratio is important for combustion efficiency and exhaust emissions. The air-fuel ratio is defined as moles of fuel per moles of air, but in the engine it is measured by volume displacement. To ensure an air-fuel ratio around a certain point, the density is used as the constraining parameter. (de Klerk, 2011)

Addition of biodiesel (FAME) is regulated differently in different geographic locations. In some regions an upper limit of 5 vol% is allowed, whereas in some regions no FAME additives are allowed (ACEA et al., 2013). FAME additives and the consumption of these is discussed in more details in Section 1.3.

1.4.3 Jet A-1 Kerosene Specifications

Unlike both diesel and gasoline, the auto-ignition properties of jet-fuel are not relevant. This is because turbine engines are continuous combustion engines, where the fuel is injected directly as an atomised spray to fuel the flame. Instead, cold flow properties are crucial for jet-fuel. This is because the fuel tanks are located in the wings of the airplane, where the temperature goes typically as low as -45°C. In addition, the jet-fuel is used as cooling medium in the airplane, which then requires the fuel to be stable when in contact with hot surfaces. Note how the jet-fuel specifications in Table 1.5 include both high temperature stability and cold flow properties such as freezing point and viscosity. (de Klerk, 2011)

Jet-fuel, Jet A-1 Kerosene			
Freezing Point	°C	max	-47.0
Viscosity @ -20°C	cSt	max	8.00
Density @ 15°C	$^{kg}/_{m^3}$		775 - 840
T10 boiling point	°C	max	205.0
Final boiling point	°C	max	300.0
Flash point	°C	min	38.0
Smoke point	mm	min	25.0
Aromatic content	$Vol\%$	max	25
Sulphur content	ppm	max	3000
Thiol content	ppm	max	30
Stability @ 260°C	$torr$	max	25.0
Specific energy content	$^{MJ}/_{kg}$	min	42.80

Table 1.5. Jet A-1 Kerosine specifications. Last revision March 2005. (Aviation, 2005)

The smoke point specification is to prevent extensive soot formation. Small soot particles will wear the turbojet engine down, when passing through the turbine at the high flow speeds encountered in a jet-engine. Note also how the total sulphur specification is relatively loose compared to the other fuel products. Though, there is a maximum of 30 ppm of thiols, which is a specific sulphur containing compound that affects stability of the jet-fuel. (de Klerk, 2011)

1.4.4 Marine Fuel Specifications

Marine fuel is a broad term for various different fuel products with different specifications. Table 1.6 lists examples of both a distillate marine fuel and a residual marine fuel. Obvious from the naming, the residual marine fuel is a heavier and lower value product than the distillate marine fuel. Though, in general these products are both the bottoms of the barrel, which are left over when the lower boiling point distillates are boiled off in the distillation units.

Marine Distillate Fuels (DMA)				Marine Residual Fuels (RMA)			
Viscosity @ 40°C	cSt		2.0-6.0	Viscosity @ 50°C	cSt	max	10.0
Density @ 15°C	$^{kg}/_{m^3}$	max	890	Density @ 15°C	$^{kg}/_{m^3}$	max	920
Micro carbon residue	$wt.\%$	max	0.3	Micro carbon residue	$wt.\%$	max	2.50
Water content	$vol.\%$	max	0.30	Water content	$vol.\%$	max	0.30
Flash point	°C	min	60.0	Flash point	°C	min	60.0
Pour point, summer	°C	max	0	Pour point, summer	°C	max	6
Pour point, winter	°C	max	-6	Pour point, winter	°C	max	0
Sulphur content[a]	$wt.\%$	max	0.1-1.50	Sulphur content[a]	$wt.\%$	max	-
H_2S content	ppm	max	2.0	H_2S content	ppm	max	2.0
Ash content	$wt.\%$	max	0.040	Ash content	$wt.\%$	max	0.040
TAN	$mg\frac{KOH}{g}$	max	0.5	TAN	$mg\frac{KOH}{g}$	max	2.5
Calc. cetane index		min	40.0				

[a] Sulphur specification varies with geografic location

Table 1.6. Marine fuel specifications based on the ISO 8217 Fuel Standard, fourth edition, 2010 (Fuels, 2012).

Note how the sulphur specification varies with geografic location. Some regions have stricter sulphur allowances than others. As mentioned in Section 1.2, a recent EU directive reduces the allowed sulphur content in marine fuel from 1.5 wt.% to 0.5 wt.% by 2020. In certain 'Sulphur Emission Control Areas', the specification is further reduced to 0.1 wt.% by 2015. (EMSA, 2010)

The above presentation reveals the significant differences between fuel specifications for different engine types. A key thing to note is the fact that the different fuels belong to a particular boiling range. By fractional distillation of the bio-crude investigated in the present study, it is possible to analyse the amount and the quality of these particular boiling ranges, and evaluate the processing required for drop-in ability.

Theory and Practice on Fractional Distillation

2

In this chapter the fractional distillation of HTL bio-crude will be presented. More precisely the distillation set-up, the applied ASTM standards and consideration related to the set-up will be presented. Here distillation profile and heteroatom content are important terms. In relation to considerations regarding the set-up, dehydration of the oil sample prior to distillation will be investigated.

2.1 Introduction to Fractional Distillation

Fractional distillation is a separation technique based on the difference in boiling points of the liquids that are separated. Crude oils are mixtures of various liquid hydrocarbons with very different properties. Fractional distillation enables separation of this mixture by evaporation of a compound from the mixture and subsequent condensing of the vapour into a product receiver. Simple distillation is used for instance when separating two liquids with a difference in boiling point of more than 25°C at atmospheric pressure. Fractional distillation is a more efficient separation technique used when separating compounds with boiling points closer than 25°C. Since the boiling point distribution of both petroleum and bio-crude oils are more or less continuous, fractional distillation must be used in this relation. (Wan, 2013), (Montemayor, 2008)

A key term within oil refining is the distillation profile, which is the main analytical result of fractional distillation. The distillation profile describes the volume and/or mass fraction distilled in a specific boiling range. More precisely, it is the boiling point distribution as a function of temperature. An illustrative drawing of a distillation curve is depicted in Figure 1.5. It can be derived from the distillation profile, whether a given crude oil is more suited for producing lighter fuel products, such as motor gasoline or heavier distillates such as jet fuel and diesel products. Likewise, the expected fraction of atmospheric and vacuum residue can be determined from the distillation profile. This is valuable information for a refiner, since residues require a lot of processing to end out as on-specification fuel relative to the LSR fractions. As a result, heavy crude oils with a large fraction of high temperature boiling points are less valuable relative to crude oils with a large LSR fraction. (Gary et al., 2007)

No conventional crude oils are the same and to quantify relevant measures of quality, so-called Hempel Assays are used in the refining industry to list properties such as distillation profile, viscosity, density, heteroatom content, pour point, coking tendency etc. for a particular crude. Table 2.1 illustrates an example of a Hempel Assay of a crude oil from the Leduc 2-field in Alberta, Canada. Some properties are given for every fraction, whereas some properties (bulk properties) only are given for the entire crude oil as a mixture. Stage 1 in the assay represents atmospheric distillation, and stage 2 represents vacuum distillation of the atmospheric residue at 40 torr. The yield of each boiling fraction is given in weight percentage along with an accumulated percentage. The vacuum residue given as the last fraction in the stage 2 part is a mix of heavy components boiling above 572°F at 40 torr. This corresponds to an atmospheric equivalent temperature (AET) of 419°C. (Gary et al., 2007)

Gravity, specific: 0.826
Gravity,°API: 39.8
Pour point, °F: below 5
Sulfur, percent : 0.30
Color: brownish green
Viscosity, Saybolt Universal at: 100°F, 38 sec
Nitrogen, percent: 0.0

DISTILLATION, BUREAU OF MINES ROUTINE METHOD

STAGE 1 - Distillation at atmospheric pressure: 746 torr
First drop: 86 °F

Fraction No.	Cut temp °C	%	Sum, %	Sp. gr. 60°F	°API. 60°F	C.I.	Refractive index,20°C	Specific dispersion	S.U. visc. 100°F	Cloud test°F
1	50	3.5	3.5	0.642	88.9					
2	75	3.0	6.5	.667	80.9	6.1	1.37486	125.8		
3	100	5.9	12.4	.718	65.6	20	1.39939	129.4		
4	125	7.0	19.4	.746	58.2	25	1.41366	133.6		
5	150	6.6	26.0	.767	53.0	27	1.42596	139.2		
6	175	5.7	31.7	.785	48.8	29	1.43611	142.6		
7	200	5.0	36.7	.800	45.4	30	1.44412	142.7		
8	225	5.1	41.8	.812	42.8	30	1.45084	142.9		
9	250	5.1	46.9	.824	40.2	30	1.45792	147.2		
10	275	6.2	53.1	.840	37.0	33	1.46614	153.7		
STAGE 2 - Distillation continued at 40 torr										
11	392	2.9	56.0	0.850	350	34			41	20
12	437	5.8	61.8	.859	33.2	34			46	35
13	482	5.3	67.1	.872	30.8	37			58	55
14	527	4.6	71.7	.883	28.8	39			82	75
15	572	5.4	77.1	.895	26.6	42			155	90
Residuum		19.9	97.0	.951	17.3					

Carbon residue, Conradson: Residuum: 7.6 percent; Crude: 1.7 percent

APPROXIMATE SUMMARY

	Percent	Sp. gr.	°API	Viscosity
Light gasoline	12.4	0.684	75.4	
Total gasoline and naphta	36.7	0.742	59.2	
Kerosene distillate	10.2	0.818	41.5	
Gas oil	14.0	0.848	35.4	
Nonviscous lubricating distillate	9.8	.863-.886	32.5-28.2	50-100
Medium lubricating distillate	6.4	.886-.901	28.2-25.6	100-200
Viscous lubricating distillate	-	-	-	Above 200
Residuum	19.9	.951	17.3	
Distillation loss	3.0			

Table 2.1. Hempel Assay of petroleum crude oil from Leduc 2-field, Alberta, Canada. (Gary et al., 2007)

The approximate summary given in the bottom of Table 2.1 is a simple analysis of the expected yields of each stream/product. The sum of the yields in the approximate summary is not necessarily 100 %, since the cut temperatures overlap. The distillation loss given in the bottom is always given in a Hempel Assay or a distillation sheet in general. (Gary et al., 2007)

2.2 Heteroatoms in Bio-Crude

Sulphur and nitrogen contents are given as total values for the petroleum crudes in the top of the Hempel Assay in Table 2.1. A major aspect of the present study is to analyse the distribution of heteroatoms in the different fractions of bio-crude. The distribution is considered as valuable quality information that is important in relation to co-processing of bio- and petroleum crude oil. It might seem surprising that the heteroatom content is not given for each fraction in the Hempel Assay. However, a common characteristic of different petroleum crude oils is that the heteroatom content is a function of boiling point. There is roughly no traces of N and S atoms in the low boiling point fractions, whereas the major part of total N and S atoms are concentrated in the high boiling components. To determine the N and S content in the different fractions of crude oil the correlations in Figure 2.1 may be used. Here the nitrogen and sulphur content as function of the true boiling point (TBP) temperature is given. The nitrogen correlation is considered valid for a range of different crudes, whereas the sulphur correlation is valid for crude oils with origin in California. Likewise, similar correlations exist for crude oils with different origin. (Gary et al., 2007)

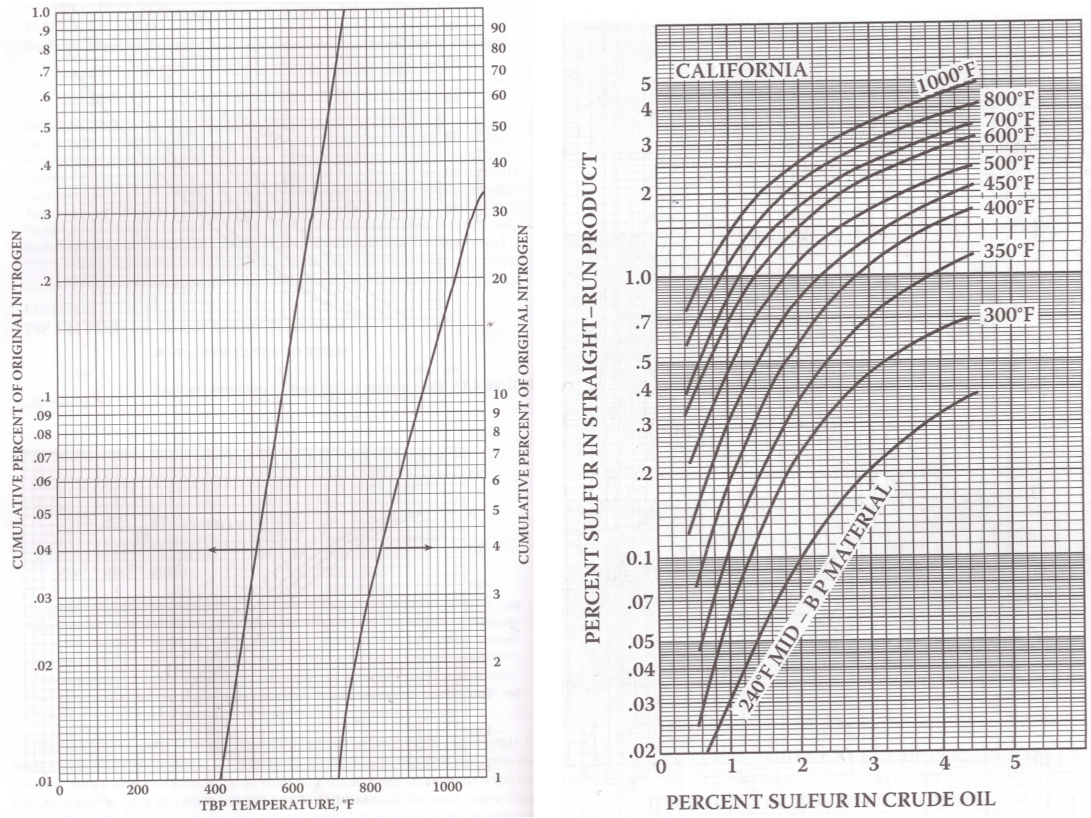

Figure 2.1. Left: General nitrogen distribution in crude oil fractions. Right: Sulphur content as function of boiling point for California crude oils. (Gary et al., 2007)

Whether or not the distribution of heteroatoms including oxygen is a function of boiling point for the HTL bio-crudes is a major question of present study. In conventional crude oil refineries the heteroatom removal is mainly performed in the residue processing by cracking, coking and hydrogenation processes with and without the presence of catalysts. If it turns out that the heteroatoms in bio-crude are distributed in a similar way as for crude oil, the bio-crude may be co-processed with the petroleum crude and the existing capacity for heteroatom removal in heavy crude may be utilised.

The distribution of heteroatoms as a function of boiling point in bio-crude can be analysed by collecting different fractions by fractional distillation and doing elemental analysis on the separate fractions. It is a major focus of this report to obtain such results of the bio-crude and compare them to Figure 2.1.

2.2.1 The Presence of Oxygenates

The elemental composition of nitrogen and sulphur are given in the Hempel Assay in Table 2.1, but note how the oxygen content is absent. This is because oxygenates are present only in low concentrations, 0.05-1.5 wt% in petroleum crude oil (de Klerk, 2011). Oxygen present as strong organic acids should be considered, due to corrosion issues. Elevated temperatures experienced throughout a refinery increases the risk of corroding the different units when strong acids are present. The amount of organic acids is quantitatively stated as the total acid number (TAN) and for crude oils a TAN above 1.0 mg KOH/g oil is considered high TAN crude oils (de Klerk, 2011).

The content of oxygenates is a major difference between petroleum crude oil and bio-crudes (Furimsky, 2013). Depending on the origin, bio-crudes contain significant amounts of oxygen. A TAN above 100 is not uncommon for pyrolysis oils (Karimia et al., 2013), (Xu et al., 2013). Likewise, the TAN measured for wood based HTL oils produced by *CBS (2014)* are in the range 30-60 mg KOH/g. Analysis of CBS oils are given in Table 2.2. Note the oxygen content above 5 wt.% and the mentioned TAN values. In relation to co-processing of the bio-crude with petroleum crude oil at existing refineries, a high TAN value is a hurdle. The refineries are not build to handle corrosive crude oils, which makes pretreatment, such as deoxygenation, of these oils relevant. This deoxygenation may be done by mild or severe HDO depending on the nature of the oxygenates (Furimsky, 2013).

	Elemental composition [wt.%]					Density @ 15°C	TAN	Pour Point
	C	H	N	S	O	[g/ml]	[mg KOH/g]	[°C]
CBS22	82.16	10.56	0.63	0.135	5.99	0.95	43.46	-9
CBS24	82.22	10.02	0.68	0.074	7.41	0.99	41.26	0
CBS25	82.04	10.49	0.32	0.119	7.23	0.97	59.90	0
CBS26	82.38	10.49	0.14	0.118	6.75		55.43	-21
CBS27	84.37	10.60	0.18	0.125	4.90	0.95	36.78	-12
CBS44	81.99	11.74	0.44	0.03	5.80			
CBS48	83.16	10.91	0.31	0.138	5.48			

Table 2.2. AITF analysis of HTL oils based on woody feedstocks. (CBS, 2014)

Thermal Cracking of Oxygenates

Hydrocarbons containing oxygenates are considered more likely to thermally crack. This is due to lower bond dissociation enthalpies (BDE) of the bonds in the oxygenates (de Klerk, 2011). However, this is not entirely true due to very different compositions of oxygenates. BDE is defined as the energy required for homolytic bond cleavage, or in other words the energy required for thermal cracking of a bond into radicals (Wade, 2013). This energy is related to the stability of the compound(s) before and after cracking. To give an example, Table 2.3 lists the BDE of a given bond in different hydrocarbons and oxygenates. Consider one of the compounds given in Table 2.3. It is quite obvious that the compound before cracking is more electron stable than the radicals after cracking. Thus, the radicals are at a higher energy state than the stable compound. This tells us that homolytic/thermal cracking of a compound is always an endothermic reaction (Wade, 2013). Likewise, an amount of energy equal to the BDE is released when the radicals recombine.

Hydrocarbons	BDE [$^{kJ}/_{mol}$]	Characteristic
H_3C—CH_3	368	Primary carbon
$(CH_3)_2CH$—CH_3	351	Secondary carbon
$(CH_3)_3C$—CH_3	339	Tertiary carbon
CH_3—C_6H_5	389	Methyl benzene
Oxygenates		
CH_3—CHO	314	Aldehyde
$C_6H_5CH_2$—$COOH$	285	Carboxylic acid
CH_3O—CH_3	335	Dimethyl ether
C_2H_5O—C_6H_5	213	Ethyl phenyl ether
CH_3CO—OCH_3	406	Methyl acetate (Ester)
$C_6H_5CH_2$—$OCOCH_3$	285	Benzyl acetate (Ester)

Table 2.3. Examples of bond dissociation enthalpies to show the influence of structure and oxygen content on cracking probability. (Zhanabai, 2014) (Wade, 2013)

Note in Table 2.3, how the BDE's vary significantly with the structure of the compound despite similar elemental composition. The BDE of a tertiary carbon is lower than that for a secondary carbon, due to the stability of the corresponding radicals (Wade, 2013). When looking through the oxygenates and comparing them to the pure hydrocarbons, it appears that for instance the carboxylic acid, and the methylether benzene requires less energy to crack. The BDE of the esters however, are very different and depend on the structural configuration. As a conclusion, it is not correct to generalise and state that all oxygenates are more likely to crack thermally, but it is evident from the examples in Table 2.3 that some oxygenates will crack at lower temperatures than the corresponding hydrocarbons. *Elliott (1980)* found that the decomposition point of wood based HTL oil is approximately 55°C below that experienced for petroleum crude oil. These observations must be kept in mind under fractional distillation, since oxygenates of unknown composition do appear in the bio-crude subject to distillation and degradation must be avoided. This leads to the procedure of fractional distillation, which will be presented next.

2.3 Distillation Set-up Related to ASTM Guidelines

ASTM has established diferent guidelines on how to perform fractional distillation. The ASTM standards D86, D1160, D2892 and D5236 can be used in the distillation of crude feedstocks (Montemayor, 2008). D86 - Distillation at Atmospheric Pressure - is designed for distilling fuels and not for products containing considerable amounts of residual material. D1160 - Distillation of Petroleum Products at Reduced Pressure - is designed to obtain approximate one theoretical plate fractionation, equivalent to one simple distillation. A theoretical plate corresponds to one vaporization-condensation cycle and thus the column efficiency increases with the number of theoretical plates. Recall that simple distillation is in relation to crude oils, where the distillition profile is more or less continous. D2892 - Distillation of Crude Petroleum (15 Theoretical Plate Column) - and D5236 - Distillation of Heavy Hydrocarbon Mixtures (Vacuum Pot-still Method) - are standard guidelines more than true test methods. Guidelines, in the sense that the methods do not specify exact cut temperatures, operating pressures or details about the necessary equipment. Instead the methods provide information on how to choose these in order to produce fractions of standardised quality. D2892 is capable of producing fractions with a final cut temperature of 400°C (AET). The method has a high column efficiency with 15 theoretical plates. D5236 is similar, but with a final cut temperature of 565°C depending of the sample. To reach this higher temperature it is recommended to use only a one theoretical plate column and a 'higher' vacuum. The lowest operating pressure of D5236 is recommended to be 0.1 torr, whereas it is 2 torr for D2892. Recall, that the lower the operating pressure the more the atmospheric boiling point is depressed. In other words, a 'higher' vacuum enables distillation of heavier components. (Montemayor, 2008)

The HTL bio-crude is expected to contain a considerable quantity of residue, and the available distillation equipment in present study is a 15 theoretical plate column. Also, the final cut of 400°C is considered sufficient, since this corresponds to the final cut temperature in a VDU (Gary et al., 2007). Thus, the *ASTM D2892 (2005)* is used as a guideline in the distillation process of the present study. A distillation procedure based on *ASTM D2892 (2005)* is made for bio-crudes and given in Appendix A. Considerations regarding the distillation set-up are given in Appendix B.

2.3.1 Fractional Distillation Set-up in Present Study

The fractional distillation set-up used in present study is illustrated in Figure 2.2. The original set-up consists of a 15 theoretical plate column with a 2 litre pot flask, and a heating mantle to heat up the lower half of the pot flask. The packed fractionating column has an inner diameter of 25mm. During distillation adiabatic conditions in the column are ideal, and thus the column is surrounded by a vacuum jacket for insulation purposes. The temperature is measured in the pot flask and in the column head (vapour temperature). A reflux condenser is placed on top of the column and below a valve is placed in order to control the reflux ratio. When the valve is open, allowing liquids/vapours to exit the column, they are fully condensed in a small condenser. From here the liquids proceed through the fractional collector and into the product receivers. A turning device in the fractional collector makes it possible to change the fraction without disturbing the distillation. From the top of the reflux condenser, the pressure is measured by a pressure transducer and controlled by the vacuum pump.

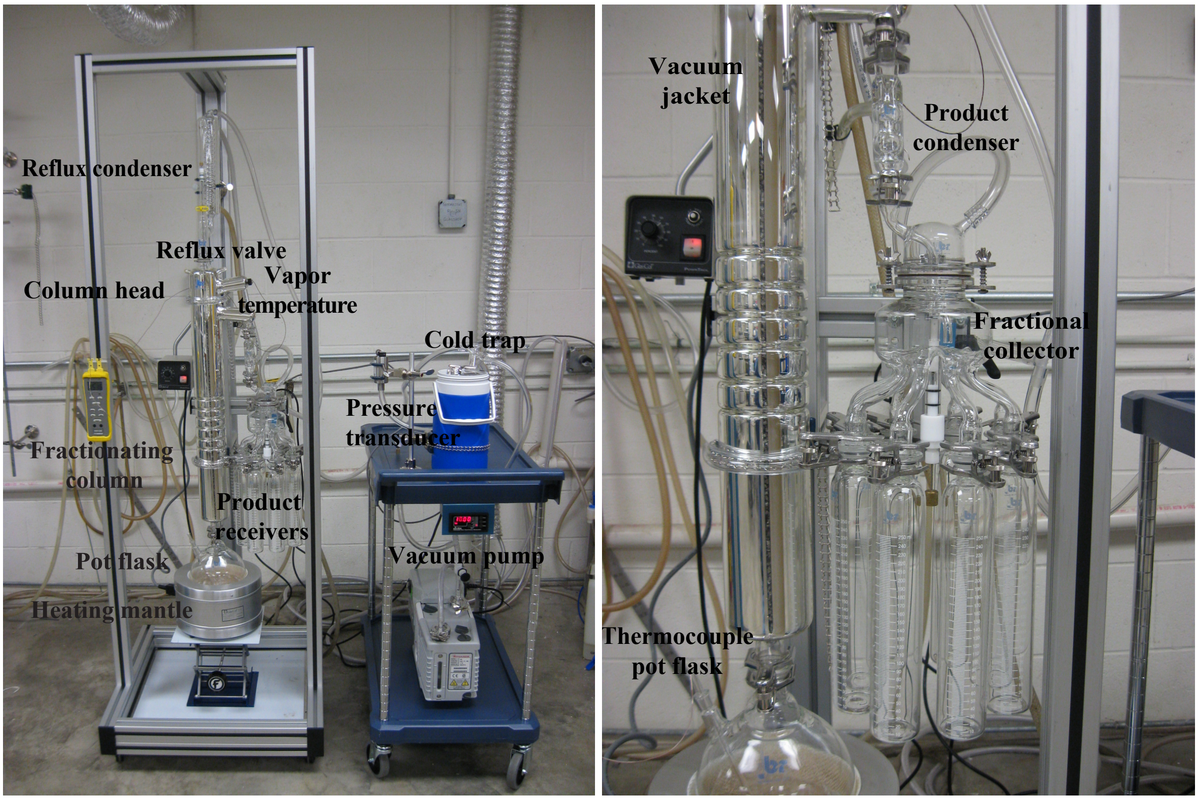

Figure 2.2. The fractional distillation set-up in present study is manufactured by BR Instruments.

Distillation efficiency or cut temperature sharpness are terms related to how accurate the difference in boiling point is measured. Distillation efficiency is related to the number of theoretical plates of the fractionating column. Recall that one theoretical plate corresponds to one vaporization-condensation cycle or in other words, one separation of a mixture with different boiling points. In order to determine the true boiling point of a compound the number of theoretical plates should be infinite and there should be perfect equilibrium between liquid and vapour corresponding to total reflux and thus no take-off.

The result of distillation with a 15 theoretical plate column will be hardly distinguishable from results of a possible infinite theoretical plate column when the reflux ratio is 15:1. However, this will increase the distillation time significantly and thus D2982 recommends a compromise between efficiency and distillation time by using a reflux ratio of 5:1. Furthermore, a reflux of 2:1 is suggested when operating below 10 torr, since a lower operating pressure decreases the distillation rate. This results in a further compromise between efficiency and distillation time. (Montemayor, 2008)

Adiabatic Conditions Obtained with Heating Jacket

Heat loss from the fractionating column is another important aspect, which affects the distillation efficiency. According to D2892 the distillation should be carried out at adiabatic conditions, meaning that no significant heat loss or gain is allowed throughout the length of the column. *ASTM D2892 (2005)*, Annex 3 describes how to measure and evaluate the column with respect to heat loss. In present study the vacuum jacket surrounding the column is not found sufficient to satisfy the guidelines of D2892. Furthermore, D2892 suggests to apply heat to the pot flask with a rate that ensures vapours to reach the column head between 20 and 50 min after start-up. This is not reached with the original set-up either. Consequently a 700W heating jacket connected to a voltage control is mounted on the fractionating column. The jacket temperature is controlled manually with the voltage control and a thermocouple mounted between the column head and the heating jacket. If the heating jacket is too cold the internal reflux will be higher compared to the reflux in the column head and opposite with a too high jacket temperature that supplies heat to the column. To speed up the column heat up, the jacket temperature is raised just below the expected vapour temperature at which the first fraction will be collected. During distillation the jacket is controlled to be between 0 and 5 °C below the vapour temperature.

Fraction Size and Crude Specific Considerations

In present study a fraction is defined as the entire volume distilled within a certain temperature range, which matches the ASTM guidelines. The temperature ranges are chosen according to the Hempel Assay in Table 2.1. The Hempel Assay cut temperatures are summarised in Table 2.4.

Fraction No.	Cut temp. °C
1	100-125
2	125-150
3	150-175
4	175-200
5	200-225
6	225-250
7	250-275
8	275-307
9	307-335
10	335-363
11	363-391

Table 2.4. The AET cut temperatures corresponding to the Hempel Assay in Table 2.1. (Gary et al., 2007)

The first three fractions in Table 2.4 corresponding to <50, 50-75°C and 75-100°C are excluded, since the bio-crudes in present study are expected not to contain any light fractions. This is expected, because the HTL oils are collected at a temperature of 40-60°C after production. Thus any fractions boiling below this temperature will be present in the gaseous product fraction.

Since no light fractions are expected, cooling water at ambient conditions is sufficient in the condensers of the distillation set-up. During distillation the distillate becomes more viscous and at high boiling points wax formation may start forming in the condenser. Thus increasing the temperature of the cooling water may be necessary. Figure 2.3 shows how the distillate is observed to crystallise in the condenser during high vacuum distillation of a HTL bio-crude in present study. To overcome this loss of distillate, the flow of cooling water may be reduced or stopped.

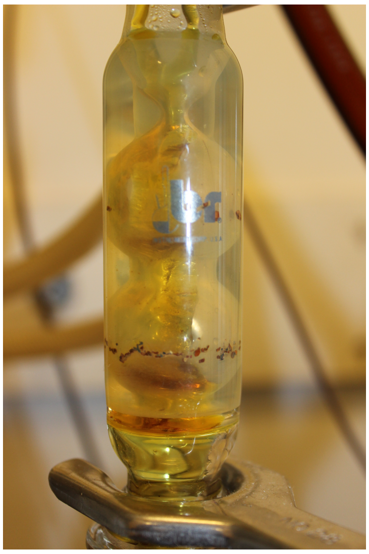

Figure 2.3. Wax formation in the condenser during high vacuum distillation in present study.

In case light fractions against expectations do appear in the oil sample, a cold trap is located as a filter between the distillation system and the vacuum pump/pressure transducer. *ASTM D2892 (2005)* states that H_2S often is evolved from crude oil and caution must be taken during distillation. A mixture of acetone and dry ice is kept in the cold trap in order to ensure that any light gases are condensed. This mixture enables a condensing temperature of -70°C in the cold trap. At atmospheric operating pressure, the boiling point of hydrocarbons heavier than propane (-42°C), and dangerous gases such as H_2S (-60°C) are condensed in the cold trap (Wan, 2013). It is however worth noting that when operating at reduced pressures, any evolved hydrogen sulphide is likely to pass through the cold trap. Hydrogen sulphide may evolve from possible cracking, which supports the importance of a safe exhaust from the distillation system. However, Table 2.2 revealed how the HTL bio-crudes are low sulphur mixtures, so the risk of hydrogen sulphide is considered lower than in relation to petroleum crude oils. It is observed in present study that a small amount of light fractions are collected in the cold trap. These constitute only around 2 % by volume of the total sample. The exact boiling point distribution of this fraction is unknown, but the sample is kept for analysis.

Allowance of Water in the Oil Sample

Presence of water in the crude oil sample can and will lead to changes in the TBP curve of compounds boiling in the range 50 - 150°C (Montemayor, 2008). It is known as steam distillation when the presence of water allows organic compounds with higher boiling points to evaporate at lower temperatures. When two immiscible liquids are present in a mixture, each phase will exert its own vapour pressure without being affected by the other phase. The resulting vapour pressure of the mixture is given as the sum of the individual vapour pressures. Thus, the resulting vapour pressure will always be higher for the mixture than that of each compound in separate phases. In relation to fractional distillation, it is thus important to remove the water in order to obtain an efficient distillation with clean cuts. D2892 states that a water content above 0.3 vol.% is too high and thus the sample must be dehydrated. In present work it has been observed that when water is present in the sample subject for distillation, an uneven boiling with bumping occurs. This makes the distillation process difficult to control. Furthermore, signs of cracking have been observed at relatively low temperatures around 190°C when water is present. The reason for this phenomenon is unknown at this stage, but the observation is interesting and it underlines the importance of dehydrating the sample subject to distillation.

2.4 Dehydration of Oil

The bio-oils used in present study all exceed the 0.3 vol.% requirement of the ASTM standard D2892 with respect to water content and thus must be dehydrated. The dehydration can e.g. be performed through centrifugation, the use of a desiccant or by distillation. These three methods are tested and the results with respect to water content are compared with the ASTM standard. The results are given in Table 2.5. Karl Fischer titration has been used to measure the water content.

Water may appear as both free water, where it appears in a separate phase, or as water-in-oil emulsions. Emulsions are single phase mixtures of water bound to the oil-molecules. Thus the dehydration method must be able to remove both free water and break possible emulsions.

Water Content After Dehydration

Feed		Original water content	Centrifugation (3500 rpm/2931·g)	Desiccant Sodium Sulphate (8 g per 100 ml)	Rotary Evaporator (5 h)	Distillation Column (130°C)
Sample 1	wt.%	1.28	-	1.04	-	-
Sample 2	wt.%	6.75	-	-	3.32	-
Sample 3	wt.%	1.40	0.76 (@ 5h)	-	-	-
Sample 4	wt.%	1.09	0.71 (@ 10h)	-	1.09	-
Sample 5	wt.%	2.05	-	-	-	<0.3

Table 2.5. Results of dehydration using desiccant, centrifugation, evaporation and distillation.

Centrifugation

By centrifugation free water will be separated from the bio-crude due to gravity and the water-in-oil emulsion will be degraded (Hahn and Mittal, 1979) However, the extent to which the emulsions will be degraded is unknown. In present work centrifugation has been carried out for 5 hours at 3500 rpm/2931·g (sample 3 in Table 2.5). However, these operating conditions have not been enough to fulfil the ASTM requirements. Thus the centrifugation time was prolonged to 10 hours at 3500 rpm/2931·g (sample 4 in Table 2.5). A result of 0.71 wt.% water is still not sufficient to meet the ASTM requirements. Based on the results it is concluded that centrifugation is not a suitable approach to reach a water content below 0.3 %.

Desiccant

The use of a desiccant in the process of drying the bio-crude is proposed in the ASTM standard D86, Distillation at Atmospheric Pressure. The standard mentions anhydrous sodium sulphate as a suitable drying agent, but it does not mention the extend to which the sample is dehydrated using this approach (Montemayor, 2008). Using 8 g anhydrous sodium sulphate per 100 ml of sample (Wan, 2013) reduces the water content from 1.28 to 1.04 % (sample 1 in Table 2.5). The desiccant was kept in the sample for around 10 min (Wan, 2013) and then removed using centrifugation. The result shows that using a desiccant like anhydrous sodium sulphate is not enough to fulfil the requirements of the ASTM standard. Wan (2013) states that sodium sulphate is an efficient but slow desiccant, so prolonging the dehydration time to more than 10 min might be effective. Though, it is also mentioned that desiccants in general remove not only water, but they also absorb other polar compounds like alcohols, amines and compounds with ketone functional groups. For this analysis it is undesired to do any 'damage' of the bio-crudes, which is a drawback for the use of desiccants for dehydration. Furthermore, the use of a desiccant is not applicable on a future large scale level, which also makes this method less relevant. As a result, it is concluded that using anhydrous sodium sulphate to dry the bio-crude prior to fractional distillation is not an option and the use of a desiccant is investigated no further.

Distillation

The ASTM standard D2892 describes dehydration through the use of a distillation set-up. Here the sample is heated until a vapour temperature of 130°C is reached (ASTM D2892, 2005). In present work a rotary evaporator has been tested to perform the dehydration. This would simplify the set-up and increase the capacity compared to a distillation column, and a rotary evaporator is based on the same principle. The rotary evaporator is tested at an AET of 150°C and the evaporation is carried out for 5 hours under vacuum. The first bio-crude sample that has been dehydrated in the evaporator contained 6.75 wt.% water and the content was reduced to 3.32 wt.%. This is given as sample 2 in Table 2.5. Secondly a bio-crude with an initial water content of 1.09 wt.% has been tested in the rotor evaporator (Sample 4 in Table 2.5). During the evaporation moisture was visible inside the flask. However, no water was removed from the sample and the water content remained the same after evaporation. Based on these result it is concluded that the rotor evaporator is capable of removing some water from the sample, but it cannot obtain a water content that fulfil the ASTM standard.

The rotary evaporator was tested because this procedure is simple and fast compared to using the 15 theoretical plate distillation column. However, as the rotary evaporator has not been capable of fulfilling the requirements of the ASTM standard, the 15 theoretical plate column is tested. The distillation was performed at atmospheric conditions but due to an uneven boiling and signs of cracking the distillation was immediately terminated. Instead vacuum distillation is proposed as a better dehydration method for the bio-crudes used in this study. Distillation under vacuum enables lower boiling points and thus no cracking. Vacuum (100 torr) distillation is performed to reach an AET of 130°C. The results of the vacuum distillation of CBS44 is shown in Figure 2.4. Here the atmospheric equivalent vapour and pot flask temperatures are shown along with the volume of the total distillate and the amount of water in the distillate. From the Figure it can be seen that the temperature of the pot flask reached 250°C and no signs of cracking occurred. After 40 min of heat up, the distillation valve is opened and the condensed vapours are collected. The vapour temperature is somewhat steady just below 100°C and the distillate separates in two phases, one organic phase and one heavier phase, given as the water phase in yellow in the figure. After 105 min the vapour temperature increases rather suddenly and the volume of the collected water phase becomes constant. This indicates that no more water is present in the sample. Another indication is the fact that the bumping during boiling suddenly stops and the boiling becomes smooth. As a result the dehydration is stopped. The organic phase of the distillate is decanted at -18°C and reintroduced into the oil sample after which the fractional distillation can start.

The water content after the dehydration has not been successfully measured using the KF titration. However, the elemental analysis, given in Table 3.4 of the original and the dehydrated CBS44 crude oil shows that the oxygen content is reduced from 5.8 to 3.6 wt.% in the dehydration. Furthermore, no water seems present in any of the collected fractions during the fractional distillation. Finally, the collected water phase in the dehydration corresponds to 2.12 vol.% of the sample. This indicates that the requirements of the ASTM standard are fulfilled using the 15 theoretical plate column to dehydrate the oil sample.

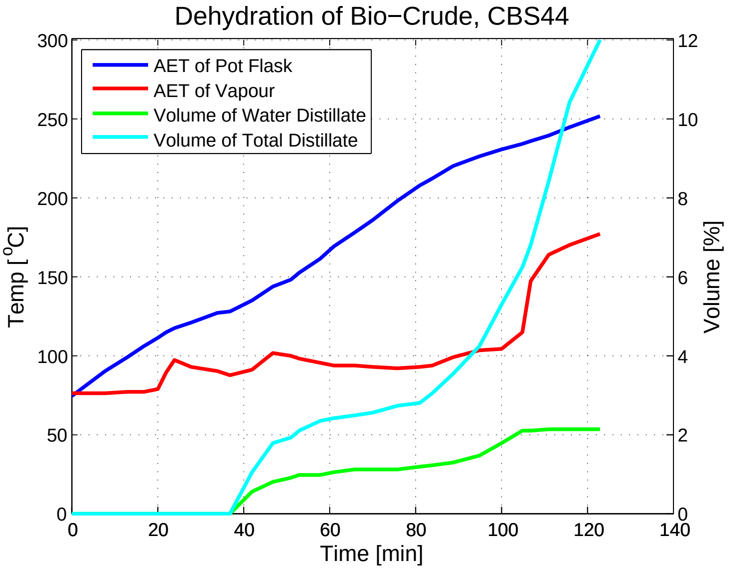

Figure 2.4. Dehydration of CBS44.

Based on present work it can be concluded that dehydration of a HTL bio-crude is a complex and time consuming process. Though very important, since distillation with water in the sample results in unsteady boiling, low distillation efficiency and control difficulties during distillation. Thus it is concluded that the dehydration in present work should be performed using the 15 theoretical plate column. After distillation the organic fraction that have been collected should be reintroduced into the oil sample after separation of the water phase. It is important to remove any residual water from the distillation column. The water is likely to get stuck in the column packing and on the glass walls and thereby be trapped in the column. During distillations in present study, shootings through the column head were observed at vapour temperatures above the boiling point of water. As a result the vapour temperature dropped, which decreases the separation sharpness. The shootings in the column are expected to be due to water trapped in the column packing. A sudden release of the water will cause it to evaporate immediately which may be visible as shootings through the column head. Thus it is important to thoroughly cleaning the column after dehydration before initiating the fractional distillation.

Distillation and Analysis of HTL Bio-Crude

3

Presentation of bio-crude distillation assays, distillation validation and analysis of the different fractions with respect to HHV, CHNS and FT-IR is the major focus of this chapter. The outcome of the fraction analyses will be used to evaluate the intermediate upgrading required for co-processing the bio-crude with petroleum crude oil.

15 theoretical plate fractional distillation of HTL bio-crude is beyond state-of-the-art, and thus the distillation profiles will be compared to distillation assays of different petroleum crudes. Distillation results and fractional analysis obtained from distillation of fast pyrolysis oils and a single HTL oil study will also be mentioned for comparison. More specifically, *Capunitan and Capareda (2013)* performed fractional distillation of corn stover pyrolysis oils at atmospheric and reduced pressure (375 torr) reaching 250 and 230°C AET respectively. There is no efficiency information given on the fractionating column used, but with respect to analysis HHV, CHNS and IR are available for comparison with the present results.

Elliott (1980) made a distillation study of HTL wood oil. The ASTM D1160 method was used in the distillation and 5 fractions were collected with a final cut temperature of 432°C. The distillate is analysed with respect to elemental analysis and HHV.

Ott et al. (2008) made a distillation study on swine manure pyrolysis oil that is called advanced distillation. Though, the distillation set-up was actually that used for simple distillation, due to the absence of a fractionating column. The vapour temperature approached 500°C at atmospheric conditions, and cracking was observed at these elevated temperatures. Sulphur distribution and IR analysis of that study will be compared to the distillates of the HTL bio-crude.

The HTL bio-crudes evaluated in the present study are described before presenting the distillation results.

3.1 Presentation of the HTL Bio-crude Subject to Distillation

An advanced hydrothermal research facility, the Continuous Bench Scale 1 (CBS), was installed at Aalborg University in 2013. It is bio-crude from this facility, designed and constructed by Steeper Energy, that is subject to distillation in present study. The CBS unit has provided very promising and state-of-the-art leading results with respect to oil quality without sacrificing yield to a significant extent. The CBS results have been obtained from processing ligno-cellulosic biomass in the form of wood, supplemented by stabilisers and hydrogen donors, at conditions higher than normally applied for liquefaction (390-420 °C and 300 bar, dry matter: 20-25 %, stable runs up to 36 hours).

During the present study, Steeper Energy is initiating a new continuous test campaign to produce a state-of-the-art steady state bio-crude. Steady state refers to an oil product that is purely HTL bio-oil. Besides water and solid biomass, the CBS feedstocks consist partly of recycled oil. At start-up of the mentioned test campaign, diesel is used to simulate the recycled oil. The oil product of each run is then used as recycle oil in the subsequent run, and in that way the amount of diesel present in the products is phased out. However, only CBS start-up bio-crudes produced from a feedstock with around 10 wt.% diesel were available within the time frame of the present study, and thus this report is based on these particular oils. However, this is not considered an issue, because the knowledge gained from bio-crude distillation, fractional analysis and subsequent deoxygenation is highly valuable for similar studies on future steady state bio-crudes. Table 3.1 lists the feedstock composition of the CBS oils used in present study. Note, that the compositions in Table 3.1 is based on the original feed. The original feed is dehydrated as described in Section 2.4 prior to fractional distillation. The dehydrated CBS oils are from now on referred to as CBS24, CBS44 and CBS48.

Feedstock	CBS24 original	CBS44 original	CBS48 original
Biomass 1^A	20.2wt.% Junkers	18.5wt.% Aspen	14.3wt.% Aspen
Additional^A			4.15wt.% Lignite
Recycled oil 1^A	18.7wt.% CBS21+22	8.0wt.% Steeper oil	6.9wt.% Steeper oil
Recycled oil 2		10.0wt.% diesel	8.6wt.% diesel
Recycled water phase	59.1wt.% CBS21	57.5wt.%	60.0wt.%
Catalyst	2.0wt.%	2.0wt.%	2.2wt.%

^{A} Dry basis

Table 3.1. Feedstock composition of CBS oils evaluated in present study. (CBS, 2014)

Note that CBS24 is an older oil without diesel in the feedstock from the summer 2013 that is not part of the mentioned campaign. This oil has been used to gain experience from preliminary distillation experiments and the fractions of this oil will not be analysed. Though, the distillation results are mentioned and thus the oil is included in Table 3.1 for completeness.

3.2 Running the Fractional Distillation

Process conditions during fractional distillation and validation of distillation profiles are presented in this section. For details on distillation procedure see Appendix A. Temperatures and the total distilled volume as function of the distillation time are given in Figures 3.1 and 3.2 for the fractional distillation of CBS44. Distillation of CBS44 was initiated with an operating pressure of 100 torr since any light fractions boiling below 75°C are unexpected. The distillation was carried out with a minimum reflux ratio of 2:1 for operating pressures below 10 torr and 5:1 otherwise.

Distillation data at an operating pressure of 100 torr is illustrated to the left in Figure 3.1. In this figure it can be seen that the heating jacket is controlled to match the actual vapour temperature to ensure adiabatic conditions. This is the case throughout the fractional distillation and the jacket and vapour temperatures are therefore excluded from the remaining figures. A maximum skin temperature of 330°C is reached at 100 torr and the maximum pot flask temperature was 250°C at 0.1 torr. At neither of these temperatures signs of cracking appeared.

Looking at the vapour temperature at an operating pressure of 100 torr it is seen that the temperature decreases after approximately 200 min. This sudden drop is related to 'shootings' that were observed in the column head. In order not to affect the separation sharpness due to the sudden temperature drop the distillate collected above 180 min (black dashed line) is poured back into the pot flask and re-distilled at a lower operating pressure. Experience shows that lowering the pressure suppress the shootings in the column head. At an operating pressure of 20 torr, the vapour AET increases rather unstable and after 150 min the temperature starts decreasing. Because of the irregular temperature profile the distillation at 20 torr is stopped and the operating pressure is lowered. Distillation at 10 and 0.1 torr in Figure 3.2 shows a smooth increase in the vapour temperature. At the time, the reason for the shootings and irregular temperatures were unknown, but through numerous distillations, experience tells that the shootings occur when the distillation column has not been properly dried after dehydration.

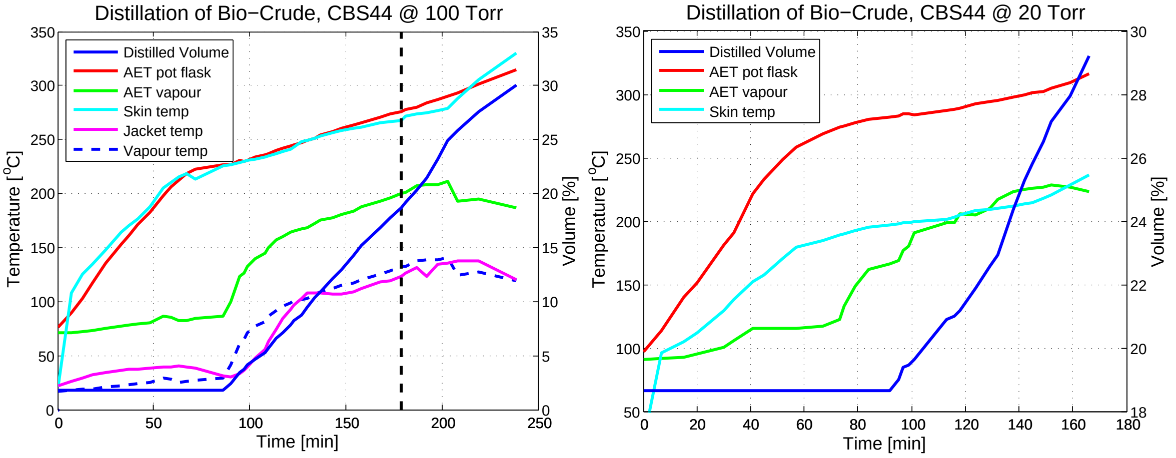

Figure 3.1. Distillation of CBS44 at 100 and 20 torr.

The distilled volume in the figures are accumulated. In total 69 vol.% of the initial CBS44 feed is distilled off in the distillation column. Without considering the cold trap, the first drop is collected at a vapour AET of 86°C and the last at 378°C. It is believed that an AET of 400°C was achievable, but due to time restrictions in the laboratory, the distillation had to be terminated, and distillation reflux could not be initiated the following day.

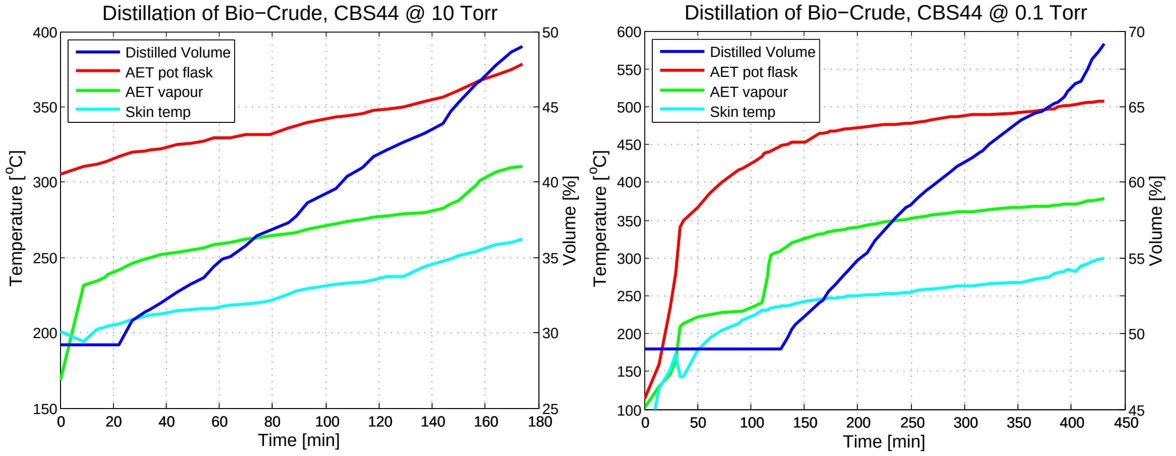

Figure 3.2. Distillation of CBS44 at 10 and 0.1 torr.

The distillation set-up used in present study has been installed and modified to follow the ASTM2892 standard. The distillation data given in the figures above indicate rather smooth distillations, and it can be concluded that experience has been gained to an extent that gives a satisfactory outcome.

3.3 Distillation Profile of CBS44

The distillation profile is the main analytical result of fractional distillation. The distillation profile represents the distilled mass or volume as a function of TBP. In Figure 3.3 the distillation profile of CBS44 is given on both a mass and volume basis. While the volume curve can be noted continuously, the mass basis profile is less resolved, because it is impossible to weigh the collector flasks during distillation with the current set-up. The boiling temperature limits of gasoline, jet fuel, diesel and fuel oil is furthermore illustrated in the figure. These limits vary depending on how a particular refinery chooses to blend the fuel to match fuel specifications (Gary et al., 2007), but are here based on *de Klerk (2011)* and *ACEA et al. (2013)*.

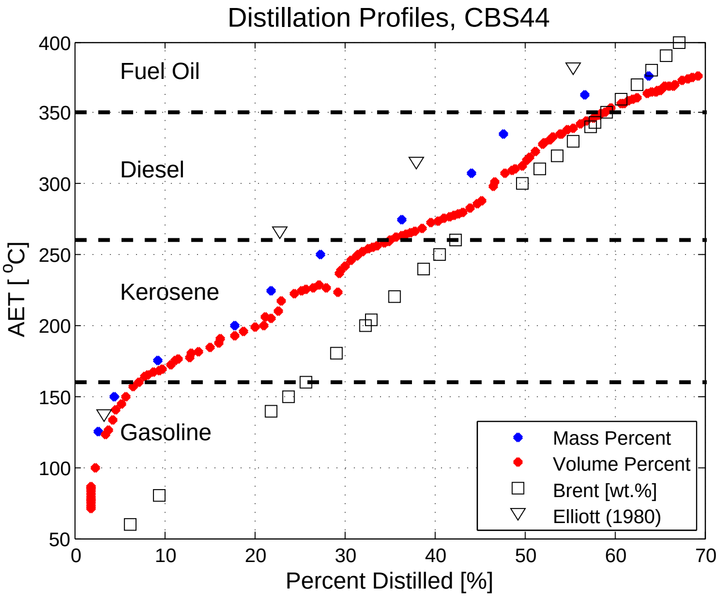

Figure 3.3. Distillation profile of CBS44 on a mass and volume basis along with the distillation profile of Brent crude oil (TOTSA, 2006) and data from *Elliott (1980)*.

At 27 % distilled the AET drops a little, while the total distilled volume increases. This corresponds to the small drop in temperature that is seen in Figure 3.1 to the right where the vapour temperature drops slightly before terminating the distillation at 20 torr.

The CBS44 distillation profiles are compared to a distillation profile of the benchmark brent petroleum crude oil (TOTSA, 2006) and distillation data of wood based HTL oil from *Elliott (1980)*. Note, that it is unknown whether *Elliott (1980)* is volume or mass percent. The comparison shows similarities between present distillation and *Elliott (1980)*. Both HTL bio-crudes have a relatively small gasoline fraction, but in general the CBS44 bio-crudes contain more LSR than the bio-crude produced by *Elliott (1980)*. This may relate to the fact that CBS44 is based on a feedstock containing diesel. However, *Elliott (1980)* also used a coal tar distillate as recycle oil in the feedstock. The HTL oils contain less gasoline equivalent compared to the Brent crude distillation profile, but the amount of residue actually seems to be lower for the CBS44 bio-crude. This is a very interesting result that needs to be documented for steady state HTL bio-crudes, because the amount of residue is an oil quality criteria.

The distillation profile reveals that the gasoline fraction of CBS44 is minor and around 6 wt.%, whereas the kerosene and diesel fractions are rather large and around 25 and 22 wt.% respectively. This is very likely related to the CBS44 feedstock containing diesel. But the fact that the kerosene fraction is larger than the diesel fraction may indicate that some diesel is decomposed during the HTL process. Also, it is interesting that the amount of residue from CBS44 is less than 30 wt.%, which is similar to that of various crude oils. Residue is referred to as the low value 'bottom of the barrel', since it requires much more processing than the LSR fractions boiling below 400°C. *BP (2014)* has published the composition of a number of different crude oils. Here the amount of residue (TBP>342°C) is between 15 and 65 wt.% (BP, 2014). As a result, the amount of residue in CBS44 is not a barrier when evaluating co-processing at a conventional refinery. Furthermore, when comparing the HTL bio-crude in present study to heavy Canadian or Venezuelean bitumen crudes that are widely used, the amount of residue is relatively small (de Klerk, 2013).

In Figure 3.4 distillates from CBS24, CBS44 and CBS48 are compared to distillates from the above mentioned BP petroleum crudes. The comparison is made with respect to the distribution of short chain hydrocarbons (C_1 to C_4), naphta, kerosene and diesel. In this comparison the boiling point ranges for the fractions are defined different than in Figure 3.3. This is due to *BP (2014)* defining the fractions differently. The compositional distribution for CBS44 and CBS48 is based on the TBP distillation profiles given in Figure 3.3 and 3.6 respectively. CBS24 is based on a simulated distillation profile provided by *CBS (2014)*.

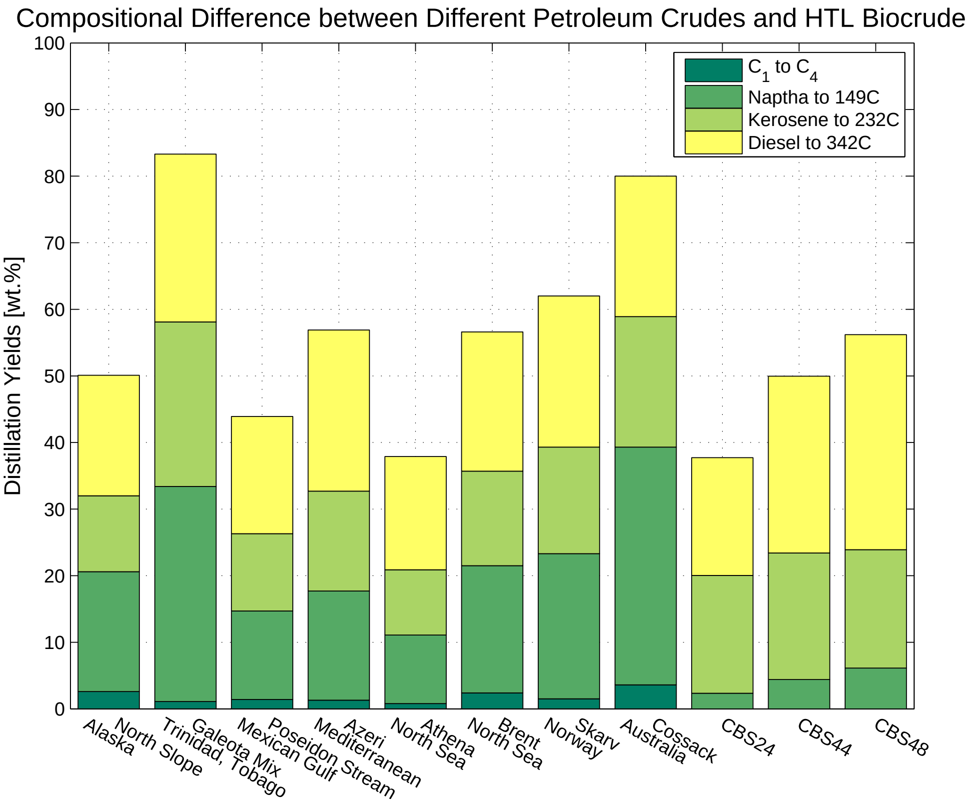

Figure 3.4. Compositional distribution of short chain hydrocarbons, naptha, kerosene and diesel. BP data are compared with CBS oils. (BP, 2014)

Short chain hydrocarbons (C_1 to C_4) are not present in the CBS oils since the oils are collected at a temperature of 40 to 60°C. In Figure 3.4 it can be seen that these are present in small amounts in the petroleum crude distillates. Furthermore, also the naptha fraction is significantly smaller in the bio-crudes. The kerosene fraction of the bio-crudes are within the range of the petroleum crudes. Finally the diesel fraction of the bio-crudes is slightly higher than for petroleum crudes, which is most likely related to the amount of recycled diesel present in CBS44 and CBS48. Remark, how the diesel fraction is smaller and the amount of residue greater for CBS24. This makes sense considering the feedstock composition, where CBS24 is produced from a feedstock with recycled HTL oil only and no diesel. Though, the feedstock composition is not believed to be the only reason. The difference is also very likely because of oil degradation during storage, since this oil is approximately one year older than CBS44 and CBS48 (CBS, 2014). And finally, hydrothermal liquefaction is believed to produce an oil with a relatively large kerosene and diesel fraction.

The size of the different fractions is highly relevant when optimising the HTL feedstock, since LSR fractions as mentioned are more valuable than residue fractions. In relation to co-processing at a particular refinery, the bio-crude distillation profile is also relevant, since a particular refinery typically is designed for a particular type of crude that e.g. has a major diesel fraction. In other words, the refineries processing the BP crude oils given in Figure 3.4, will be designed differently due to the difference in crude oil composition.

3.3.1 Verification of TBP Distillation through TGA

Thermogravimetric Analysis (TGA) is a technique to monitor the change in mass of a substance as it is subjected to a controlled temperature program and atmosphere (PerkinElmer, 2010). *Li et al. (2001)* have used TGA to obtain simulated distillation curves of coal tar. They found that when using a special shaped pan the results are in agreement with the true distillation curve. The special pan has a narrow neck that corresponds to simple distillation, where some vapours will condense as they try to leave the pan. This increases the accuracy of the simulated distillation. In present study the shape of the crucible used in the TGA analysis does not allow the vapours to condensate and accuracy is decreased. The TGA results and the TBP curve are not expected to be identical, but the use of TGA to verify fractional distillation has been proposed.

During TGA the sample is simply heated, while monitoring the change in mass as the temperature increases and mass evaporates. To avoid combustion in the chamber it is purged with nitrogen. The simulated distillation performed by *Li et al. (2001)* is carried out from an initial temperature of 100°C to 600°C with a heating rate of 10°C/min. In present study the temperature ranges from 50 to 960°C. Three different heating rates are tested in order to obtain reliable results. Heating rates of 5, 10 and 20°C/min are tested. The TBP distillation profile given in Figure 3.3 is compared to the TGA simulated distillation curves in Figure 3.5.

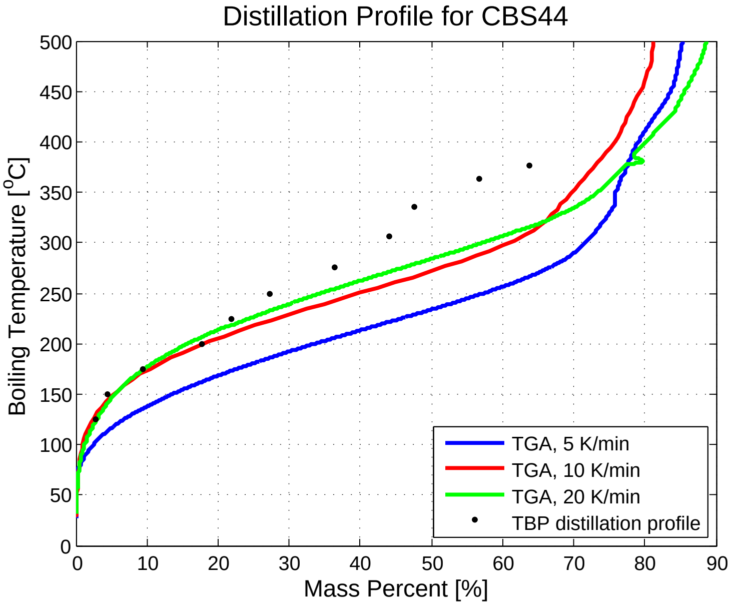

Figure 3.5. TBP distillation profile of CBS44 compared with simulated distillation profiles through TGA at different heating rates.

The heating rate of 5°C/min deviates from both the heating rates of 10 and 20°C/min and the TBP distillation curve. It can be seen that mass is evaporated too fast at a low heating rate compared to the TBP distillation curve. At boiling temperatures below 250°C, the simulated curves at heating rates of 10 and 20°C/min are similar to the TBP distillation curve. Above this boiling temperature the simulated curves indicate that more mass is evaporated compared to the TBP curve. The deviation occurs at temperatures above 250°C and it might be related to cracking of the sample. If cracking occurs longer carbon chains might be degraded to lower boiling point compounds that will evaporate and increase the mass percent compared to the TBP distillation curve.

Based on the TGA measurements it is concluded that the results below 250°C are reliable since the TGA and TBP distillation curves are alike. Though TGA is not considered an efficient tool for distillation validation.

To further verify the fractional distillation, the HTL bio-crude CBS48 has been distilled twice in order to show repeatability. A simulated distillation curve using TGA is furthermore compared to the TBP distillations. The results are given in Figure 3.6. It might seem strange that CBS48 and not CBS44 is used in this verification. However, as explained the CBS test campaign uses recycled oil in subsequent runs and thus no CBS44 was left for verification purposes. The deviation between the TBP distillation and the TGA simulated distillation is similar to the one in Figure 3.5 and is expected to be due to ineffecient separation and cracking as previously described.

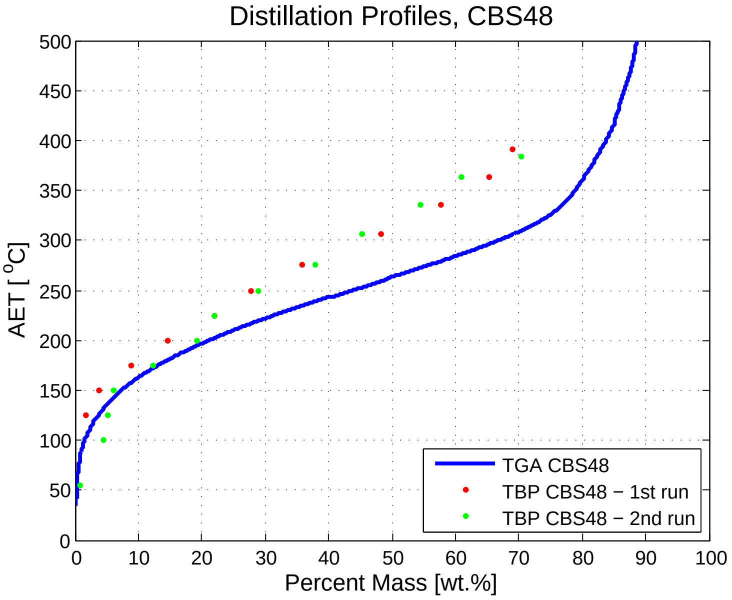

Figure 3.6. TBP distillations and TGA measurement of CBS48 to show repeatability.

Running the fractional distillation is a complex task and many parameters may affect the process. The heating mantle, the heating jacket and the vacuum pump must be controlled, data regarding temperatures, pressures and volumes must be collected and the reflux estimated and controlled. Despite these parameters that may affect the distillation accuracy Figure 3.6 shows similar TBP distillation curves for the first and second run. This is a very satisfactory result that further supports the validity and repeatability of the distillations done in present study.

3.4 Analysis of the Bio-Fractions

Characteristics of the feed and the fractions from distillation of CBS44 are given in a complete assay in Table 3.2. Information regarding TBP, distilled mass and volume, estimated density and HHV is given for the feed, the collected fractions, the cold traps and the residue. Furthermore, the yield and the accumulated yield of the distillation is given on a volume basis. A picture of the feed, the cold trap, the fractions and the residue is shown in the bottom of Table 3.2. The order of the flasks in the picture corresponds to the order in the table with the feed to the far left and the residue to the far right. The structure of Table 3.2 is based on that of a Hempel Assay and is considered a major result of the present study. The cold traps include the distillate collected in the cold trap at all operating pressures and it is treated as one light fraction boiling below 100°C. The content of the cold traps has a strong smell and caution is taken. Analyses of the cold trap is limited to heating value and FT-IR.

From Table 3.2 it is seen that the initial mass is 1039.0 g and the sum of the fractions, the cold trap and the residue is 1029.7 g which gives a recovery of 99.1 wt.%. Thus 0.9 wt.% is lost in the distillation. The majority of the loss is probably due to hold-up, but the exact amount is not determined. Hold-up is the mass trapped in the distillation column after the distillation is terminated and cooled. The remaining distillation loss that is not due to hold-up can be explained with light components that are not condensed in the cold trap. *ASTM D2892 (2005)* limits the distillation loss to maximum 0.4 wt.% excluding hold-up, and the distillation should be discarded if the loss is greater. Though, this limit cannot be exactly determined without measuring the hold-up. This is however neglected and subject for further improvements in the distillation procedure, since a loss of 0.9 wt.% is considered more than satisfactory for the present investigation. In Table 3.2 the volume of the distillation loss is determined by assuming a density equal to that of the feed.

The exact volume of the residue in unknown. The residue has a high viscosity at room temperature, which makes it difficult to pour the residue into a pitcher where the volume can be determined without loosing mass. Furthermore, approximately 47 g of boiling stones are added to the sample. Removing the boiling stones will result in a further mass loss. However, the volume of the residue can be estimated by difference.

Fractional Distillation Results, CBS44

	TBP AET [°C]	Mass [g]	Volume [ml]	Yield [vol.%]	Accumulated Yield [vol.%]	Estimated Density [g/ml]	HHV [kJ/g]
CBS44		1039.0	1120			0.93	41.19
Cold trap^A		12.4	20	1.8	1.8	0.62	42.20
Fraction 1	100-125	15.9	22	2.0	3.8	0.72	39.53
Fraction 2	125-150	17.5	22	2.0	5.7	0.80	42.36
Fraction 3	150-175	51.2	64	5.7	11.4	0.80	44.09
Fraction 4	175-200	87.6	105	9.4	20.8	0.83	43.92
Fraction 5	200-225	42.9	50	4.5	25.3	0.86	43.67
Fraction 6	225-250	55.9	64	5.7	31.0	0.87	43.39
Fraction 7	250-275	93.7	106	9.5	40.5	0.88	42.85
Fraction 8	275-307	81.5	91	8.1	48.6	0.90	42.33
Fraction 9	307-335	36.9	43	3.8	52.4	0.86	42.86
Fraction 10	335-363	94.1	104	9.3	61.7	0.91	43.12
Fraction 11	363-391	73.1	81	7.2	68.9	0.91	42.55
Residue	391-	367.0	338^B	30.2	99.1	1.09	38.71
Σ Sum		1029.7	772	99.1			
Distillation Loss		9.3 (0.9 %)	10^C	0.9			

^{A} Corrected for water content
^{B} Calculated by difference
^{C} Based on density of feed, CBS44

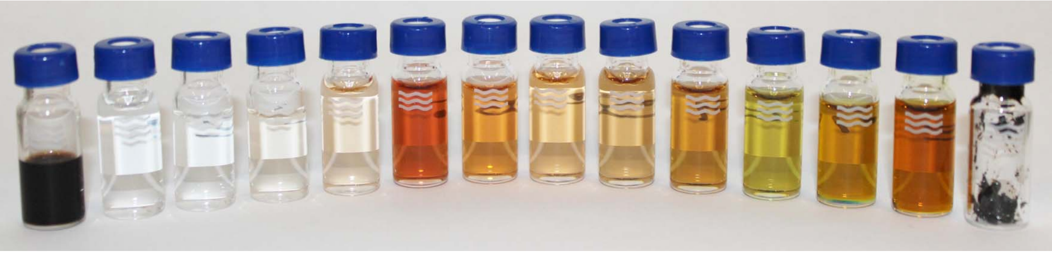

Table 3.2. Fractional distillation assay of CBS44. The fractions are depicted in the bottom with CBS44, cold trap, fraction 1-11 and residue from the left.

Based on the cut temperatures given in Figure 3.3 fractions 1, 2 and partly 3 are classified as gasoline and 3, 4, 5, 6 and partly 7 are kerosene. Fractions 7, 8, 9 and partly 10 covers the diesel range, whereas the remaining two fractions 10 and 11 are in the fuel oil boiling range.

3.4.1 Density

The density in Table 3.2 is estimated from the mass and volume at room temperature. From the table it is seen that the density increases with increasing boiling point, which matches expectations. Fraction 9 has a lower density than fractions 6, 7 and 8, which is unexpected. Fraction 9 is relatively small and an inaccurate volume reading may affect the estimation of the density.

In general the densities of the bio-fractions are heavier than those of petroleum crude boiling in the same range. This is visualised by Figure 3.7, where the densities of the different fractions of CBS44 and CBS48 are compared to the corresponding fractions of two crude oils from *Gary et al. (2007)*. Please note that the bio-fraction densities are estimated with low accuracy at room temperature and thus should only be used as guidance. In comparison, the densities from *Gary et al. (2007)* are given at 15°C. Note in the legend how the bulk density of the bio-crudes are also heavier than the petroleum crudes. Especially, the residue fractions of the bio-oils are heavier than the residue of petroleum crude. The oxygen content of the bio-fractions is expected to be the reason for a higher density in general.

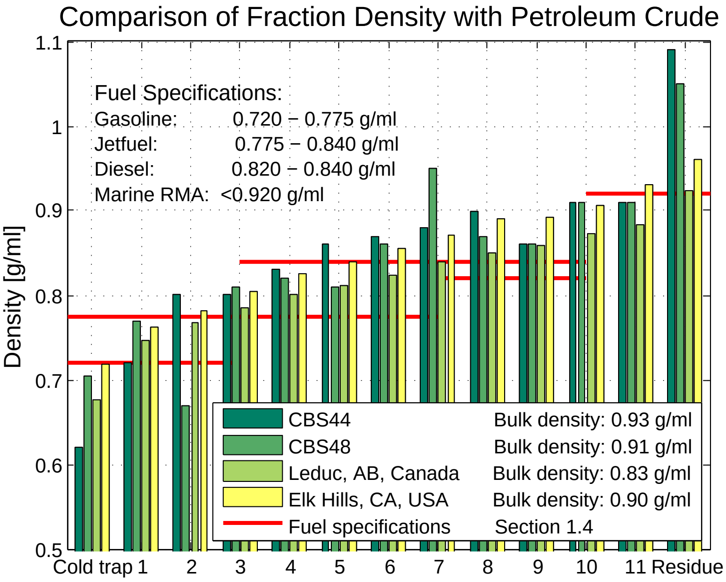

Figure 3.7. Comparison of fraction densities used as guidance. The density of bio-crudes is estimated with low accuracy, whereas the petroleum crudes are from *Gary et al. (2007)*. Fuel specifications are from Section 1.4.

Fuel specifications regarding density are also given with red lines for the respective boiling fractions in Figure 3.7. This depicts, how the bio-fractions are within or just above the fuel specifications. Hydrotreating of the kerosene and diesel fractions to remove oxygenates and saturate double bonds is most likely sufficient to fulfil the density specification. However, co-processing is the main objective, and based on Figure 3.7, the densities will definitely not become a barrier for co-processing.

3.4.2 Higher Heating Value

The higher heating value is determined using a bomb calorimeter. The HHV is tested twice for each compound, and in all cases consistent data were obtained. The average value of the two measurements is given in Table 3.2. During the measurements it was observed that the ash content of the sample crucible decreased as the higher boiling point fractions were tested. Figure 3.8 shows the crucible after measuring the HHV of the feed, fraction 4, 11 and the residue. The lower boiling point fractions leave a large amount of ash compared to the higher boiling point fractions. Note, how the feed (CBS44) is the sample that leaves the least ash content. The reason for this is unknown.

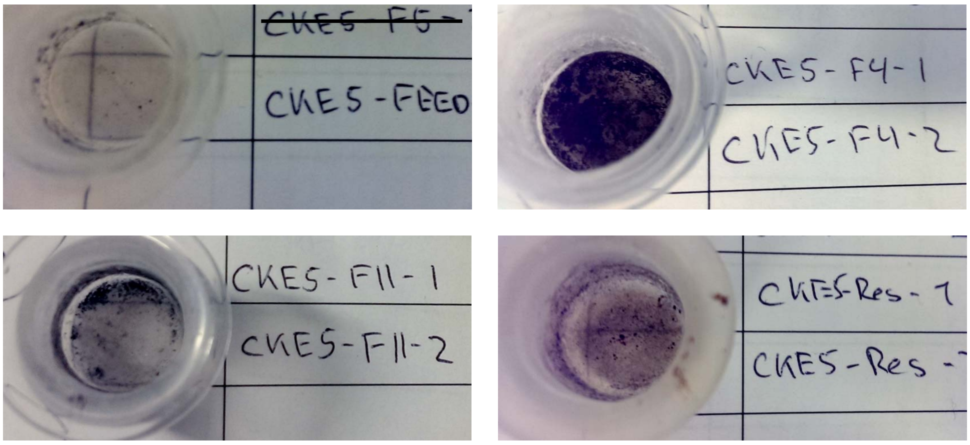

Figure 3.8. The crucible with ash content after measuring the HHV of fraction 4, 11, CBS44 and the residue.

The HHV of fraction 1 (100-125°C) is low when comparing to the higher boiling point fractions. As will be documented with FT-IR spectroscopy in Section 3.4.4 this fraction contains alcohols that generally have a lower heating value than the corresponding hydrocarbon. In general the HHV of the bio-crude fractions is slightly lower than for conventional petroleum crude. To enable comparison Table 3.3 lists the HHV of petroleum crude oil, CBS44, corn stover pyrolysis oil, wood based HTL oil and the HHV of their equivalent gasoline and diesel fractions. No fraction boiling in the diesel range was distilled by *Capunitan and Capareda (2013)*, so the 180-250°C is used for comparison. It is clear how the pyrolysis oil and the wood based HTL oil and their fractions are significantly lower, whereas the CBS44 and its fractions are slightly lower than the conventional crude oil and the respective gasoline and diesel equivalent.

Crude Equivalent		**Gasoline Equivalent**		**Diesel Equivalent**	
Compound	**HHV [kJ/g]**				
Crude oil	45.5^{A}	Conventional gasoline	46.5^{A}	Low sulphur diesel	45.6^{A}
CBS44	41.2	CBS44 fraction 1-3	42.9^{B}	CBS44 fraction 7-10	42.8^{B}
Corn stover PO	35.4^{C}	Fraction (100-180°C)	37.3^{C}	Fraction (180-250°C)	37.0^{C}
Wood based HTL oil	36.8^{D}	Fraction (Up to 138°C)	37.2	Fraction (266-382°C)	35.9
NA		Bio-ethanol	29.8^{A}	FAME	40.2^{A}

A: (Boundy et al., 2011) B: Weighted average C: (Capunitan and Capareda, 2013)
D: (Elliott, 1980)

Table 3.3. Comparison of HHV of different crudes and the equivalent gasoline and diesel fractions.

In Table 3.3 the HHV of bio-ethanol and FAME are also given for comparison with the HTL bio-fractions. As documented, these biofuels are presently used to a great extend worldwide, but with limitations on drop-in ability and mileage. Considering the HHV only, the HTL bio-crude shows potential as a sustainable fuel providing a longer mileage than bio-ethanol and FAME. Furthermore, an ulimited drop-in ability is believed to be achievable by deoxygenation prior to co-processing.

In Chapter 4 upgrading of the bio-crude with respect to deoxygenation is investigated and the change in heating value will be examined. It is expected that the deoxygenation will increase the HHV and thus approach those of petroleum crudes. But first it is crucial to investigate in what fractions of the HTL bio-crude the oxygen is trapped.

3.4.3 Elemental Analysis

Elemental analysis of CBS44 and the distilled fractions have been done externally at the Institute of Chemistry at Aarhus University. The elemental distribution in the different fractions are given in Table 3.4 along with H/C and O/C molar ratios. Apart from the residue fraction, the H/C molar ratios are generally quite high, indicating a parafinnic nature of the distillates. A H/C ratio of 1.38 for the residue indicates the presence of aromatic structures. Note how the H/C molar ratio is decreasing with the increasing boiling point of the fractions. This is partly due to the fact that the carbon number increases with boiling point, minimising the influence of the terminal hydrogens on a linear alkane. Though, it is also expected that the amount of cyclic and aromatic structures increase with boiling point, which then matches a decreasing H/C ratio.

Elemental Analysis of CBS44 and Fractions

	C [wt.%]	H [wt.%]	N [wt.%]	S^A [wt.%]	O^C [wt.%]	H/C ratio	O/C ratio
CBS44, orig.	82.00	11.74	0.44	0.03	5.59	1.71	0.053
CBS44	84.09	11.86	0.42	0.02	3.60	1.68	0.032
Fraction 1	74.47	12.05	0.49	0.14	12.86	1.93	0.130
Fraction 2	80.76	12.60	0.37^B	0.16	6.11	1.86	0.057
Fraction 3	84.25	13.13	0.19^B	0.08	2.36	1.86	0.021
Fraction 4	84.68	12.84	0.13^B	0.11	2.24	1.81	0.020
Fraction 5	84.46	12.60	0.13^B	0.19	2.62	1.78	0.023
Fraction 6	84.55	12.42	0.09^B	0.28	2.66	1.75	0.024
Fraction 7	83.85	12.68	0.24^B	0.46	2.78	1.80	0.025
Fraction 8	82.71	12.48	0.63	0.02	4.16	1.80	0.038
Fraction 9	83.99	12.64	0.48	0.02	2.87	1.79	0.026
Fraction 10	85.05	12.39	0.35	0.01	2.20	1.74	0.019
Fraction 11	84.87	11.89	0.32	0.01	2.91	1.67	0.026
Residue	83.07	9.60	0.38	0.02	6.93	1.38	0.063

^{A} S below calibration level ^{B} N below calibration level ^{C} By difference

Table 3.4. Elemental analysis of CBS44, orig. (before dehydration), CBS44 and the distilled fractions.

It is characteristic for petroleum crude oils that heteroatom content is a function of TBP. This was previously documented with Figure 2.1. Whether this is also true for HTL bio-crudes is very relevant in order to evaluate the potential for co-processing bio-crude at a petroleum refinery. Figure 3.9 presents the heteroatom distribution of the table above as function of TBP. Note that the sulphur content is below the calibration level for the elemental analysis instrument, and the oxygen is calculated by difference.

Oxygen Distribution

Figure 3.9 reveals a higher concentration of oxygenates in the distillates boiling below 150°C. Especially fraction 1 has a high oxygen content of 12.86 wt.%, which explains the lower HHV of this fraction. Likewise, the residue contains a significant amount with 6.93 wt.% oxygen. The remaining fractions have a relatively constant oxygen content around 2-4 wt.% as clear from Figure 3.9.

Elemental analysis of wood based HTL oil by *Elliott (1980)* also reveals oxygen in all fractions. Opposite CBS44, the lowest oxygen content is found in the first fraction (9.7 wt.%) and the residue fraction (10.4 wt.%). Fractions 2-5 (138-382°C) contain somewhat steady oxygen contents of 12.1-13.4 wt.%. The bulk HTL crude excluding water contains 11.1 wt.% O. In general the oxygen content is higher and it has a different distribution trend in the HTL oil produced by *Elliott (1980)* compared to CBS44. In general, the oxygen content of CBS44 is relatively low compared to pyrolysis and vegetable bio-crudes (Ott et al., 2008), (Capunitan and Capareda, 2013), (Zheng and Wei, 2011).

The distribution of oxygen as function of TBP in petroleum crudes is unknown, but it is generally present in concentrations around 0.05-1.5 wt.% (de Klerk, 2011). For comparison, CBS44 contains 3.60 wt.% and above 10 wt.% in specific fractions. As a conclusion, deoxygenation is needed to enable co-processing.

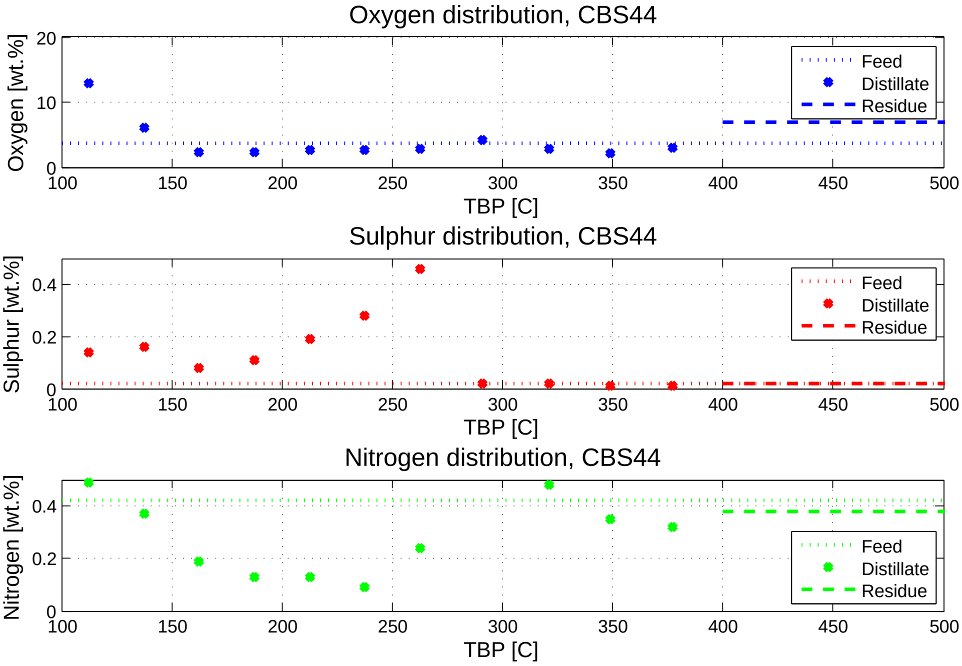

Figure 3.9. Heteroatom (O, S and N) distribution as function of TBP for CBS44.

Sulphur and Nitrogen Distribution

The sulphur and nitrogen concentrations in CBS44 do not seem to be highest in the residue fraction as expected. Figure 3.9 illustrates how the sulphur concentration is actually highest in the kerosene and light diesel boiling range. This is similar to the sulphur distribution in pyrolysis oil from swine manure. *Ott et al. (2008)* states that the sulphur is located in LSR fractions, and almost completely absent above an AET of 386°C.

Nitrogen is mostly found in fractions boiling above 250°C for petroleum crude oil (de Klerk, 2011). In the CBS44 crude oil, nitrogen seems to be distributed rather evenly, but with the least nitrogen in the kerosene fraction. In this boiling range the nitrogen content is below 0.2 wt.%, whereas it is around 0.4 wt.% for the remaining fractions.

Petroleum crude oils may contain up to 2 wt.% nitrogen, but mostly below 0.5 wt.% (de Klerk, 2011). With respect to sulphur, crude oils mostly contain between 0.5 and 5 wt.% (de Klerk, 2011). For comparison the CBS44 crude contains 0.42 and 0.02 wt.% N and S respectively. Based on this comparison, the CBS44 HTL bio-crude can be concluded to be low on sulphur and average on nitrogen content compared to petroleum crude oils. Thus, the nitrogen and sulphur concentrations are not considered too high to enable co-processing.

The distribution of N and S heteroatoms is however different from petroleum crudes, which may constitute an issue in relation to co-processing. To give an example, the bio-crude gasoline fractions, containing around 0.4 wt.% nitrogen, may not be forwarded to gasoline reforming units in a conventional refinery without the risk of catalyst poisoning. Thus, it will be interesting to evaluate if a mild deoxygenation step also will remove N and S heteroatoms located in the low boiling fractions. Likewise, the distribution of nitrogen and sulphur is different in the residue fraction of CBS44 compared to petroleum crude oil. A relatively low concentration of N (0.38 wt.%) in the bio-residue enables catalytic upgrading, which increases the range of processes that the bio-residue is compatible with. FCC is for instance a catalytic residue upgrading process widely used for gasoline production. Usual FCC catalysts are sensitive to nitrogen, but since the bio-residue has a low concentration of nitrogen the bio-residue is a suitable feed for an FCC unit. Thereby, the relatively low LSR gasoline fraction of bio-crude can be supplemented by a residue upgrading process producing mostly gasoline products. This is an advantage of the bio-crude compared to petroleum crude.

Elemental analysis of the CBS44 crude and corresponding fractions reveals the need for a deoxygenation step prior to potential co-processing. The severity of such a deoxygenation step depends on how the different oxygenates are bounded to the bio-crude. FT-IR enables analysis of major functional groups in the bio-crude including oxygenates.

3.4.4 FT-IR Spectroscopy

Infrared spectroscopy is a relatively cheap method to analyse what functional groups are dominant in a sample. In this respect it is interesting to analyse the bio-crude for aromatic, olefinic and parafinnic content. Likewise, in relation to upgrading it is very interesting to analyse how the oxygen is bounded in the oil. In particular, how the oxygenates vary in the different fractions of the distilled bio-crude.

Infrared light is absorbed by organic compounds and consequently vibrations of the molecules increase. Different bonds and thus functional groups absorb the infrared light at different wavelengths. By interpreting the absorption spectra obtained from FT-IR, the types of functional groups present in moderate concentrations can be identified. The absorptions vary not only in wavelength, but also shape and intensity. For instance, if an amine functional group is present, the FT-IR spectra will show two or three distinct peaks at a wavenumber ($\widetilde{v} = \frac{1}{\lambda}$) of 3450-3400 cm^{-1} with medium to weak intensity. Intensity refers to percentage absorption between 0 and 100 % of the infrared light. Equation 3.1 defines, how absorption wavenumber is related to bond strength and atom masses. (Wade, 2013) (Wan, 2013)

$$\widetilde{v} \propto \sqrt{\frac{k}{\mu}} \qquad [cm^{-1}] \tag{3.1}$$

k is a force constant related to bond stiffness, and μ is related to the molar masses of the bonded atoms. Based on Equation (3.1) it is clear why the absorption wavenumber of a double bond is higher than that of a single bond. Likewise, how a C-O bond absorbs at lower wavenumbers than a C-H bond, because O is a heavier atom than H. Figure 3.10 shows how the absorption wavenumber vary with the different bonds. Even though N is heavier than O it can be seen that the absorption wavenumber is higher for the N-H bond compared to the O-H bond. This is due to the bond stiffness of the N-H and O-H bonds. Figure 3.10 has transmittance as the secondary axis, which is just the opposite of absorbance. The infrared light that is not absorbed is transmitted and detected by the IR instrument. That is why no absorbance corresponds to 100 % transmittance. (Wade, 2013)

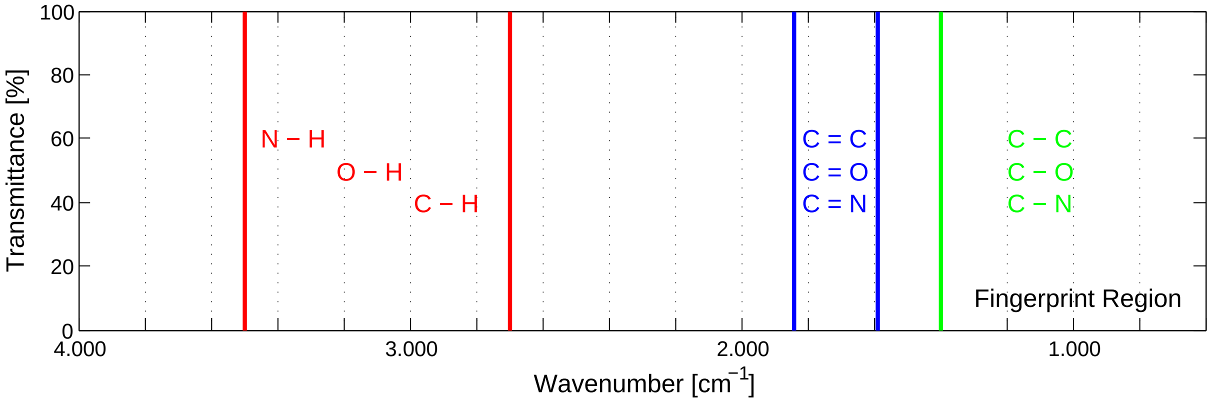

Figure 3.10. The absorption wavenumber variation for different bonds. (Wade, 2013)

Continuing the amine functional group example, the concentration of a group must be at a certain level for it to appear in the absorption spectra. Consequently, S and N containing functional groups will not appear in the FT-IR spectra presented in the following, since the concentration of S and N are well below 1 wt.% for the bio-crudes analysed in present study. FT-IR becomes particularly useful when the bio-crude is separated by fractional distillation. FT-IR of the crude may indicate different functional groups, but if present in relatively low concentrations a particular absorption peak is likely to hide in the noise of the spectra. Distinct peaks are more probable in FT-IR spectra of fractions separated by boiling point, since the variety of different functional groups in a certain boiling range is expected to be narrower than that of the bio-crude. Table 3.5 lists the characteristics and absorption maxima of the functional groups expected visual in the absorption spectra of the bio-crude fractions. Interpretation of the different spectra will mainly be based on this table. Also, it should be noted that the spectra are normalised in order to compare absorption, which will not define, but indicate differences in concentration. In the end of this section a table summarises the expected hydrocarbon structure and functional groups of the feed, the fractions and the residue. Furthermore, the results of the IR spectra of CBS44 are compared to literature.

IR Correlation Chart

Functional Group	Bond	Absorption maxima [cm^{-1}]	Characteristics
Alkane	C-H	2850 - 2960	strong, sharp
Alkane	C-C	1450	medium, sharp, CH_2 scissoring
Alkene	C=C	1620 - 1680	medium, sharp
Alkene/Aromatic	C-H	3010 - 3095	medium, sharp
Aromatic	C=C	1450 - 1600	3 peaks, medium, sharp
Alcohol	O-H	3300 - 3600	strong, broad
Alcohol	C-O	1050 - 1150	strong
Ketone	C=O	1680 - 1750	medium-strong, sharp
Aldehyde	C=O	1630 - 1780	medium-strong, sharp
Aldehyde	C-H	2750 - 2850	2 weak peaks, W-shaped
Carboxylic acid	C=O	1710 - 1780	medium-strong, sharp
Carboxylic acid	O-H	2500 - 3000	medium-strong, very broad
Ester	C=O	1735 - 1750	medium-strong, sharp
Ester	C-O	1200 - 1300	weak-medium, sharp
Ether	C-O	1200 - 1300	weak-medium, sharp

Table 3.5. Characteristics of the different functional groups expected to be present in the HTL bio-crude in concentrations high enough, for them to be visual in the FT-IR spectra. (Wan, 2013), (Wade, 2013), (Nakanishi, 1962)

The table shows that for e.g. alkenes to be present as a functional group both C-H and C=C bonds must be identified with absorption maxima within the given ranges. For alkanes to be present it must be mentioned that additional peaks at 1375 and 720 cm^{-1} must be identified. These indicate bending vibrations of CH_3 and CH_2 groups and are not included in the table. (Wade, 2013)

FT-IR of CBS44

Figure 3.11 presents the FT-IR spectra of the CBS44 distillation feed. 3 medium-strong sharp C-H peaks around 2853-2955 cm^{-1} along with the C-C peak at 1452 cm^{-1} and absorptions at 1375 and 721 cm^{-1} indicate parafinnic hydrocarbons (See Table 3.5) as expected (Wade, 2013).

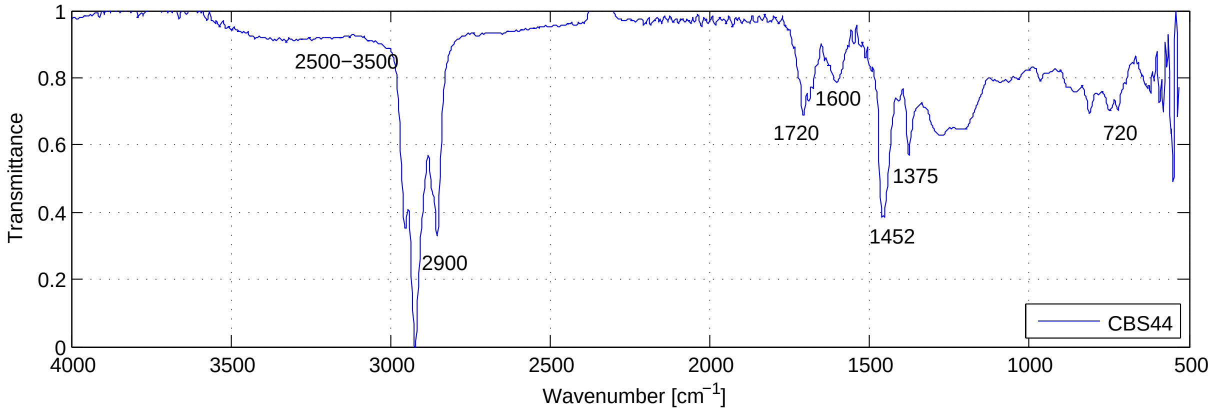

Figure 3.11. FT-IR spectra of the CBS44 feed.

Besides the clear sign of alkanes, the FT-IR of CBS44 indicates absorption at a variety of different wavenumbers, which is expected due to many different functional groups being present in the bio-crude. A weak peak around 1600 cm^{-1} indicates the presence of carbon double bonds, perhaps aromatics. A broad O-H peak is observed at wavenumbers between 2500 - 3500 cm^{-1} which indicates presence of carboxylic acids or alcohols. The O-H peak along with a carbonyl C=O peak at around 1720 cm^{-1} correspond to presence of carboxylic acid. But whether this C=O peak is also due to ketones, esters or aldehydes is hard to distinguish, but a variety of these is likely to be present. For alcohols to be present a C-O bond must be identified along with the O-H peak. If C-O bonds are present (alcohols, esters, ethers) a strong absorption is present around 1000 - 1300 cm^{-1}, but other bonds also absorb in this region (referred to as the fingerprint region) (Wade, 2013). Consequently, the absorption in this region in Figure 3.11 does not imply C-O bonds, but if no absorption is discovered in this region, absence of C-O bonds can be concluded. Though, all in all the FT-IR of the bio-crude is hard to interpret precisely, since it clearly contains a variety of different functional groups as expected.

FT-IR of CBS44, Fractions 1 and 2

Analysing the different fractions provides more knowledge of the present functional groups and how they, in particular the oxygenates, vary. FT-IR spectra of fractions 1 and 2 are compared to the CBS44 feed in Figure 3.12. It is clear how fewer and more distinct peaks are present for the fractions compared to the bio-crude. The IR spectra of fraction 1 shows peaks at 3400 and 1050 cm^{-1} which indicates presence of alcohols. This is accompanied by a lower heating value of this fraction. Alcohols are generally high octane compounds, and since fraction 1 is in the gasoline boiling range, removal of these may not be necessary. It may even decrease the value of this fraction as a potential gasoline blend.

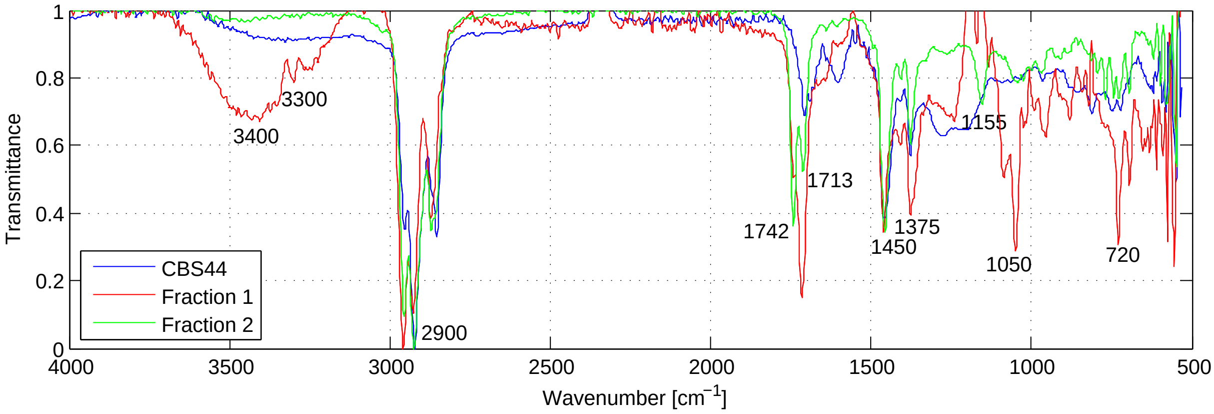

Figure 3.12. FT-IR spectra of the CBS44 feed, and fraction 1 and 2 from distillation.

In Figure 3.12 it is worth noting that fractions 1 and 2 show no sign of carboxylic acids as no broad peak at 2500 - 3000 cm^{-1} is identified. This despite the clear presence of carboxylic acids in the IR spectra of the CBS44 feed. Consequently, the carboxylic acids must sit elsewhere in higher boiling fractions. Fraction 1 has an interesting sharp, weak absorbance around 3300 cm^{-1}. This peak value does not appear in Table 3.5, but according to *Wade (2013)* it could be the C-H stretch of a terminal alkyne, but such would also be associated with a peak at 2250 cm^{-1}, which is not the case. It could also be due to an overtone, which is absorption at a double wavenumber. This would imply strong absorption around 1650 cm^{-1}, which is not the case either. Finally, it could indicate presence of an amine or amide group. This is surprising considering a nitrogen content of 0.49 wt.% in fraction 1. Figure 3.12 indicates with peaks around 2900, 1450, 1375 and 720 cm^{-1} that both fraction 1 and 2 contain mainly alkanes. Peaks in the range 690-800 cm^{-1} suggests the presence of substituted aromatics (Nakanishi, 1962), but the 1450-1600 range does not indicate significant absorption of aromatics. Though, note how there are two different distinct peaks in the carbonyl range for especially fraction 2. One with the absorption maxima at exactly 1713 cm^{-1}, and the other at 1742 cm^{-1}. The first one is typically an acyclic ketone, whereas the one at 1742 cm^{-1} indicates a ketone sitting on a 5-membered cyclic structure (Nakanishi, 1962). The indication of cyclic ketones is interesting in relation to the subsequent upgrading, since the severity of deoxygenation conditions depends on the structure of the oxygenates. This will be discussed further in Subsection 4.2. The medium peak around 1155 cm^{-1} of fraction 2 may be due to the presence of esters or ethers (Nakanishi, 1962).

FT-IR of Fractions 4, 5 and 6

FT-IR of fraction 3 is skipped, since the spectra is very similar to that of fraction 2. Figure 3.13 compares the FT-IR spectra of fraction 4, 5 and 6 with that of kerosene. These fractions are boiling in the jet-fuel range and thus it is interesting to compare with kerosene. Firstly, note how the IR spectra of kerosene is more distinct and less noisy than the IR spectra of the bio-crude fractions. This is due to the pure, and parafinnic nature of the kerosene. The IR spectra of the bio-crude fractions show all the characteristic peaks for alkanes at 2900, 1450, 1375 and 720 cm^{-1}. In comparison with kerosene, it is clear how some upgrading is required for the bio-fractions to have similar absorption.

Again the carbonyl absorption is significant for all bio-crude fractions indicating the presence of oxygenates. Fraction 4 has a strong absorption at 1705 cm^{-1}, indicating a carbonyl group sitting on a 7-membered ring or larger (Nakanishi, 1962). The peak at 1742 cm^{-1}, indicating a ketone sitting on a 5-membered ring is also present like for fraction 2. Fractions 5 and 6 have similar peaks. The 2 fractions have the strongest carbonyl absorption at 1688 cm^{-1} which is believed to indicate a ketone sitting on an aromatic ring (Nakanishi, 1962). In relation to the varying carbonyl absorptions, recall how the absorption wavenumber depends on the stiffness of the bond. An aromatic ring is resonance stabilised making the carbonyl C=O bond less stiff. In comparison, a 5- and 7-membered ring suffers from angle strain. A 5-membered ring is more strained than a 7-membered, which is why their absorption frequencies are higher (Wade, 2013).

The carbonyl absorptions of fractions 4-6 suggest the presence of ring structures. Absorptions in the range 1450 to 1600 cm^{-1} supports this statement. The IR spectra indicates alcohol and/or acid functionalities with the broad absorption above 3000 cm^{-1}. It is likely that alcohol groups and carboxylic acids exist in this boiling range, which requires removal in the upgrading. Finally, minor absorptions around 1260 and 1155 cm^{-1} should be noted. This could together with the carbonyl group indicate esters, but it is difficult to determine precisely.

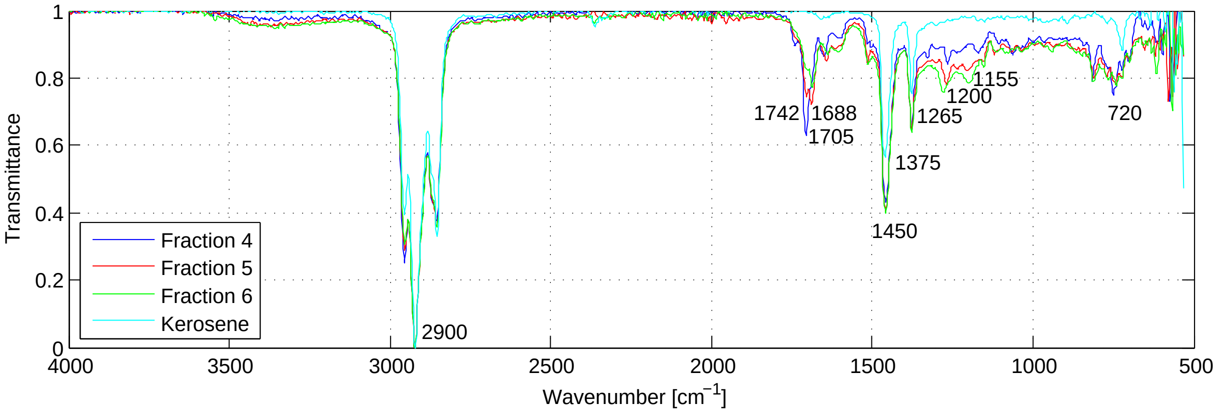

Figure 3.13. FT-IR of kerosene compared to fractions 4, 5 and 6 of the CBS44 distillation.

FT-IR of Diesel Fractions 7, 8, 9 and 10

Figure 3.14 presents the IR spectra of fraction 7, 8, 9 and 10 compared to that of a diesel sample, which has similar boiling points. The four fractions are presented together, because they have similar spectra. Diesel must be of parafinnic nature to ensure a high cetane number, which is apparent from the IR spectra of diesel. Spectra of the 4 fractions indicate presence of alkanes with peaks at 2900, 1450, 1375 and 720 cm^{-1}. Furthermore, absorptions at 1500 and 1600 cm^{-1} indicate some aromatic compounds. The identified peaks around 700-850 cm^{-1} suggest that the aromatic compounds are substituted aromatics (Nakanishi, 1962). Hydrogenation of these cyclic structures under upgrading would improve the quality of fractions 7-10, since they become similar to diesel.

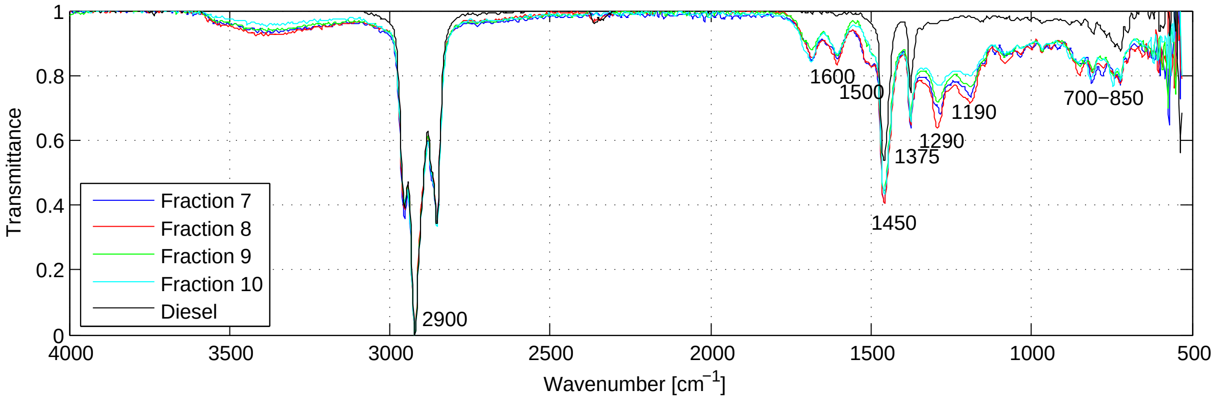

Figure 3.14. FT-IR of a diesel sample compared to fraction 7, 8, 9 and 10 of the CBS44 distillation.

The IR spectra for all four fractions also indicate C-O bonds with two distinct peaks at 1190 and 1285-1295 cm^{-1}. The minor O-H absorption above 3000 cm^{-1} could be related to a C-O absorption indicating the presence of alcohols (Nakanishi, 1962). However, the C-O peaks can also represent ethers or due to the presence of carbonyl bonds at 1688 cm^{-1} it may represent esters. In relation to the upgrading the structure of the oxygenates is important because it affects the conditions at which deoxygenation is efficient. However, in relation it is considered more important if the oxygenates are part of an aromatic ring or sitting on an alkane.

FT-IR of the Distillation Cold Trap and Residue

FT-IR of fraction 11 is neglected, since it is similar to fraction 10 and no new inputs can be inferred from it. Figure 3.15 presents the IR spectra of the cold trap fraction and the distillation residue. These fractions are not plotted in the same figure for comparison, but rather to avoid explanation of similar peaks twice.

It is clear that the cold trap fraction consists of mainly alkanes. Though, carbonyl groups are present, indicated by the absorption around 1720 cm^{-1}.

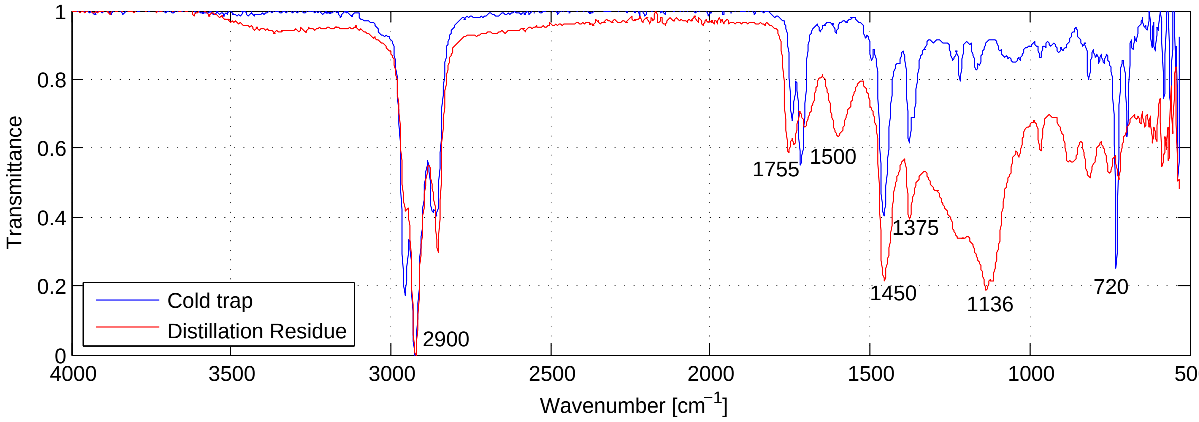

Figure 3.15. FT-IR of the cold trap fraction and the residue fraction from distillation of CBS44.

Based on a H/C ratio of 1.38, the residue fraction is expected to contain aromatics, and probably polycyclic aromatics (Furimsky, 2013). Thus it is rather surprising that only minor absorption is present just above 3000 cm^{-1}. However, there is a broad significant peak with absorption maxima at exactly 1600 cm^{-1} along with different peaks around 700-850 cm^{-1} indicating substituted aromatics. The clear C-H peaks around 2900, 1450 and 1375 cm^{-1} cannot be ignored, and they are probably related to substitutions on aromatic rings.

A strong broad peak at 1136 cm^{-1} indicates C-O bonding of some kind, which along with the carbonyl peak around 1755 cm^{-1} could indicate esters. Esters and ethers sitting in aromatic and polyaromatic compounds are difficult to hydrotreat. Such will probably require severe conditions, which is discussed in Section 4.2. Finally, it seems that the residue fraction contains carboxylic acids due to the broad O-H peak in the range from 2500 - 3500 cm^{-1} and the carbonyl peak at 1755 cm^{-1}. The presence of carboxylic acids have been less apparent in the lower boiling fractions. Thus the FT-IR spectra indicates that the acids present in the spectra of the bio-crude in Figure 3.11 is located in the residue fraction.

FT-IR analysis compared with literature

The results of the FT-IR analysis are compared to results of *Ott et al. (2008)* and *Capunitan and Capareda (2013)* who performed distillation of swine manure and corn stover pyrolysis oils respectively. Through analysis of the IR spectra *Ott et al. (2008)* found that the distillate contains water and aliphatic hydrocarbons. The presence of further compounds is not described. After examining the IR spectra of *Ott et al. (2008)* it is concluded that the spectra furthermore indicates presence of carbonyl groups, which matches the above discussion..

Capunitan and Capareda (2013) found that fraction B (100-180°C) and C (180-250°C) contain alkanes and substituted aromatics. Compared to present study alkanes are also expected present in the equivalent fractions. However, the presence of substituted aromatics is expected at higher boiling point fractions (250°C +) than indicated by *Capunitan and Capareda (2013)*. Carbonyl functional groups and C-O bonds in the 1000 - 1250 cm^{-1} range are identified in both fraction B and C of *Capunitan and Capareda (2013)*. The presence of carbonyl bonds matches the results of the IR spectra in present study.

Summary of the FT-IR analysis

The expected compounds of the fractions and the residue according to the IR spectra are summarised in Table 3.6.

Potential Composition of Bio-Fractions

Sample	Hydrocarbon structure	Functional Groups
Cold trap	Alkanes	Acyclic ketones
Fraction 1	Alkanes	Alcohols Acyclic ketones
Fractions 2 and 3	Alkanes	Acyclic ketones 5-membered cyclic ketones Esters/ethers
Fraction 4	Alkanes	Alcohols Esters/Ethers 7-membered cyclic ketones 5-membered cyclic ketones
Fractions 5 & 6	Alkanes	Alcohols Esters/Ethers Aromatic ketones
Fractions 7, 8, 9, 10 & 11	Alkanes Substituted aromatics	Esters/Ethers Carbonyl groups
Residue	Substituted aromatics	Esters/Ethers Carboxylic acids Carbonyl groups

Table 3.6. Summary of the expected distribution of hydrocarbons and potential functional groups according to FT-IR spectra.

3.4.5 Observations Regarding Miscibility

Petroleum crude oil hydrocarbons are almost entirely unpolar, due to the minor content of oxygen, sulphur and nitrogen. This is different from HTL bio-crude as shown with the FT-IR spectra, since the functional groups containing oxygen affects the polarity of the bio-hydrocarbons. Miscibility issues of the bio-crude distillate is proved by the two fractions depicted in Figure 3.16, where two and numerous layers are visible in the left and right picture respectively. Figure 3.16 also depicts how slight immiscibility is visual in the condenser during distillation. This is interesting and could be due to different functional groups being present in the different layers of the same boiling fraction. Once most of the functional groups are removed by the upgrading step, this miscibility issue is expected to be resolved. However, what is more important is, whether or not this phenomenon affects the separation efficiency of the distillation?

Recall, how dehydration of the oil sample subject to distillation is required, since steam distillation will occur if water is present (ASTM D2892, 2005). Steam distillation is actually suppression of the boiling point of two or more compounds, when present in an immiscible mixture. In theory the same phenomenon might happen during distillation of bio-crude due to the polarity of the mixture. This is most likely also the case for pyrolysis oils, due to larger amount of oxygenates and strongly polar carboxylic acids. Though, it is not discussed in neither *Elliott (1980)*, *(Capunitan and Capareda, 2013)*, *(Ott et al., 2008)* nor *(Zheng and Wei, 2011)*. The influence of bio-crude polarity on the distillation efficiency is unknown, but expected to be less significant than the influence of water. This is because water and bio-oil is completely immiscible at the distillation conditions, whereas the bio-fractions are only slightly immiscible. However, it is subject for further work to investigate if distillation efficiency is reduced due to slight miscibility issues for polar bio-crudes.

Figure 3.16. Layers are visible in the distillation flasks (left and right), and miscibility issues are visible on the condenser walls (center).

3.4.6 Colour Change

Stability issues have been observed through colour change during storage of the distillation products. Figure 3.17 illustrates the colour change that is observed in only 3 days of storage. The samples are ordered from left to right as CBS44, cold trap, fraction 1-11 and the residue.

Figure 3.17. Colour change observed during 3 days of storage in contact with oxygen. Top: Before - Bottom: After.

The colour change is believed to be caused by degradation of the distillates when in contact with air or more specifically oxygen. The reason for suspecting the oxygen and not for instance light is the phenomenon depicted in Figure 3.18. Here the distillates are left over night in the distillation column under a little vacuum, and it is clear how only the top part that is in contact with the gas phase (air) has changed colour. As a consequence after realising the problem, the samples are flushed with nitrogen upon storage and every time the flasks are opened for analysis. When flushing with nitrogen, the rate of colour change during storage is reduced significantly.

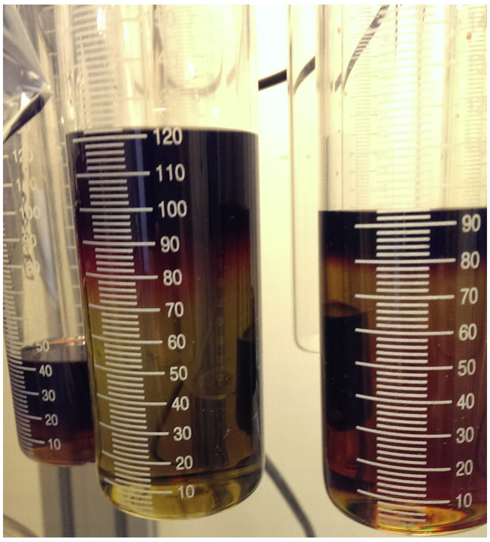

Figure 3.18. Partly degradation of distillates left over night under vacuum with contact to air.

This is a very important observation that indicates the presence of reactive components in the bio-crude. What specific functional groups that might cause the problem is unknown at this stage, but *Zheng and Wei (2011)* tests stability by measuring the increase in viscosity over time under heated conditions. *Zheng and Wei (2011)* performs vacuum distillation (15 torr) of rice husk pyrolysis oil and obtains a single fraction with a yield of 61 wt.% at an AET of 193°C. The stability test is made for both the feed and the distilled fraction. It is concluded that the distillate viscosity hardly increases, whereas the pyrolysis oil degrades significantly. The reason for the distillate being more stable is concluded to be due to the lower oxygen content. Thus, it might be the presence of oxygenates that causes the stability issues of the HTL bio-crude. The observation underlines the importance in investigating intermediate upgrading, since e.g. hydrotreating most likely will stabilise these reactive components by either saturation or functional group removal using hydrogen.

3.5 Partial Conclusion

A fractional distillation set-up has been successfully installed and modified to follow the ASTM D2892 guidelines. Smooth distillations have been carried out, repeatability and a mass recovery of 99.1 % is obtained. A major result of this chapter and the present study in general is the distillation profile of the CBS44 HTL bio-crude. The equivalent gasoline fraction of CBS44 is relatively small at 6 wt.%, whereas the jet-fuel and diesel fractions are relatively large at 25 and 22 wt.% respectively. Less than 30 wt.% residue is also satisfactory and within the range found for various petroleum crudes. As a result, it is considered appropriate to drop-in the HTL bio-crude prior to the ADU, due to the similar distillation profile of HTL bio-crude and petroleum crude oil.

Estimated densities are within or just above fuel specifications for the corresponding boiling range. Only the residue fraction has an estimated density that is significantly higher than the petroleum crude equivalent. CBS44 has a HHV of 41.19 kJ/g, which is significantly higher than those found in literature for pyrolysis and vegetable oils. The CBS44 distillates have HHV in the range 42.2-44.1 kJ/g while it is

38.7 kJ/g for the residue fraction. This is quite high compared to that of bio-ethanol and bio-diesel, but slightly lower than the HHV of petroleum products.

Based on FT-IR and H/C molar ratio, CBS44 is concluded to be generally parafinnic in nature, but with substituted aromatics mostly located in fraction 7 and higher. Since CBS44 contains a large jet-fuel and diesel fraction, a parafinnic nature is good, because it relates to a high cetane number and relatively good cold flow properties. The IR spectra indicates that oxygenates appear as alcohols, esters, ethers, carbonyl groups in both parafinnic and cyclic structures as well as a minor content of carboxylic acids located in the residue fraction.

Compared to petroleum crude oil, the CBS44 is average on nitrogen content with 0.42 wt.% and very low on sulphur with 0.02 wt.%. The nitrogen and sulphur distributions in CBS44 are however completely different from the characteristic distributions of these elements in petroleum crude oil. Sulphur is mainly present in the distillates boiling below 275°C, whereas nitrogen is distributed rather evenly as a function of TBP. In relation to co-processing nitrogen is a catalyst poison, and thus an even distribution is an advantage with respect to residue refining, since the major part of nitrogen appear in the residue fraction of petroleum crude. But in relation to e.g. gasoline reforming, an even nitrogen distribution is an issue, since gasoline fractions of petroleum crude are free of nitrogen.

Elemental analysis and FT-IR show that the oxygen content is distributed relatively even throughout the boiling fractions. Though, with 12.9 wt.% and 6.9 wt.%, fraction 1 and the residue are above average with respect to oxygen content. Oxygen in every fraction is problematic in relation to co-processing, since LSR fractions of petroleum crude oil require little refining due to the relatively low content of heteroatoms. Due to this characteristic, conventional refineries are not suited for major deoxygenation of low boiling fractions. These statements support the incentive to investigate intermediate upgrading or more specifically deoxygenation. This might also relieve the stability issues observed, when the bio-fractions are stored in air.

Upgrading of HTL Bio-Crude 4

Refining is required in order to utilise HTL bio-crude as a liquid drop-in biofuel. Refining is a broad term for the processes needed on the path towards producing on specification fuel products. The major refining processes are fractional distillation, heteroatom removal, thermal and catalytic cracking and reforming processes. It was concluded in the previous chapter that pre-refining/upgrading of HTL bio-crude is needed no matter what the drop-in location is chosen to be. However, the required deoxygenation of HTL bio-crude in order to co-process with petroleum crude, is little compared to the complete refining required for producing pure biofuels that matches fuel specifications.

The aim of this chapter is to study upgrading or more specifically deoxygenation of HTL bio-crude from the perspective of conventional petroleum refining. It is logic to use the methodology of conventional refining, since co-processing is the major subject of this report. Relevant conversion chemistry for heteroatom removal and fuel quality improvement will be briefly described. In this relation, it must be kept in mind that the scope of this report includes bio-crude evaluation and process possibilities rather than detailed chemistry evaluations, such as formulation of reaction routes, estimation of kinetics and evaluation of catalyst performance and deactivation. Instead, a literature study presented in this chapter is used to choose appropriate process conditions for the deoxygenation of HTL bio-crude.

4.1 Chemistry of Heteroatom Removal

Heteroatoms such as sulphur, nitrogen, oxygen and metals present in any crude oil must be removed to a certain extent in order to match for instance sulphur specifications of the fuel products (see Section 1.4 for fuel specifications). Furthermore, especially nitrogen is undesirable, since it is likely to deactivate certain catalysts throughout the refinery units. Likewise, presence of metals introduce the risk of plugging for instance the bed reactors used in a refinery. Small concentrations in the range ppm will eventually accumulate to large quantities with the processing of large volume flows. Certain oxygenates are undesirable due to e.g. stability concerns and corrosivity. As a result, heteroatom removal is crucial and widely used in any crude oil refinery. (Gary et al., 2007), (de Klerk, 2011)

Heteroatoms are generally removed by hydrotreating. Hydrotreating is a metal catalysed process that basically rips off the heteroatoms and saturates the free spot with hydrogen. Hydrotreating may be used as either a pretreatment step or a product polishing step in a fuel refinery. The products from the pretreatment step requires further refining to match fuel specifications, whereas the polishing step is used to produce for instance final diesel fuel that matches the sulphur regulation. Furthermore, hydrotreating has the advantage that the bulk density is reduced by addition of hydrogen, which is good since liquid fuel products generally are sold on a volume basis. (Gary et al., 2007) (de Klerk, 2011)

As previously mentioned the heteroatom content is generally higher in the residue products of petroleum crude oil. Thus, common residue upgrading processes, mainly designed for cracking purposes, are also designed to remove heteroatoms. Hydrotreating is as mentioned a metal catalysed process. But when heteroatom removal is done in relation with residue upgrading it can also be done with bifunctional catalysis or even through thermal cracking. These different conversions will be briefly described in the following, because this is considered beneficial in order to evaluate a suitable upgrading path for the HTL bio-crude.

4.1.1 Catalytic and Thermal Conversion Chemistry

The refining path of crude oil into fuel products consists of a wide range of reactions. Cracking reactions are used to reduce the boiling point of the residue fraction, addition reactions are used to form liquid products from gaseous hydrocarbons. Isomerisation reactions are used to change the structural composition of hydrocarbons to for instance introduce branching and thereby improve octane or cold flow properties. Hydrogenation reactions are used to saturate an olefinic feed with hydrogen or replace heteroatoms with hydrogen. (Gary et al., 2007) (de Klerk, 2011)

The above mentioned reactions will all occur simultaneously to some extend, and thus a conversion equilibrium exists at given operating conditions. To give an example, addition reactions will to a certain degree also occur under cracking conditions. However, it is obviously desirable to enable control of the reactions that occurs in a particular unit. Whether or not equilibrium is reached depends on the reactor residence time and the kinetics of the different reactions. Kinetics depend on temperature and pressure, so this is one way of controlling the output. But also the use of catalysts may favour one reaction path over another. Catalysts does not change the chemical equilibrium, but an appropriate catalyst increases the reaction rate of the desired reaction. This provides control and the distribution of reaction products can be shifted towards desirable. Though it is important to note that the different reactions will occur simultaneously to some extend. (Wade, 2013) (de Klerk, 2013)

Catalytic Conversion Chemistry

A variety of different catalysts are developed for very specific refining purposes. However, a general understanding of the key properties of different types of catalysts is beneficial. The present description is very limited and should only be used as guidance, where important aspects such as catalyst structure, pore size and catalyst activity is neglected, since it is beyond the scope of the present study.

Metallic site catalysis primarily supports hydrogenation/dehydrogenation reactions. Thus an alkene and a hydrogen may be produced by dehydrogenation of an alkane as illustrated with the top part of Figure 4.1. The equilibrium favours dehydrogenation at high temperatures and low pressures indicating an endothermic reaction. (de Klerk, 2013)

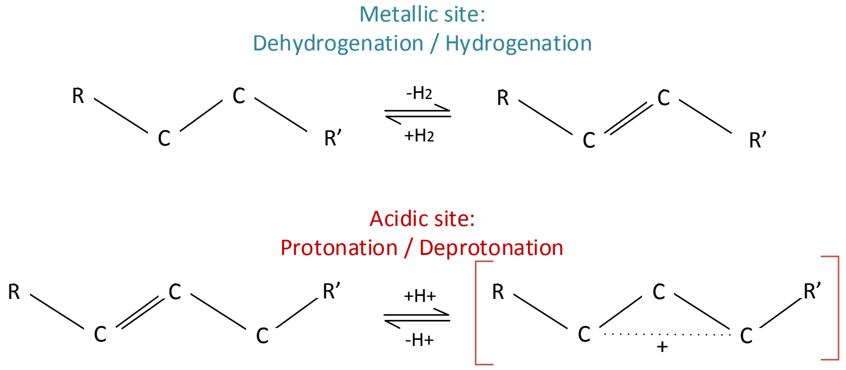

Figure 4.1. Basic principle behind metal supported hydrogenation and acid supported protonation.

Acidic site catalysis enables protonation of an alkene, and in this relation the stability of the carbocation is important. A primary carbocation is rare and less stable than a secondary carbocation, which is again less stable than a tertiary carbocation. Once protonated, the hydrocarbon may isomerise towards a more stable composition. In other words, the charge of a secondary carbocation is likely to move to a tertiary carbocation if possible. This is basically the principle behind isomerisation, and thus an acidic catalyst may be used to introduce isomerisation to improve cold flow properties. (de Klerk, 2013), (Wade, 2013)

Alkenes are reactive molecules that can be easily modified by use of acid catalysis. Alkanes however, are relatively stable molecules and can be protonated only at severe conditions by very strong acids. Though, by using the dehydrogenation ability of metal catalysis to convert the alkanes to alkenes, the conversion chemistries possible with acidic catalysis are enabled. This forms the principle of bifunctional catalysis, where isomerisation or cracking reactions can be introduced to relatively stable alkanes. The princip of bifunctional catalysis is illustrated in Figure 4.2. Basically, the path is dehydrogenation of the alkane, protonation of the alkene, subsequent conversions such as isomerisation or cracking reactions, then deprotonation of the carbocation and finally hydrogenation to produce for instance a stable alkane isomer of the feed. (de Klerk, 2013)

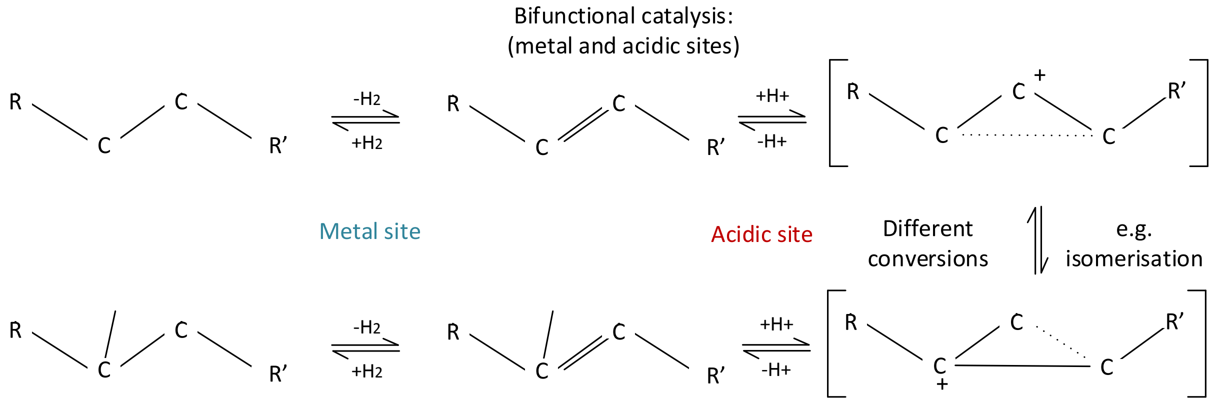

Figure 4.2. Bifunctional catalysis with both metal and acidic sites enable conversion of relatively stable alkanes.

Continuing the simplified description, the ratio between metal and acidic sites on a particular catalyst can be used to predict, whether hydrogenation/dehydrogenation or protonation/deprotonation reactions are favoured. If the catalyst is mainly metallic, the reactions will stay in the left part of Figure 4.2. Whereas, with mainly acidic sites alkene protonation and isomerisation reactions are favoured and nothing will happen to any alkanes due to the stability of these. Thus, an appropriate catalyst composition depends on the feed and desired products. (de Klerk, 2013)

Thermal Conversion Chemistry

Thermal cracking occurs when the temperature is high enough to facilitate homolytic bond cleavage. Recall how BDE is the energy required for thermal cracking. Figure 4.3 simply illustrates the free radical formation/depletion under thermal cracking/addition reactions.

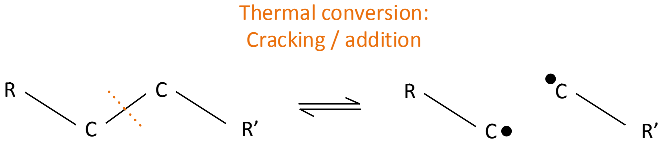

Figure 4.3. Free radical formation/depletion by thermal cracking/addition.

Note that the free radical position is on the terminal carbon when formed under thermal cracking. In combination with a metal hydrogenation catalyst and a hydrogen rich atmosphere, the free radicals can be saturated. This is called hydrocracking, and the products of this process are mainly parafinnic due to the position of the radical. In comparison, the products of catalytic cracking are more branched and aromatic in nature, due to the instability of primary carbocations. If diesel is the main product, parafinnic products are appropriate to ensure a high cetane number, and thus hydrocracking is often used in this relation. Free radical addition reactions are favoured under high pressure and relatively low temperature conditions. Just like thermal cracking, the products from free radical addition reactions are more linear than those of acid supported reactions.

Based on the desired product quality, a particular catalytic or thermal upgrading path may be superior. But also the feed to the process is important. A high nitrogen content in the feed will introduce the risk of acid catalyst poisoning. As a result, a residue fraction containing significant amounts of nitrogen is likely to be cracked thermally, to reduce catalyst poisoning (Gary et al., 2007). The nitrogen content of the CBS44 bio-crude was previously documented to 0.42 wt.%. The use of catalyst with this concentration of nitrogen should not be a problem (de Klerk, 2013). The above given rough description form a nice basis for understanding the effect the chosen upgrading path has on product quality. (Wade, 2013), (de Klerk, 2013)

4.2 Deoxygenation of HTL Bio-crude

Deoxygenation of petroleum crude oil has received little attention, because the oxygen content usually is below 0.5 wt.% (de Klerk, 2013) (Furimsky, 2013). In relation to bio-crudes however, deoxygenation is the major object of heteroatom removal. Deoxygenation of bio-crude is most likely to follow one of three different reaction paths. The three reactions are given in Figure 4.4 and are known as hydrodeoxygenation (HDO), decarbonylation and decarboxylation. A fourth hydrogenation reaction is also given, since this is considered an important intermediate reaction in the deoxygenation of bio-crude. More on this shortly.

Note how the decarboxylation reactant is a carboxylic acid, and how the decarbonylation reactant is an aldehyde. As documented, FT-IR spectra of the CBS44 bio-crude indicates no presence of aldehydes and only minor concentration of carboxylic acids. Instead, carbonyl groups in the form of ketones or esters is observed in major concentrations. By the hydrogenation reaction given in Figure 4.4 intermediates such as alcohols, carboxylic acids or aldehydes may be formed from the carbonyl groups. Consequently carbonyl groups are also expected to follow one of the three deoygenation reactions. For instance, a ketone may be hydrogenated into the corresponding alcohol as indicated in the figure, and then follow the HDO path to produce pure hydrocarbons. (Furimsky, 2013), (Furimsky, 2000)

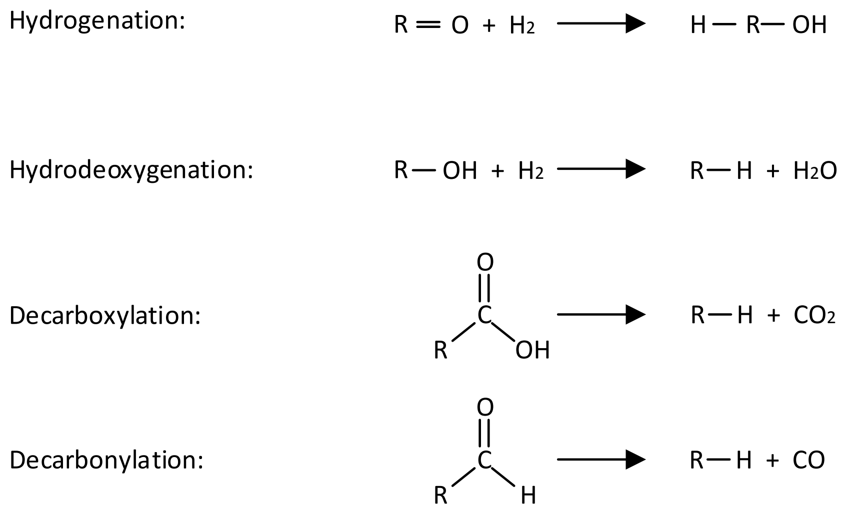

Figure 4.4. Reaction paths that the deoxygenation of bio-crude will follow. (Mohammad et al., 2013) (Furimsky, 2000)

In relation to deoxygenation of the HTL bio-crude, decarbonylation and decarboxylation reactions are desirable since they do not consume hydrogen for deoxygenation. Furthermore, the H/C ratio is increased by these reactions, since both suffer a carbon in the removal of oxygen (Furimsky, 2013). A higher H/C ratio is related to quality improvement and thus this is an advantage. Though, as will be presented later, catalyst deactivation can be avoided by ensuring a relatively high hydrogen pressure during reaction (Furimsky, 2013). And a high partial hydrogen pressure supports the HDO path, relative to the decarbonylation and decarboxylation paths (Furimsky, 2013). Thus, a compromise between the desired reaction path and catalyst performance is to be made.

In Chapter 5 deoxygenation of CBS44 bio-crude will be presented. Here it will be described how water is present in the deoxygenation products, indicating that HDO reactions have taken place during deoxygenation. Unfortunately, gas phase analysis have not been possible during the present study, and thus the formation of CO and CO_2 from decarbonylation and decarboxylation reactions cannot be proven.

4.2.1 Extend of Deoxygenation to Enable Co-processing

Heteroatom removal in petroleum crude oil refining is mainly an issue for the high boiling fractions, since the LSR fractions are rather pure hydrocarbons. In relation to bio-crude co-processing in existing utility, a similar distribution of heteroatoms in the bio-crude is required. However, Subsection 3.4.3 revealed with elemental analysis that oxygenates appear in significant quantities throughout every fraction of the CBS44 bio-crude. FT-IR spectra visualised, how the oxygenates appear in different configurations depending on the boiling range. Different oxygenates have different reactivity, which is highly relevant when choosing the process conditions for deoxygenation of the whole CBS44 crude or a particular boiling fraction. Figure 4.5 orders the HDO reactivity and hydrogen consumption during HDO of different oxygenates.

By comparing the FT-IR summary in Table 3.6 with Figure 4.5, it can be derived that the oxygenates present in CBS44 are mainly medium to high HDO reactivity compounds, such as alcohols, carbonyls and carboxylic acids. This is satisfactory, since the process conditions can be eased and the hydrogen consumption will be in the low end. This makes the deoxygenation step prior to co-processing less costly. Though, based on the FT-IR some phenols, cyclic ketones, esters and ethers are also expected in the higher boiling fractions. Most likely as part of polycyclic structures in the residue fraction, in which the oxygen content is relatively high at 6.93 wt.% compared to the bulk concentration. Deoxygenation of these requires more severe conditions and consumes more hydrogen due to hydrogenation of the aromatics. Meanwhile, it may turn out that mild HDO will convert enough medium to high HDO reactivity oxygenates to facilitate co-processing at a refinery. In fact, it is considered an ideal outcome, if the deoxygenation step prior to co-processing can be designed to convert all the medium to high HDO reactivity oxygenates in the bio-crude. Thereby, only the low HDO reactivity oxygenates that require severe process conditions and consume relatively large amounts of hydrogen are remaining in the bio-crude. These cyclic oxygenates are based on Table 3.6 mostly expected in the high boiling (≥fraction 7) and residue fractions, which is beneficial in relation to refinery co-processing. High boiling and residue fractions of petroleum crude are directed to process units, where severe conditions are used to remove heteroatoms and reduce the boiling point distribution by cracking reactions (Gary et al., 2007). The process conditions used in these particular units, should be sufficient to convert the remaining oxygenates present in the bio-crude into pure hydrocarbons.

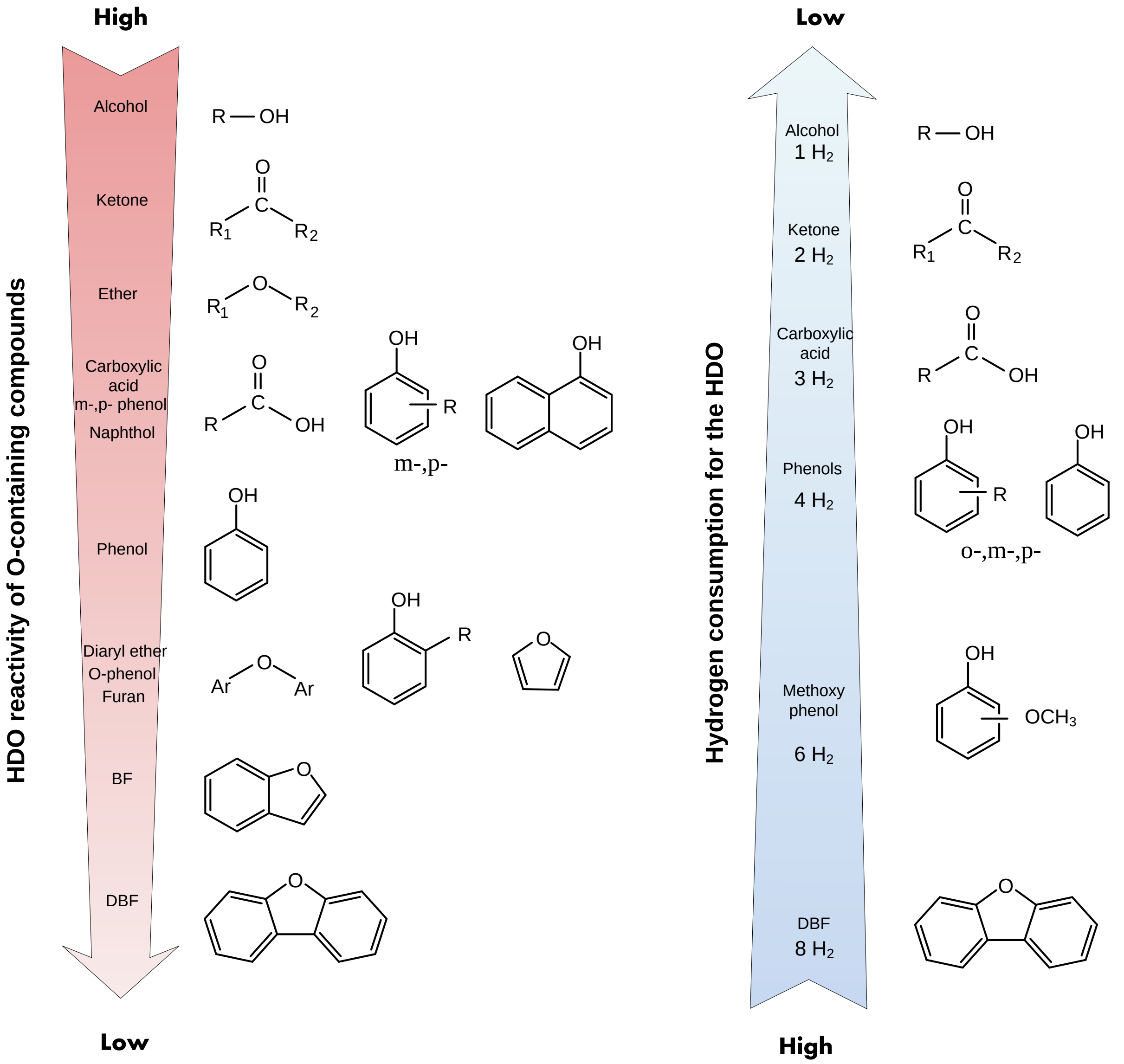

Figure 4.5. HDO reactivity and hydrogen consumption associated with complete deoxygenation of different oxygenates by HDO. (Hoffmann, 2013)

The above given objective is believed to include both the cost perspective and a quality compromise that both the refiner and HTL producer can match. Mild process conditions and a minimum hydrogen consumption minimises the costs associated with the deoxygenation step. Meanwhile, the outcome of such a setup delivers a bio-feed with a quality and nature that enables co-processing at existing utility without the need for major refinery modifications. Based on this discussion and argumentation, deoxygenation of the whole bio-crude rather than specific fractions will be performed.

4.2.2 Literaturestudy on Bio-crude Upgrading

A literature study based on deoxygenation of bio-crudes of different origin is presented in the following. The focus of the literature study is the choice of catalyst. *Furimsky (2013)* presents an extensive state-of-the-art literature study on hydroprocessing of different bio-crudes including vegetable oils, pyrolysis oils and HTL oils from both ligno-cellulosic feedstocks and algae. Different catalysts including conventional hydroprocessing catalysts (CoMo, NiMo etc.) are discussed along with noble catalysts.

Conventional Catalysts

Removal of water from HTL bio-crude is difficult and requires distillation, as found in Section 2.4. Thus, H_2O in small amounts is very likely to be present in the bio-crude subject to deoxygenation. Furthermore, water is a major product of HDO. *Furimsky (2013)* states that water reduces the catalyst performance of conventional hydroprocessing catalysts, with NiMo/Al_2O_3 being more sensible to water than CoMo/Al_2O_3. Furthermore, it is stated that the catalyst support must be considered when water is present in the feed. Carbon supports are hydrophobic, whereas γ-Al_2O_3 supports often are observed to gradually degrade in water. On the other hand, carbon supports do not have the acidic behaviour that enables isomerisation reactions and thus improved cold flow properties of diesel and jet fractions. Recall the feature of acid catalysis in Figure 4.2. (Furimsky, 2013) (Pstrowska et al., 2014) (Ardiyanti et al., 2011)

Nitrogen has an inhibitive effect on conventional catalyst activity (Furimsky, 2013), (de Klerk, 2011) so the low nitrogen content in bio-oil from ligno-cellulosic biomass is advantageous. Though, with the introduction of other high N feedstocks such as e.g. waste slurry in the next generation of HTL bio-crudes, the inhibitive effect nitrogen has on the upgrading catalyst must be kept in mind.

Activity of conventional hydroprocessing catalysts are improved with the presence of H_2S. Generally, the catalysts are first pre-activated by H_2S. Then during processing the catalysts stay active, when processing e.g. petroleum gas oil with relatively high amounts of sulphur, since H_2S is the main product of HDS. Though, HTL bio-crudes from ligno-cellulosic feedstocks are low in sulphur, and thus a H_2S generating agent may be added to the bio-crude during upgrading to achieve a steady catalyst performance. This is used in relation to HDO during Fischer-Tropsch synthesis. *de Klerk (2011)* states that catalyst deactivation occurs during Fischer-Tropsch synthesis, when an unsulphided base metal (e.g. nickel or copper) is used in relation with carboxylic acid containing feeds. The solution is to add a sulphur generating agent. However, addition of a sulphur agent to an otherwise sulphur free feed, will result in contamination of the upgrading products. This is undesirable and a significant issue within conventional hydrotreating of bio-crudes. (Furimsky, 2013) (Ardiyanti et al., 2011) (de Klerk, 2011)

Coke deposition on the catalyst surface is also a well known reason for catalyst deactivation (Gary et al., 2007). The coking tendency of HTL bio-crude is expected to be lower than that of pyrolysis oils due to a higher H/C ratio of the HTL bio-crude. Also, coking deposition may be reduced by increasing the hydrogen pressure during deoxygenation. (Furimsky, 2013)

Catalysts Containing Noble Metals

To avoid the need for pre-sulphiding and addition of a H_2S generating agent to the bio-crude, the use of nonconventional catalysts containing noble metals are gaining attention within bio-crude upgrading (Ardiyanti et al., 2011) (Furimsky, 2013). On the other hand, *de Klerk (2011)* states that in relation to Fischer-Tropsch synthesis, noble metal catalysts are considered too active for HDO and hydrogenation reactions. Heat management becomes a problem in relation to catalysts that are too active.

Furimsky (2013) states that catalysts containing noble metals are considered more stable towards water than the conventional catalysts. However, there is a lack of studies evaluating the effects that both water, H_2S, NH_3 and coke have on noble metal catalysts. Even though the noble metal catalysts may be considered more resistant to water during bio-crude upgrading, deactivation of Pd/C catalyst has been observed during co-processing of petroleum fractions and vegetable oil. The deactivation increased with the amount of vegetable oil in the blend, and the cause of deactivation was stated to be coke deposition and product gases such as CO and CO_2 (Furimsky, 2013). Based on an experimental study *Ardiyanti et al. (2011)* concluded that the deoxygenation activity of noble metals is higher per gram of metal than the conventional CoMo/Al_2O_3.

Catalyst in Present Study

Choudhary and Phillips (2011) are used to summarise the above advantages and disadvantages in te choice of deoxygenation catalyst. They state that the ideal bio-oil upgrading catalysts need high activity for deoxygenation, must be able to withstand large quantities of coke and minimise coke formation. Furthermore, the applied catalyst must have a high tolerance to water for steady performance during HDO. Finally the catalyst must be able to regenerate through a simple process, and the catalyst must be available in large amounts at a reasonable price if the upgrading should be utilised on a wide scale. (Choudhary and Phillips, 2011)

Furimsky (2013) states that $NiMo/Al_2O_3$ are the most widely used catalyst in the hydroprocessing of bio-oils. In present study, a batch of conventional hydrotreating catalyst $NiMo/Al_2O_3$ has been provided by *Shell Danmark A/S (2014)*. The batch was preactivated and sulphided and is used by *Shell Danmark A/S (2014)* for hydrotreating diesel range petroleum products. Typical process conditions are 340°C, 60 bar, LHSV equal to $1.5h^{-1}$ and a H_2:oil molar ratio around 2 (Shell Danmark A/S, 2014). NiMo and Al_2O_3 are both sensible to water, which might affect the deoxygenation. Furthermore, the HTL bio-crude is low on sulphur and thus the activity might decrease. Though, catalyst activity and regeneration is beyond the scope of present work.

In the following some relevant upgrading studies using $NiMo/Al_2O_3$ are presented to select appropriate process conditions for the current deoxygenation experiments.

4.2.3 Selection of Deoxygenation Studies Using $NiMo/Al_2O_3$

Pstrowska et al. (2014) performed hydroprocessing of rapeseed pyrolysis oil using a conventional presulphided $NiMo/Al_2O_3$ catalyst in a continuous flow reactor. At 350°C, 30 bar H_2 pressure and LHSV of 2 h^{-1}, and using raw pyrolysis oil containing 9.5 wt.% water, the oxygen content was reduced from 9.45 wt.% to 2.82 wt.%. A lower operating temperature was observed to decrease the deoxygenation. Catalyst deactivation was observed and stated to be due to the high water content and coke deposition. To overcome this a dehydration step (vacuum distillation to AET 120°C) was done and the residence time was varied. In the second series the feed contained 2.1 wt.% water, and the oxygen content was reduced from 6.43 % to 1.46 %. The HDO conversion was highest using the longer LHSV of 0.5 h^{-1}. In relation to the present study using batch reactors, a LHSV of 0.5 h^{-1} is equivalent to a residence time of 2 hours. Furthermore, the bio-oils in present deoxygenation study have been dehydrated, which by *Pstrowska et al. (2014)* was found to reduce catalyst deactivation.

Xu et al. (2013) presents a successful two-step catalytic deoxygenation study of pyrolysis oil. The pyrolysis oil is first stabilised to overcome coke deposition under 'mild' HDO conditions (300°C, 100 bar) using a noble metal catalyst on carbon support (Ru/C). During mild HDO, the oxygen content was reduced from 48 % to below 10 %. Considering the clearly higher quality of HTL bio-crudes compared to this particular pyrolysis oil, the stabilising HDO step is considered unnecessary for HTL deoxygenation. The second deoxygenation step, referred to as deep HDO by *Xu et al. (2013)*, was done in a continuous flow reactor at 400°C and 130 bar, using a conventional pre-sulphided hydroprocessing catalyst ($NiMo/Al_2O_3$). A H_2:oil molar ratio around 4 to 8 was continuously supplied to the reactor. The deep HDO products had similar characteristics to petroleum crude oil, with reduction of the oxygen content from 9.3 % to below 1 %, HHV around 45 kJ/g and no indication of oxygenates in the FT-IR spectra. These properties are including 10-30 wt.% solvent (e.g. diesel) added during mild HDO, but the deoxygenation is considered satisfactory by *Xu et al. (2013)*.

Krar et al. (2011) converted sunflower oil into paraffins by the use of $NiMo/Al_2O_3$ catalyst and exhibited high deoxygenation activity. The yield of the target product was 48.6 % at 380°C, 40 bar H_2 pressure, LHSV of 1.0 h^{-1} and H_2:sunflower oil molar ratio of approximately 6. A high isoparaffin content of 11.8-17.3 wt.% resulted in good cold flow properties and a high cetane number of 91. Based on these improved properties *Krar et al. (2011)* concludes that sunflower oil can successfully be converted to blending components in the gas-oil boiling range.

Simacek et al. (2009) investigated HDO of rapeseed oil at temperatures from 260 to 340°C at a hydrogen pressure of 70 bar using a NiMo/alumina catalyst. *Simacek et al. (2009)* found that the reaction was incomplete at low temperatures, whereas pure hydrocarbons were formed at temperatures above 310°C.

Srifa et al. (2014) investigated the effect of operating temperature, hydrogen pressure, residence time and H_2:oil ratio using a $NiMoS_2/\gamma\text{-}Al_2O_3$ catalyst in the conversion of palm oil. A product yield of 90.0 % and a n-alkane content of more than 95.5 % was obtained at 300°C, 30-50 bar hydrogen pressure, 1-2 h^{-1} and a H_2:oil molar ratio of approximately 7.5-10.

Wildschut (2009) performed mild hydrotreatment of pyrolysis oil at 250°C and 100 bar and deep hydrotreating at 350°C and 200 bar using a range of different noble and conventional catalysts, including $NiMo/Al_2O_3$. Deoxygenation conversion levels up to 90 % was achieved. The products contained less organic acids, aldehydes, ketones and ethers than the feed, whereas the phenolic and alkane content increased. Furthermore, the heating value was about twice that of the feed. Though, the quality of the pyrolysis oil used as feed by *Wildschut (2009)* was remarkably lower (HHV<20MJ/kg, O>40 wt.%) than the quality of the HTL bio-crudes used in present study.

A literature study by *Mortensen et al. (2011)* shows that HDO at several different operating conditions with different catalysts have been tested. In general the pressure in these studies is in the range of 80-200 bars, the temperature in the range 300-400°C and the residence time for batch reactors is 3-4 hours. The resulting oil yield is between 26 and 84 wt.%.

Summarisation of Deoxygenation Conditions

The above studies are all performing the deoxygenation process with satisfactory results using the conventional hydrotreating catalyst $NiMo/Al_2O_3$. The product qualities are significantly improved and characteristics more or less similar to conventional products are obtained. It should be emphasized that the references are all working on pyrolysis or vegetable oils. These oils generally contain more oxygen than the HTL bio-crude. As a result, a lower amount of hydrogen and less severe operating conditions are expected to be sufficient for the deoxygenation in present study.

Table 4.1 lists ranges for operating conditions based on the above literature study. Also, those provided by *Shell Danmark A/S (2014)* for the particular catalyst used in present study are listed. Finally, the operating conditions that are used in the present deoxygenation experiments are given. Note how the choice of operating conditions are more severe than those used by *Shell Danmark A/S (2014)* for hydrotreatment of petroleum fractions, but milder than those used in relation with pyrolysis and vegetable oils. This choice is made, because the oxygenates present in the HTL bio-crude are expected to have a higher HDO reactivity compared to those present in pyrolysis oils.

Summarisation of Deoxygenation Conditions using $NiMo/Al_2O_3$

	Temperature [°C]	Pressure [bar]	H_2:oil ratio	Reaction time [h]
Literature study	250-400	80-200	4-8:1	2-4
Shell Danmark A/S (2014)	340	60	1:1	0.7
Present study	295-365	100	2:1	2

Table 4.1. Summarisation of deoxygenation conditions used in the literature presented in Subsection 4.2.3. The operating conditions used by *Shell Danmark A/S (2014)* and in present study are also given.

This above selection of deoxygenation literature shows that the process is complex and many parameters may be varied in order to affect the deoxygenation results. Based on the literature study and the operating conditions provided by *Shell Danmark A/S (2014)*, an operating temperature in the range 295-365°C is chosen. Meanwhile, the amount of catalyst, the residence time, molar ratio and operating pressure are kept rather constant. However, as will be presented in Chapter 5 it is found that the catalyst treatment is crucial in the deoxygenation process in order to obtain repeatability and reliable results.

Deoxygenation Setup and Results 5

The first experimental deoxygenation facility in the laboratory at Aalborg University has been designed and installed as part of the present study. Likewise, catalyst, a hydrogen station and to some extend instruments for product analysis have been purchased and installed to enable deoxygenation experiments and subsequent product analysis. Presentation and evaluation of the deoxygenation set-up is provided in this chapter.

Additionally, this chapter will present how use of the commercial modelling software VMGsim has been initiated. In this relation, how the fractional distillation results from Chapter 3 are included in the simple modelling approach. Modelling is used only as a shortcut to predict operating pressure and molar ratio at a certain operating temperature, when making the deoxygenation recipe prior to the experiments.

Last but not least, an experimental study on deoxygenation of HTL bio-crude using the designed set-up will be presented. Previously, it is concluded that oxygen is present in all distilled fractions of the HTL bio-crude. And as documented, an appropriate path towards co-processing compatible bio-feed includes deoxygenation of the whole bio-crude rather than of specific fractions. In present study fraction 7 from the distillation of CBS44 and the bio-crudes CBS44 and CBS48 are used as feeds in the deoxygenation experiments. The experiments are given the abbreviation CKU throughout this chapter.

5.1 Presentation of Deoxygenation Set-up

Deoxygenation experiments in the present study are performed using 25ml Swagelok microbatch reactors, a fluidised sandbath and a specially designed shaking device to enable mixing of the reactants. Figure 5.1 depicts the designed set-up. The sandbath enables rapid heat-up and cool down, steady temperature control and multiple experiments at a time. A Techne SBL-2D sandbath with automatic temperature control is used.

Microbatch Reactors

25ml Swagelok microbatch reactors are relatively inexpensive to build, they can easily be used in a sandbath, and they facilitate deoxygenation of sufficient sample to enable subsequent product analysis. In general, batch reactors are believed to be the feasible choice in relation to parameter studies, where the effect of numerous parameters needs to be examined to understand the process completely. Additionally, micro batch reactors enable the ability of rapidly achieving desired reaction conditions. The microbatch reactors have been designed from Swagelok tubings and fittings to facilitate up to 220 bar at 400°C. Figure 5.1 depicts a microbatch reactor to the right. The reactors consist of a bottom part with the major reaction volume and a top part with a valve, a pressure transducer and a clamp for mounting to the shaker. The valve and pressure transducer do not resist the high temperatures of the sandbath, and thus these are kept above the sandbath. The reactors are designed to maximise the volume that is inside the sandbath during reaction. This is because the cold part of the reactor induces an undesired uncertainty that is difficult to predict. The 'cold' reactor volume has been minimised to 2.48ml, which is 10 % of the entire reactor volume.

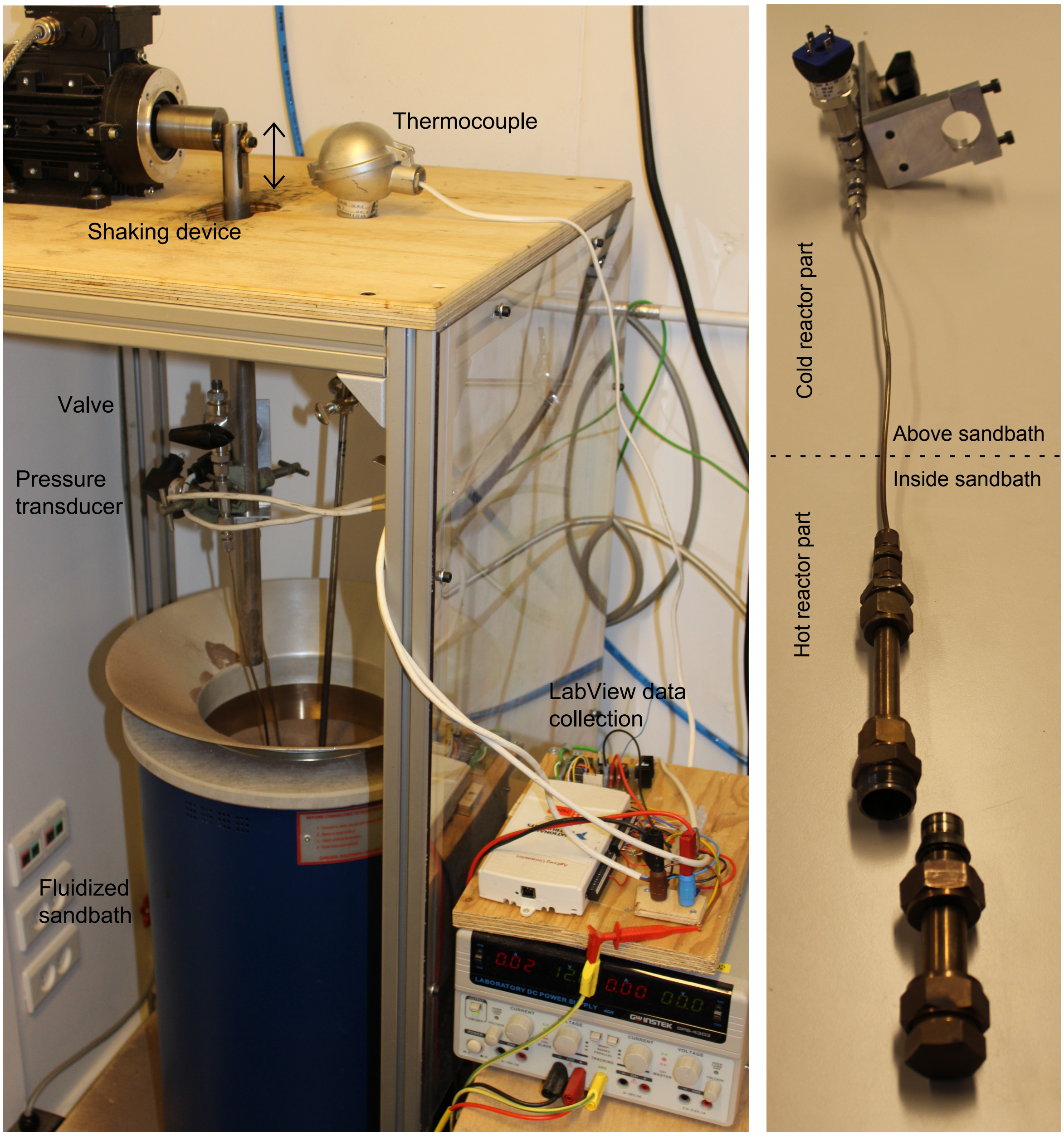

Figure 5.1. Left: Deoxygenation setup consisting of microbatch reactors, a sandbath and a shaking device has been designed during the present study. Right: Close up of microbatch reactor.

Shaking Device

A shaking device is proposed in order to improve conversion and simulate the extensive reactant mixing that will occur in a large scale continuous flow reactor. This shaker is designed as a solid steel rod mounted 10mm from the centre on an engine shaft. By mounting the reactor on the rod, the reactor is moved 20mm vertically at a desired speed of approximately 5Hz. Approximately 0.2 g of 1mm glass spheres are added to the reactants to induce mixing. Delay of the shaker setup and hydrogen supply made a bottleneck in the project, which limited the amount of experimental work that was possible before project deadline. However, once installed the shaker works very satisfactory, and it has a clear effect on reactant mixing, which will be illustrated in Figure 5.3.

Temperature and Pressure Measurements

It is important to know the exact reaction temperature, but it has been observed that the temperature in the sandbath does not match the set-point on the display. Furthermore, it is not possible to measure the temperature inside the batch reactor during reaction due to space limitations and concerns regarding the sealing ability. As a result, the temperature is measured using a PT100 thermocouple located in the sandbath approximately 50mm above the bottom of the microbatch reactor. Furthermore, reaction pressure is measured using a Wika A-10 pressure transducer, mounted in the top of the reactor. It has been observed that pressure follows temperature changes relatively fast, and thus it is considered sufficient to measure the sandbath temperature and avoid additional design of reactors with internal temperature measurement. Finally, it should be mentioned that a LabView program has been programmed and set up to collect, interpret and save the signals of the two measurements.

5.2 Modelling of Deoxygenation Experiments

Prior to the deoxygenation experiments there is a desire of operating at a certain pressure and hydrogen to oil molar ratio at a specific temperature. Modelling of the bio-crude enables prediction of these parameters, when making the deoxygenation recipe. Matching these reaction conditions by guessing a recipe becomes quite difficult without a reasonable model. It becomes even more complex, when taking into account that the microbatch reactors contain both a cold and a hot volume as mentioned above. To short-cut guesses a simple model has been made to help predict the reaction conditions.

5.2.1 Modelling of Bio-crude in VMGsim

Correct modelling of the oil phase as components or pseudo components is the difficult part of modelling oil refining processes (Kaes, 2011). VMGsim is a steady state process modelling software that is designed with the petroleum refining industry in mind (VMG, 2014). The software enables modelling of a crude oil based on the TBP distillation profile. Other parameters such as density, molecular weight distribution and heteroatom content may also be entered to improve modelling accuracy (Kaes, 2011). Based on the given parameters, VMGsim divides the crude oil distillation profile into a number of fractions / pseudo components. Thermodynamic properties are then modelled for the pseudo components by empirical models (Kaes, 2011). Initial use of this tool has been tested and applied in the present modelling, where an 'Advanced Peng Robinson' property method has been used. The 'Advanced Peng Robinson' is based on the Peng Robinson model, but with improved density estimations and better modelling of polar compounds (Kaes, 2011). VMGsim is believed to have promising abilities for accurate modelling of bio-crude, but it is beyond the scope of the present study to look into detailed modelling and model validation. However, the distillation profiles obtained from fractional distillation of CBS44 and CBS48 are applied in the basic VMGsim modelling used in the present study. The basic model shows satisfactory performance with respect to modelling the pressure increase during heat up. This will be described in relation to Table 5.1.

VMGsim is designed to match petroleum crude oils (Kaes, 2011), and a significant difference between petroleum and bio-crude is the oxygen content. Thus, current modelling may underestimate the molecular weight of the bio-crude pseudo components. This will underestimate the hydrogen to oil molar ratios that will be given for the deoxygenation experiments. The model predicts the CBS44 bio-crude to have an average molecular weight of around 250 g/mole. Analysis of the molecular weight distribution is not available for the HTL bio-crude but the oxygen content of the CBS44 is minor at 3.6 wt.%. Based on this the basic VMGsim model, where distillation profiles are applied, is assumed adequate for the current study.

5.2.2 Deoxygenation Modelling

The deoxygenation model is used to derive a recipe that achieves a particular operating pressure at a certain sandbath temperature. It is not used to model e.g. the consumption of hydrogen or production of water during deoxygenation. Figure 5.2 presents a flow diagram used in the deoxygenation modelling in VMGsim. The model is basically based on pressurisation and heating of a mixture of bio-crude and hydrogen. Furthermore, the model includes the fact that the microbatch reactors have a 'cold' volume of 2.48ml located above the sandbath. The temperature, T_{cold}, inside this part has been estimated from an experiment, where nitrogen is heated up gradually, while pressure and temperature increase is measured. This experiment is described in Appendix C, and it is concluded that T_{cold} can be assumed to be 100°C at the temperature range used in this deoxygenation study. Furthermore, it is assumed in the model that the cold volume contains hydrogen only. Relatively high operating pressures reduce vaporisation of the bio-crude and thus gravity forces will keep the liquid bio-crude in the bottom part of the reactors.

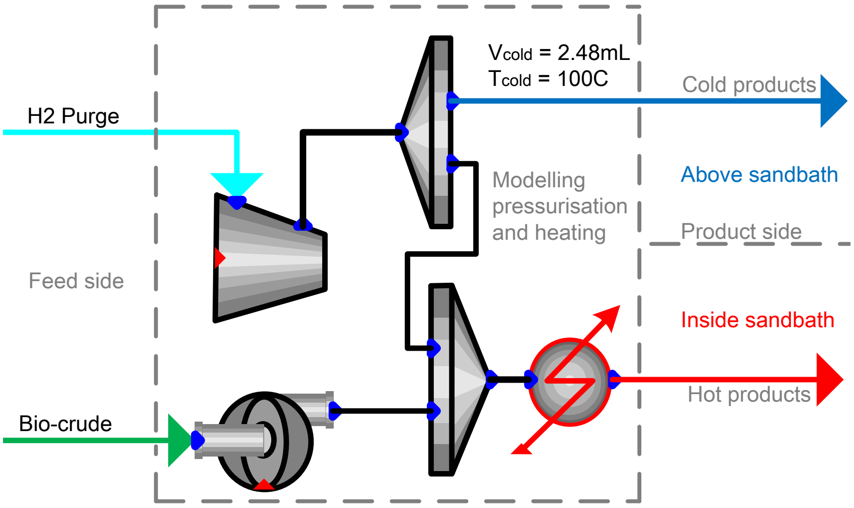

Figure 5.2. Flow diagram of the VMGsim deoxygenation model. Note the distinction between volume inside and above the sandbath during reaction.

Figure 5.2 visualises how hydrogen is compressed to the operating pressure and split into a 'cold' and a mixing stream. The 'cold' stream V_{cold} represents the reactor volume located above the sandbath during reaction. The mixing hydrogen stream is mixed with pressurised bio-crude prior to heating. The predicted model pressure is estimated by ensuring constant reactor volume at the feed and product side. The flow diagram of the deoxygenation model may seem very simple, but it fulfils the demand of the current work nicely. By using this model, it is relatively easy to derive the deoxygenation recipe that ensures a specific pressure and hydrogen to oil molar ratio.

5.3 Evaluation of Deoxygenation Set-up

Once the designed deoxygenation set-up was finished and installed, a deoxygenation experiment of fraction 7 (250-275°C) from the distillation of CBS44 was made to evaluate the potential of the set-up. This experiment is referred to as CKU2, and the reaction conditions are listed in Table 5.1. Figure 5.3 presents a temperature and pressure profile, IR spectra and a picture comparing the feed and products of experiment CKU2. Based on FT-IR spectra fraction 7 is expected to contain esters, ethers and carbonyl groups. The expected outcome of CKU2 is removal of these functional groups to produce a relatively pure hydrocarbon mixture boiling in the diesel range.

The temperature profile of Figure 5.3 is fluctuating with an amplitude of 20°C, due to the automatic control of the sandbath switching on and off. This is not satisfactory, but as experience with the sandbath was gained, the temperature fluctuations were reduced to below 5°C. This will be clear from the temperature profiles presented in the end of this chapter.

During the reaction the pressure profile of CKU2 in Figure 5.3 is generally decreasing due to consumption of hydrogen. It should be emphasized that this decrease is not due to a leakage, since the reactors are leak tested in a water bath after end of reaction. The decrease of operating pressure during reaction constitute a key issue with the current set-up. Deoxygenation is not performed under a constant pressure, but in a range, which is likely to affect the conversion. It is subject for future work to evaluate if it is beneficial to improve the set-up by constantly purging the batch reactor with hydrogen to ensure a constant pressure during reaction.

The hydrogen purge pressure of CKU2 is approximately 28 bar, whereas the final pressure after cool down is 8 bar, indicating hydrogen consumption. The change in hydrogen pressure is indicated as ΔP in Figure 5.3. The picture in the top right corner of the figure shows a significant colour change. Note that the picture does not illustrate the yield from CKU2, it only visualises the change of colour. The FT-IR spectra in Figure 5.3 reveals that the product is significantly improved. The O-H bond above 3000 cm^{-1} and the indication of carbonyl bonds around 1750 cm^{-1} are completely removed. Furthermore, the indication of C-O bonds in the fingerprint region is significantly reduced. Note also the hydrogenation of aromatic bonds indicated with a lower absorbance around 1600 cm^{-1} for the CKU2 product. This hydrogenation is supported by the presence of hydrogen and the metal sites of the $NiMo/Al_2O_3$ catalyst. Since fraction 7 is boiling in the diesel range, it is also worth mentioning that the hydrogenation of aromatic compounds increases the cetane number of the fraction.

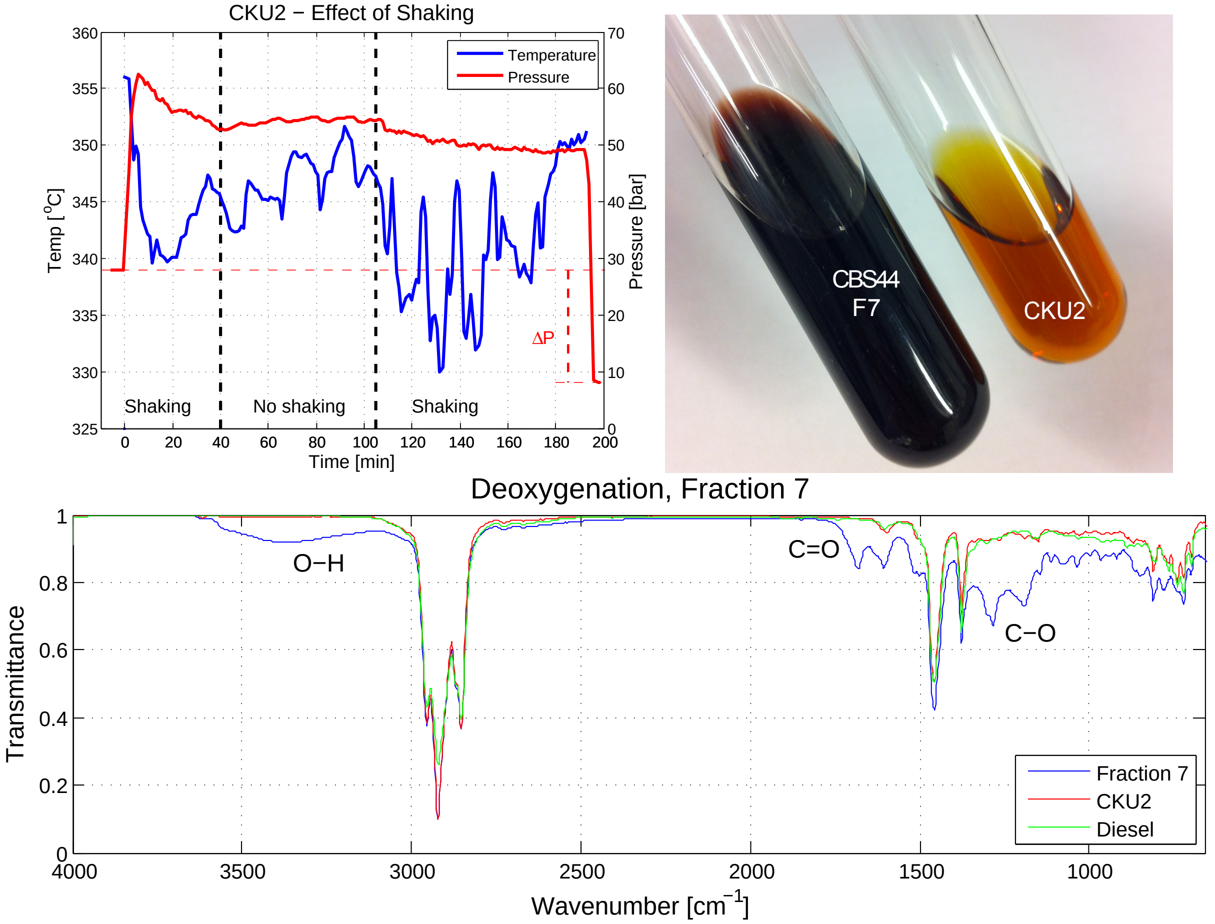

Figure 5.3. Temperature and pressure profile of CKU2 along with picture and FT-IR spectra of feed and CKU2 product to visualise successful deoxygenation.

In fact, it is difficult to show a difference between the IR spectra of the CKU2 product and that of diesel. The HHV is improved from 42.85 kJ/g for fraction 7 to 45.14 kJ/g for the CKU2 product. Recall from Table 3.3 that low sulphur petroleum diesel has a HHV around 45.6 kJ/g. Based on these results the CKU2 deoxygenation experiment is concluded to be successful, since the product is very similar to petroleum diesel.

Effect of Shaking Device

An interesting observation from CKU2 is the affect the shaker has on the deoxygenation activity. Looking at the temperature and pressure profile in Figure 5.3, two vertical dashed lines indicate periods with and without shaking. When the shaker is active it is clear that the pressure decreases, indicating hydrogen consumption. When the shaker is off, the pressure is constant or slightly increasing due to temperature, indicating no hydrogen consumption. These initial results show the importance of the shaking device as a tool to enable good mixing of reactants in the batch reactor and thus increase deoxygenation conversion.

Rapid Batch Reactor Heat-up and Cool Down

Rapid heat-up and cool down of the reactants and reaction products are enabled with the designed set-up. When lowering the reactor into the sandbath, the pressure increases instantly as can be seen at 0 minutes in Figure 5.3. In addition the reactor is rapidly cooled in a waterbath, which can be seen with the immediate pressure drop around 190 minutes. More specifically, maximum pressure is reached within 3 minutes after reactor loading in the sandbath. Likewise, a steady pressure is reached in around 2 minutes after cool down. Thus, the heating / cooling rate is at least 100°C per minute.

The rapid heat-up and cool down is important in order to control the reactions that occur during the experiment. Recall from Subsection 4.1.1 that various reactions occur simultaneously, but some are favoured at e.g. high temperatures and others at lower temperatures. Alkene addition is for instance favoured at lower temperatures (de Klerk, 2011), and by allowing a slow cool down, this type of reaction may occur during cool down. Residence time and reaction kinetics affect the reaction rate and by introducing rapid heat-up and cool down the amount of undesired reactions are minimised. This is successfully achieved with the deoxygenation set-up designed in present study.

5.4 Experimental Deoxygenation Results

This section will present the results of deoxygenation experiments, where the objective is to evaluate mild deoxygenation of HTL bio-crude as a viable route to enable co-processing. However, a lot of experiments, a lot of time and a lot of bio-oil is required to completely understand the effect of the numerous parameters that may be varied in such experiments. Recall from the literature study in Section 4.2 that the choice and amount of catalyst, the residence time, temperature, purge and operating pressure and the H_2 to oil molar ratio all affect deoxygenation. Restricted time and resources (bio-crude) limit the amount of deoxygenation experiments possible in present work. Thus, choices regarding the extent of the present analysis must be made. It is chosen to vary the operating temperature, while keeping the other parameters rather constant. During the experiments, where the operating temperature is varied, repeatability issues are observed. This prevents conclusions on the effect of temperature from being made. However, it provides knowledge about another important aspect, which is catalyst handling and repeatability.

The experimental procedure of deoxygenation is described in Appendix D. Temperature and pressure profiles, feed and product pictures and FT-IR spectra of all experiments are given in Appendix E. Operating conditions and deoxygenation reactants are summarised in Table 5.1 for every experiment along with HHV of the products. The amount of catalyst is given as a percentage of the amount of feed. Note that the catalyst pellets are crushed (appart from CKU11), before being added in the reactor in order to increase the catalyst surface area. P_{purge} is the hydrogen purge pressure, P_{max} and P_{final} are the maximum operating pressure just after heat-up and the pressure after cooling respectively. These can be read off from the pressure profiles given in Appendix E. P_{model} is the VMGsim modelled operating pressure, which should be compared to P_{max}.

Deoxygenation Experiments

		CKU2	CKU5	CKU6	CKU7	CKU8	CKU10		CKU11	
	Unit						R1	R2	R1	R2
Reactant		Frac.7	CBS44	CBS44	CBS44	CBS44	CBS48		CBS48	
Bio-crude	g	3.90	4.90	5.02	5.04	4.82	4.93	5.04	4.94	4.98
Catalyst	$\%$	20.0	21.9	19.8	19.9	20.0	21.9	20.8	19.3	19.3
Glass beads	g	0.15	0.24	0.20	0.17	0.18	0.17	0.17	0.19	0.17
Time	min	193	119	123	121	189	121		120	
Temp	$^\circ C$	345	365	330	295	330	330		330	
Molar ratio^A		1.7	2.0	1.9	1.9	2.0	2.0	2.0	2.0	2.0
P$_{purge}$	bar	27.7	49.5	48.6	49.5	47.9	48.9	49.7	49.0	49.2
P$_{max}$	bar	63	120	99	97	109	110	103	95	96
P$_{model}$	bar	56	101	94	90	93	95	96	94	94
P$_{final}$	bar	8.1	30.4	19.0	33.4	36.4	25.6	33.0	18.2	19.6
HHV	kJ/g	45.14^B	42.50^C	43.81^C	42.40^C	42.76^C	43.94^D	43.34^D	44.41^D	44.34^D

^{A} VMGsim model ^{B} Frac.7: 42.85 [kJ/g] ^{C} CBS44: 41.19 [kJ/g] ^{D} CBS48: 42.11 [kJ/g]

Table 5.1. Table with the operating parameters used in the deoxygenation experiments and HHV of reaction products. CKU10 and CKU11 included use of two reactors (R1 and R2) simultaneously.

The VMGsim model is used to define a receipe for each experiment that will achieve a certain operating pressure and a certain hydrogen to oil molar ratio. The model underestimates the operating pressure as can be seen in Table 5.1. However, the deviation from the actual pressure P$_{max}$ is between 1 and 16 %, which is satisfactory considering the simplicity of the VMGsim model. In fact, detailed evaluation of the VMGsim modelling software in relation to HTL bio-crude is considered very interesting as future work.

Product Analysis and Observations

Water droplets have been observed in the products of every deoxygenation experiment presented in Table 5.1. Water formation indicates that deoxygenation follows the HDO mechanism. It is expected that carbonyl groups are hydrogenated into an alcohol intermediate by the metal sites of the NiMo/Al_2O_3 catalyst. Then the alcohol can be converted to the corresponding hydrocarbon under HDO by formation of water.

Analysis of the gaseous deoxygenation products has not been possible during the present study. The composition after reaction will indicate to what extent decarbonylation and decarboxylation reactions have taken place. This will be indicated by the presence of CO and CO_2. Additionally, such analysis will show how much of the hydrogen is actually consumed. Though, such information cannot be provided for the present study, but it forms a subject for future work.

Stability and miscibility issues have been observed during fractional distillation of the HTL bio-crude as documented in Subsection 3.4.6. It is expected that the deoxygenation will improve the bio-crude stability by removing or saturating reactive compounds. Accurate stability analysis is subject for future work, but colour change of the upgraded products have not been observed.

The deoxygenated products are compared to the feeds with respect to HHV and FT-IR spectra. An IR spectra is not able to determine the amount of oxygen in a sample, but the spectra indicates the presence of oxygen bonds and reductions or removal of these. By analysing the difference in IR absorbance, it can be estimated to what extent the oxygenates are converted. HHV is used to compare the different deoxygenation experiments and quantify how similar the upgraded bio-crude is to petroleum crude oil. An elemental analysis has been made of feed and products of the final CKU11 deoxygenation experiment.

5.4.1 Temperature Analysis Indicates Repeatability Issues

FT-IR spectra of CKU5, CKU6 and CKU7 performed at operating temperatures of 365, 330 and 295°C respectively are given in Figure 5.4. From Table 5.1 it is clear that apart from temperature the operating parameters are rather constant for the three experiments. The IR spectra shows changes compared to the feed in all three experiments. However, the highest deoxygenation conversion is seen for CKU6 at 330°C. Here the O-H bonds above 3000 cm^{-1}, the carbonyl bond indication around 1750 cm^{-1} and the C-O indication in the fingerprint region is reduced the most compared to the feed. In addition Table 5.1 shows a higher pressure drop between P$_{purge}$ and P$_{final}$ for CKU6 compared to CKU5 and CKU7, which indicates a higher hydrogen consumption. Finally the HHV is increased from 41.19 kJ/g in the feed to 42.50, 43.81 and 42.40 kJ/g for CKU5, CKU6 and CKU7 respectively.

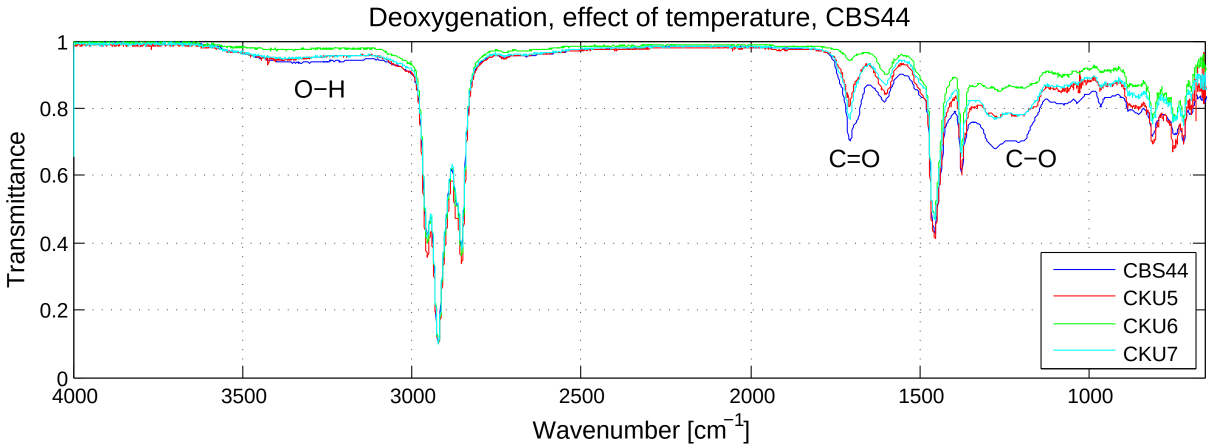

Figure 5.4. FT-IR spectra of CKU5, CKU6 and CKU7 (365, 330 and 295°C respectively) compared to that of the feed. These results indicate that CKU6 with an operating temperature of 330°C results in the highest deoxygenation conversion.

Based on the results of CKU5, CKU6 and CKU7 an operating temperature of 330°C is chosen in the subsequent experiments.

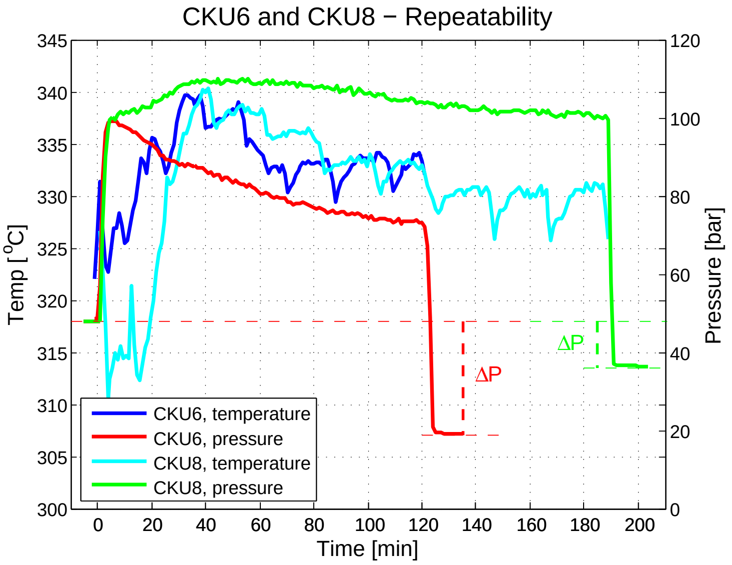

Figure 5.5. Temperature and pressure profile for CKU6 and CKU8. The only difference between CKU6 and CKU8 is the residence time. Repeatability issues are observed due to different pressure profiles.

In Figure 5.5 the residence time is prolonged to 3 hours. The only difference between CKU6 and CKU8 is the residence time and thus the pressure profile is expected to be similar. However, as can be seen in Figure 5.5 the pressure profiles are obviously different. In CKU6 the pressure decreased with time, whereas it increases for CKU8 and then decreases with a different rate. This despite a very similar temperature profile and otherwise matching conditions.

As a result, the comparison between CKU6 and CKU8 in Figure 5.5 shows that repeatability is not possible with the applied deoxygenation procedure. The reason for this is unknown, but it needs to be addressed in order to make reliable results with the designed deoxygenation set-up.

5.4.2 Addressing the Repeatability Issue

After realising that repeatability is an issue, the deoxygenation set-up is extended to handle two reactors at the same time. This way two experiments with identical temperature profiles can be made. After CKU8 no more CBS44 feed is available. Consequently CBS48 is used throughout the repeatability experiments CKU10 and CKU11.

In CKU10 the same deoxygenation procedure as in the earlier experiments has been conducted. The procedure is given in Appendix D. This means that the catalyst pellets are crushed. Figure 5.6 illustrates temperature and pressure profiles of the CKU10 experiment. Again repeatability is not observed, since the pressure develops differently in the two experiments. For reactor 1 (R1) it seems that the catalyst is not active until 40 min after being lowered into the sandbath, whereas reactor 2 (R2) shows immediate deoxygenation. Furthermore, the HHV in Table 5.1 and the IR spectra given in Appendix E show better results for R1 compared to R2, which supports the indication that more hydrogen is consumed in R1. But unfortunately it also supports the conclusion about no repeatability.

After approximately 60 minutes the shaker is briefly turned off (illustrated with the black dashed line) in order to switch the position of the two reactors in the sandbath to investigate if location affects the deoxygenation. However, no change in pressure profile is seen and thus repeatability issues related to the sandbath are disproved.

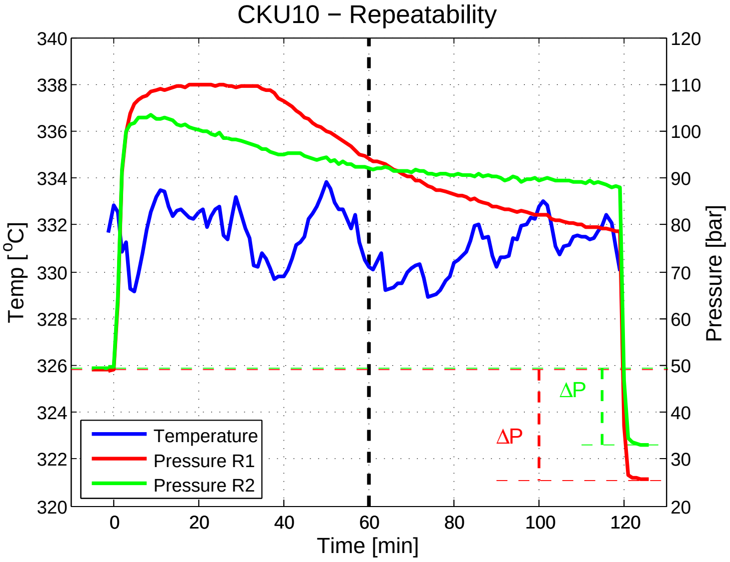

Figure 5.6. Temperature and pressure profile of CKU10 with crushed catalysts. Repeatability cannot be seen.

Based on the experience gained in CKU10 a final experiment CKU11 is conducted, where the catalyst is added without crushing the pellets. Figure 5.7 shows similar pressure profiles for the two reactors. Furthermore, the HHV and the IR spectra are very similar. The pressure profile shows that hydrogen is still consumed in the reactor after 2 hours indicating deoxygenation. Though, the rate of consumption is decreasing, which may be related to catalyst deactivation, the constantly falling operating pressure or reactants and products approaching equilibrium. Looking more closely at the pressure profile, R1 shows a slightly higher pressure drop compared to R2, which indicates a higher hydrogen consumption. The reason for this deviation is unknown. However, the observation is accompanied by the IR spectra showing a slightly higher removal of carbonyl bonds and C-O bonds for R1 compared to R2. Finally the HHV of R1 is slightly higher than R2. Despite the minor deviations the results of CKU11 show repeatability, which is very satisfactory. It is found that the catalyst must be kept in pellet form and not crushed in the deoxygenation experiments in order to obtain repeatable results.

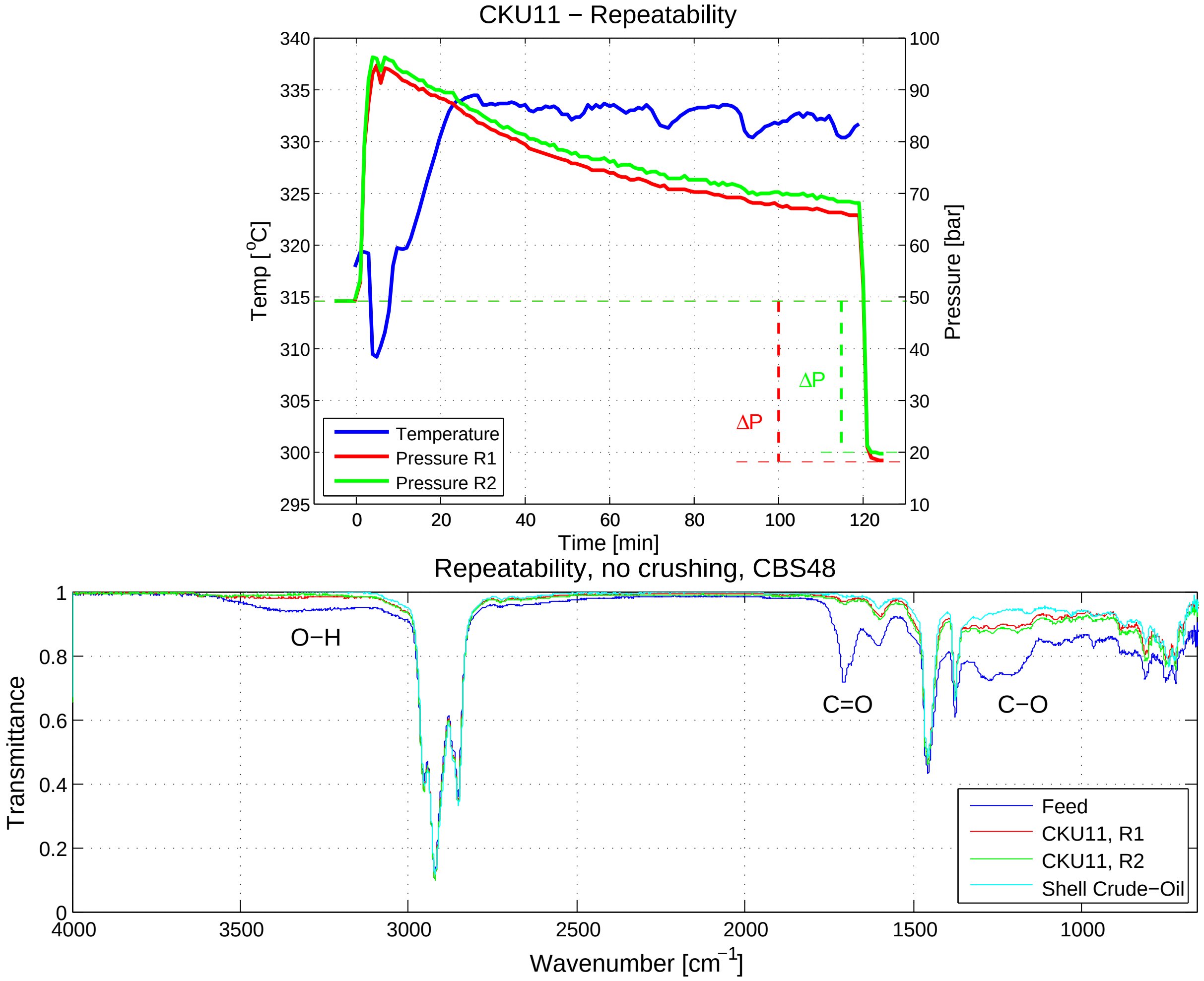

Figure 5.7. Temperature and pressure profile of CKU11 along with FT-IR spectra. Catalyst is uncrushed and repeatability is seen. Furthermore, it is seen that the deoxygenated products are similar to crude-oil with respect to IR spectra.

5.4.3 Evaluating the Deoxygenation of HTL Bio-crude

CKU11 is considered a reliable deoxygenation experiment, since repeatability is obtained. The HHV is increased from 42.11 kJ/g in the CBS48 bio-crude to 44.41 and 44.34 kJ/g in the products of R1 and R2 respectively. This is listed in Table 5.1. For comparison petroleum crude oil has a HHV of around 45.5 kJ/g (Boundy et al., 2011). A slightly lower HHV of the upgraded bio-crude indicates the presence of remaining oxygenates.

In Figure 5.7 the FT-IR spectra of the CKU11 products are compared to that of crude-oil provided by *Shell Danmark A/S (2014)*. It is seen that the indication of carbonyl bonds at 1750 cm^{-1} is almost completely removed in the deoxygenation, which matches the crude-oil spectra. In general the IR spectra shows good similarities to that of the Shell crude oil, though it seems that some oxygenates are still present in the bio-crude. This is also observed from the elemental analysis of CBS48 and CKU11 products given in Table 5.2.

		CBS48, dehydrated	CKU11, R2
C	[wt.%]	83.16	85.49
H	[wt.%]	10.91	11.85
N	[wt.%]	0.31	0.30
S	[wt.%]	0.14	0.04
O^A	[wt.%]	5.48	2.32
H/C ratio		1.56	1.65
O/C ratio		0.05	0.02

^{A} Oxygen by difference

Table 5.2. Elemental analysis of reactants and products of the CKU11 deoxygenation experiment.

Denitrogenation

The elemental analysis in Table 5.2 shows that the nitrogen content is rather unchanged, which is not surprising considering relatively mild reaction conditions. Within petroleum refining, HDN generally requires more severe operating temperatures than HDS (Gary et al., 2007) (Speight, 2011). Conditions ranging between 340-450°C, 100-170 bar and 6-16 H_2:oil ratios are used in residue hydroconversion units in petroleum refining (de Klerk, 2013). During co-processing of heavy vacuum gas oil and canola bio-oil, *Chen et al. (2013)* observed 55 % HDN conversion at 360°C, whereas it was 95 % at 395°C. Though, the HTL bio-crude already has a lower nitrogen content than most petroleum crude oils. Thus HDN of bio-crude is not believed to be a requirement for co-processing.

Desulphurisation

The sulphur content is reduced with 71 % to 0.04 wt.% which is within the fuel specification of jet and marine fuel, and well below the sulphur content of petroleum crude oils. Recall from Figure 1.3 how the average sulphur content in crude oils used in U.S. refineries is above 1.4 wt.%. This gives the bio-crude additional value compared to petroleum crude.

Deoxygenation

The oxygen content during CKU11 is reduced with 58 % to 2.32 wt.%. This is satisfactory considering the relatively mild reaction conditions (330°C, 95bar, 2:1 H_2:oil). Depending on the upper limit that a particular refinery will accept, these deoxygenation conditions might be sufficient to enable co-processing.

Remaining oxygenates are probably low HDO reactivity compounds that is not converted by the mild deoxygenation conditions of CKU11. If this is the case, these remaining oxygenates are not expected to be a problem in relation to co-processing the upgraded bio-crude with petroleum crude oil. This is due to the expected boiling point of such polycyclic structures, which locate them in the residue fraction. In a conventional refinery the residue fraction is exposed to rather severe cracking and hydroprocessing conditions, at which the remaining oxygenates can be converted. This statement is an interesting conclusion of the present study, but it needs to be documented by future work.

5.5 Partial Conclusion

An experimental deoxygenation set-up with a fluidised sandbath, a shaking device and 25ml microbatch reactors with pressure transducers has been designed. Preactivated NiMo/Al_2O_3 catalyst has been purchased and used throughout all upgrading experiments. The deoxygenation set-up enables a rapid heat-up and cool down with rates above 100°C per minute. Likewise, the shaking device is proven to be important for good reactant mixing, since hydrogen consumption is eliminated when the shaker is turned off. The set-up has been evaluated by a deoxygenation experiment of fraction 7 from the distillation of CBS44. The deoxygenation experiment is carried out at 345°C, 63 bar, 3 hours and a H_2:oil molar ratio of 1.7. The pressure profile of the experiment indicates hydrogen consumption and the carbonyl, O-H and C-O absorptions in the FT-IR spectra of fraction 7 are completely removed. In fact the IR spectra of the upgraded products matches that of petroleum diesel. The HHV is increased from 42.85 to 45.14 kJ/g, which is very close to that of diesel (45.6 kJ/g).

A simple model is developed to assist making a deoxygenation recipe that ensures a given operating pressure and H_2:oil molar ratio at a specific temperature. Use of the modelling software VMGsim has been initiated, and the modelling of bio-crude is based on the TBP distillation profile obtained from fractional distillation. The model underestimates the operating pressure, but deviations are within 1-16 %. This is satisfying considering the simplicity of the model. In general VMGsim is believed to be very appealing for future work on bio-crude modelling.

The operating temperature has been varied (365-295°C) in upgrading experiments (CKU5-CKU7) with CBS44 as feed in order to evaluate the impact operating temperature has on deoxygenation activity. However, repeatability issues are observed and thus focus is changed to obtain repeatable results in the deoxygenation. The set-up is extended to handle two reactors with the same temperature profile. Based on CKU10 and CKU11 it is concluded that the repeatability issue arises due to the way the catalyst is treated. When crushing the catalyst consistent data is not obtained. Thus the results of CKU5, CKU6 and CKU7 cannot be used to conclude at which temperature the deoxygenation activity is the highest. However, the study reveals that handling of catalysts highly affect the deoxygenation, which is an important observation. The impact of operating temperature, pressure, residence time and molar ratio is then left for future work.

Reliable results are obtained in CKU11, where deoxygenation of the HTL bio-crude is carried out with two reactors at 330°C, 95 bar and a H_2:oil molar ratio of 2.0 for 2 hours. Repeatability is seen both from FT-IR, HHV and the pressure profiles. Elemental analysis shows that the nitrogen content is rather unaffected by the deoxygenation. Sulphur is reduced by 71 % to 0.04 wt.%, which is within fuel specifications for both jet and marine fuel. Oxygen is reduced by 58 % to 2.32 wt.%, which is satisfactory considering relatively mild reaction conditions.

Remaining oxygenates are expected to be located in high boiling aromatic compounds. If this is the case, the deoxygenation achieved in CKU11 is considered adequate to enable co-processing at a refinery, since heteroatom removal of residue streams can be done through co-processing in existing utility.

Future Work 6

The HTL bio-crudes analysed in present study is produced from a feedstock containing 8-10 wt.% diesel, because the oils were start-up oils part of a larger test campaign. Future work includes fractional distillation of a steady state HTL oil to obtain a distillation curve and HHV, CHNS and FT-IR of the fractions. In this relation, the procedure of present work regarding distillation of bio-crude is suitable.

Sligt immiscibility issues have been observed during fractional distillation of the HTL bio-crude. This may affect distillation efficiency in a similar manner as steam distillation. The effects strong polarity and slight immiscibility have on distillation efficiency should be investigated, as fractional distillation of various bio-crudes is likely to gain more attention.

Instability of the HTL bio-crude was observed during storage of distillates in air. Stability of the HTL bio-crude is believed to increase significantly by deoxygenation. A proper analysis that could quantify this hypothesis is considered valuable future work. Such analysis can also document that there is a need for hydrotreating the HTL bio-crude in order to prevent degradation over time.

A large parameter study on deoxygenation of HTL bio-crude is to be made to achieve optimum reaction conditions and knowledge of how different parameters affect the conversion. Such work includes analysis of different catalysts with respect to structure, activation and performance. Furthermore, temperature, pressure, hydrogen to oil molar ratio and residence time are parameters that affect the deoxygenation conversion and thus the impact of these should be investigated. The deoxygenation set-up designed in present study is considered suitable for such parameter study.

Prior to an extensive deoxygenation study, it may be beneficial to improve the deoxygenation set-up to maintain a constant operating pressure. This can be achieved by constantly supplying hydrogen during reaction. Furthermore, separation of deoxygenation products makes it possible to calculate the deoxygenation yields. The inability of gas product analysis is another drawback of the present deoxygenation procedure. Such analysis provides detailed knowledge on the degree of hydrogen consumption. Furthermore, the amount of CO and CO_2 in the gas products can be compared to the extent of water formation, which provides knowledge on the deoxygenation mechanism. Thus, analysis of the gaseous deoxygenation products is considered valuable future work.

Remaining oxygen in the deoxygenation products of CKU11 is expected to be located mainly in cyclic and polycyclic structures in the residue fraction. Future work includes documentation of this hypothesis in order to verify that removal of these oxygenates is unnecessary to enable co-processing.

Finally future work implies further investigation of the prospects in VMGsim as a modelling tool for bio-crude processing. VMGsim is designed for petroleum hydrocarbon processing, and the software seems appealing considering the similarity of petroleum and bio-crude. The accuracy of modelling bio-crude using a TBP distillation profile, density and heteroatom distribution is believed to be superior compared to the use of e.g. model compounds. Additionally, such modelling approach is straightforward.

Conclusion 7

Evaluation of HTL bio-crude as a potential refinery co-processing feedstock is the major objective of this study. For this purpose, it is necessary to characterise the heteroatom distribution and oxygen is a particular focus. Oxygen appear throughout the bio-crude and mild deoxygenation is proposed as a viable route to enable co-processing without the need for major refinery modifications.

Fractional distillation using a 15 theoretical plate column has been performed on HTL bio-crude to an AET of 376°C. The distillation equipment has been modified to follow the ASTM D2892 guidelines for fractional distillation of petroleum crude oils. Dehydration of bio-crudes is important to avoid steam distillation, bumping and thermal cracking during distillation. It is found that the fractional distillation equipment can effectively be used to dehydrate the bio-crude by distillation at 100 torr to an AET of 150°C.

A smooth distillation of the CBS44 bio-crude results in a 99.1 wt.% recovery and no signs of cracking are observed. The use of TGA for validation purposes is disproved. Instead repeatability of two distillations of the same bio-crude validates the distillation results. A TBP distillation profile of CBS44 is the main analytical result of the fractional distillation. The profile reveals that the gasoline equivalent of CBS44 is 6 wt.%, which is low compared to the benchmark Brent petroleum crude oil. The jet-fuel and diesel equivalents are rather large at 25 wt.% and 22 wt.% respectively. Though, it must be emphasised that the CBS44 is produced from a feedstock containing 10 wt.% diesel. Finally, the amount of CBS44 residue is below 30 wt.%, which is lower than that in the Brent petroleum crude.

11 distillate fractions and a residue fraction is obtained in the fractional distillation. These are analysed with respect to elemental composition, HHV, estimated density and FT-IR. The densities of fractions 1-11 are estimated to be within or just above fuel specifications for the corresponding boiling range. The HHV of CBS44 is 41.19 kJ/g, which is significantly higher than for pyrolysis and vegetable oils, but lower than petroleum crude. Fraction 1-11 of CBS44 have HHV's in the range 42.2-44.1 kJ/g, while it is 38.7 kJ/g for the residue fraction. FT-IR and H/C molar ratios between 1.93 and 1.67 documents that fractions 1-11 are generally parafinnic in nature, but with some substituted aromatics located mainly in fraction 7 and up. The residue fraction with a H/C ratio of 1.38 contains mostly cyclic and polycyclic compounds.

Elemental analysis and FT-IR reveal that the oxygen distribution is relatively constant (2-4 wt.%) as function of TBP. Though, fraction 1 (12.9 wt.%) and the residue fraction (6.9 wt.%) are above average with respect to oxygen content. IR spectra indicates that oxygenates appear as alcohols, esters, ethers, linear and cyclic carbonyl groups and a minor content of carboxylic acids that are located in the residue fraction. In particular the oxygenates bounded to parafinnic structures in fractions 1-11 are considered medium to high HDO reactivity compounds that may be removed by mild deoxygenation.

The CBS44 bio-crude is very low on sulphur (0.02 wt.%) and average on nitrogen content (0.42 wt.%) compared to petroleum crude oil. The nitrogen and sulphur distributions are however completely different from the characteristic distributions in petroleum crude oil. Sulphur is mainly present in the distillates boiling below 275°C, whereas nitrogen is distributed rather evenly as a function of TBP. This means that the nitrogen content of the CBS44 residue fraction (0.38 wt.%) is low compared to petroleum residues. This is an advantage in relation to co-processing, since the bio-residue can be treated catalytically without the risk of catalyst poisoning. Oppositely, the CBS44 bio-crude contains both nitrogen, sulphur, but mostly oxygen in the LSR fractions. This is a problem in relation to co-processing, since the equivalent petroleum fractions require little refining due to a relatively low content of heteroatoms. Consequently, conventional refineries are not suited for major heteroatom removal in low boiling fractions.

These statements support the incentive to investigate mild deoxygenation, where the objective is to remove medium to high reactivity oxygenates, since these are expected in the LSR fractions. For this purpose an experimental deoxygenation set-up consisting of a sandbath, 25ml microbatch reactors and a shaking device is designed. A conventional preactivated NiMo/Al_2O_3 hydrotreating catalyst is used. The set-up enables rapid heat-up and cool down, good reactant mixing with the shaker and temperature and pressure measurements during reaction. Successful deoxygenation of fraction 7 under mild conditions (345°C, 63 bar, 3h, 1.7:1 H_2:oil molar ratio) resulted in HHV and FT-IR spectra very similar to diesel. This documents that the designed deoxygenation set-up works satisfactory. Water formation during all deoxygenation experiments indicates that HDO is a major conversion mechanism. Future work includes analysis of gaseous products to investigate if the decarbonylation and decarboxylation mechanisms are also occuring. A basic VMGsim model is developed to assist preperation of the deoxygenation experiments, and the software is found appealing in relation to future modelling of bio-crude processing.

Issues related to repeatability of the deoxygenation experiments have been observed during a small study on the effect of operating temperature. Thus focus is changed and crushing of the catalyst is concluded to cause the repeatability issue. The CKU11 experiment with two different reactors containing uncrushed catalyst documents repeatability through matching FT-IR, HHV and pressure profiles. Under mild (330°C, 95 bar, 2h, 2:1 H_2:oil molar ratio) deoxygenation of CBS48, a HHV of 44.3 kJ/g is obtained. The sulphur content is reduced by 71 % to 0.04 wt.%, which is very low compared to petroleum crude and within jet and marine fuel specifications. Carbonyl, O-H and C-O absorptions in the IR spectra are significantly reduced. Elemental analysis specifies that the oxygen content of the CKU11 products is reduced by 58 % to 2.3 wt.%. This reduction may be further improved through an extensive parameter study, which is left for future work.

Supported by IR the remaining oxygenates are expected to be low HDO reactivity oxygenates of mainly cyclic and polycyclic nature. These are very likely located in the high boiling fractions of the bio-crude. In such case, mild deoxygenation may be sufficient to enable co-processing, since the remaining oxygenates will be exposed to severe operating conditions in the residue upgrading units of a conventional refinery.

Co-processing enables a gradual phase-in of HTL bio-crude, where feasibility of co-processing and availability of both bio- and petroleum crude oil can be balanced. In order to enable co-processing it is an issue that the distribution of oxygen, nitrogen and sulphur is concluded to be different from that characteristic of petroleum crude oil. Though, a mild deoxygenation step can be used to remove high HDO reactivity oxygenates in the LSR fractions, and thereby the consequences of a difference in heteroatom distribution can be minimised. As a conclusion, a mild deoxygenation step is considered to be sufficient to enable the synergy of co-processing without the need for major refinery modifications.

Bibliography

ACEA, Alliance, EMA and JAMA (2013), Worldwide fuel charter, september 2013, Technical report, Worldwide Fuel Charter Commitee.

Ardiyanti, A.R., A. Gutierrez, M.L. Honkela, A.O.I. Krause and H.J. Heeres (2011), 'Hydrotreatment of wood-based pyrolysis oil using zirconia-supported mono and bimetallic (pt, pd, rh) catalysts', *Applied Catalysis A: General* **407**, 56–66.

ASTM D2892 (2005), Standard test method for distillation of crude petroleum (15-theoretical plate column), Technical report, ASTM International.

ASTM D5236 (1999), Standard test method for distillation of heavy hydrocarbon mixtures (vacuum potstill method), Technical report, ASTM International.

Aviation, Exxon Mobile (2005), World jet fuel specifications with avgas supplement, Technical report, Exxon Mobil Aviation International Ltd.

Boundy, Bob, Susan W. Diegel, Lynn Wright and Stacy C. Davis (2011), *Biomass Energy Data Book, 4th Edition*, Office of the Biomass Program, U.S. Department of Energy. ISBN:978-3-527-32605-1.

BP (2014), *Assays*. BP Global.

Capunitan, Jewel A. and Sergio C. Capareda (2013), 'Characterization and separation of corn stover bio-oil by fractional distillation', *Fuel* **112**, 60–73.

CBS (2014), *HTL Bio-crudes from CBS unit and related analysis results*. Steeper Energy Aps.

Chen, Jinwen, Hena Farooqi and Craig Fairbridge (2013), 'Experimental study on co-hydroprocessing canola oil and vacuum gas oil blends', *Energy and Fuels* (27), 3306–3315.

Choudhary, T.V. and C.B. Phillips (2011), 'Renewable fuels via catalytic hydrodeoxygenation', *Applied Catalysis A: General* **397**, 1–12.

de Klerk, Arno (2011), *Fischer-Tropsch Refining, First Edition*, Wiley-VCH Verlag GmbH & Co. KGaA. ISBN:978-3-527-32605-1.

de Klerk, Arno (2013), *Content of course in Refining of oil and synthetic liquids*. Department of Chemical Engineering, University of Alberta.

EASAC (2012), The current status of biofuels in the european union, their environmental impacts and future prospects, Technical report, German National Academy of Sciences.

EG FTF (2011), Future transport fuels, Technical report, European Expert Group on Future Transport Fuels.

EIA (2012), Biofuels issues and trends, Technical report, U.S. Department of Energy.

EIA (2013), *When was the last refinery built in the United States?* www.eia.gov, PDF file attached.

EIA (2014*a*), *International Energy Statistics*. www.eia.gov.

EIA (2014*b*), *U.S. Refinery Crude Oil Input Qualities*. www.eia.gov.

Elliott, Douglas C. (1980), 'Process development for biomass liquefaction', *U.S. Department of Energy's Biomass Liquefaction Experimental Facility at Albany, Oregon* , 257–263.

EMSA (2010), The 0.1% sulphur in fuel requirement as from 1 January 2015 in SECAs, Technical report, European Maritime Safety Agency.

Fogassy, Gabriella, Nicolas Thegarid, Guy Toussaint, Andre C. van Veen, Yves Schuurman and Claude Mirodatos (2010), 'Biomass derived feedstock co-processing with vacuum gas oil for second-generation fuel production in fcc units', *Applied Catalysis* **96**, 476–485.

Fuels, Exxon Mobile Marine (2012), Marine fuels specifications, Technical report, Exxon Mobil Marine Fuels.

Furimsky, Edward (2000), 'Catalytic hydrodeoxygenation', *Applied Catalysis A: General* **199**(2), 147–190.

Furimsky, Edward (2013), 'Hydroprocessing challenges in biofuels production', *Catalysis Today* **217**, 13–56.

Gary, James H., Glenn E. Handwerk and Mark J. Kaiser (2007), *Petroleum refining, Technology and economics, 5. Edition*, CRC Press. ISBN:0-8493-7038-8.

Hahn, A.U. and K.L. Mittal (1979), 'Mechanism of demulsification of oil-in-water emulsion in the centrifuge', *Colloid and Polymer* **257**, 959–967.

Hoffmann, Jessica (2013), Biooil production, process optimization and product quality, Technical report, Aalborg University.

Huber, George W., Paul O'Connor and Avelino Corma (2007), 'Processing biomass in conventional oil refineries, production of high quality diesel by hydrotreating vegetable oils in heavy vacuum oil mixtures', *Applied Catalysis* **329**, 120–129.

Kaes, Gerald L. (2011), *VMGsim 7.0 Manual, Chapter: Oil Characterization*, Virtual Materials Group, Inc.

Karimia, Elham, Ivo Freitas Teixeiraa, Ariel Gomezc, Eliane de Resendea, Christopher Gissanea, Jay Leitcha, Veronique Jollet, Isabella Aignere, Franco Berrutie, Cedric Briense, Peter Franshamf, Brent Hoffg, Nick Schrierg, Rochel M. Lagob, Stefan W. Kyciac, Richard Heckh and Marcel Schlaf (2013), 'Synergistic co-processing of an acidic hardwood derived pyrolysis bio-oil with alkaline red mud bauxite mining waste as a sacrificial upgrading catalyst', *Applied Catalysis* .

Krar, Marton, Tamas Kasza, Sandor Kovacs, Denos Kallo and Jeno Hancsok (2011), 'Bio gas oils with improved low temperature properties', *Fuel Processing Technology* **92**, 886–892.

Li, Fan, Li-Ping Chang, Peng Wen and Ke-Chang Xie (2001), 'Simulated distillation of coal tar', *Energy Sources* **23**(2), 189–199.

Maxwell, J. B. and L. S. Bonnell (1957), *Industrial Engineering Chemistry*. Vol. 49, pp. 1187-1196.

Mercader, Ferran de Miguel, Michiel J. Groeneveld, Sascha R. A. Kersten, Christophe Geantet, Guy Toussaint, Nico W. J. Way, Colin J. Schaverienc and Kees J. A. Hogendoorn (2007), 'Hydrodeoxygenation of pyrolysis oil fractions, process understanding and quality assessment through co-processing in refinery units', *Energy and Environmental Science* **4**, 985–997.

Milhench, Claire (2011), 'Analysis: Eu carbon costs may force refiners to relocate, close', *Reuters* . www.reuters.com.

Mohammad, Masita, Thushara Kandaramath, Zahira Yaakob and Yogesh Chandra Sharma (2013), 'Overview on the production of paraffin based-biofuels via catalytic hydrodeoxygenation', *Renewable and Sustainable Energy Reviews* **22**, 121–132.

Montemayor, Rey G. (2008), Distillation and vapor pressure measurement in petroleum products, Technical report, ASTM International.

Mortensen, P.M., J.D. Grunwaldt, P.A. Jensen, K.G. Knudsen and A.D. Jensen (2011), 'A review of catalytic upgrading of bio-oil to engine fuels', *Applied Catalysis A: General* **407**, 1–19.

Nakanishi, Koji (1962), *Infrared absorption spectroscopy, practical.*, Holden-Day, San Francisco.

NREL, National Renewable Energy Laboratory (2009), Biodiesel, handling and use guide - 4th edition, Technical report, U.S. Department of Energy.

Ott, Lisa Starkey, Beverly L. Smith and Thomas J. Bruno (2008), 'Advanced distillation curve measurement: Application to a bio-derived crude oil prepared from swine manure', *Fuel* **87**, 3379–3387.

PerkinElmer (2010), *Thermogravimetric Analysis (TGA) - A Beginner's Guide*. PerkinElmer.

Pstrowska, Katarzyna, Jerzy Walendziewski, Rafal Luzny and Marek Stolarski (2014), 'Hydroprocessing of rapeseed pyrolysis bio-oil over nimo/al2o3 catalyst', *Catalysis Today* **223**, 54–65.

Shell Danmark A/S (2014), *Contact: Technical Manager Kristen Kristensen*. Shell Danmark, Fredericia.

Simacek, Pavel, David Kubicka, Gustav Sebor and Milan Pospisil (2009), 'Hydroprocessed rapeseed oil as a source of hydrocarbon-based biodiesel', *Fuel* **88**, 456–460.

Speight, James G. (2011), *The Refinery of the Future*, Elsevier Inc. ISBN-13:978-0-8155-2041-2.

Srifa, Atthapon, Kajornsak Faungnawakij, Vorranutch Itthibenchapong, Nawin Viriya-empikul, Tawatchai Charinpanitkul and Suttichai Assabumrungrat (2014), 'Production of bio-hydrogenated diesel by catalytic hydrotreating of palm oil over nimos$_2$/γ-al$_2$o$_3$ catalyst', *Bioresource Technology* **158**, 81–90.

Toor, Saqib, Lasse Rosendahl and Andreas Rudolf (2011), 'Hydrothermal liquefaction of biomass : A review of subcritical water technologies', *Energy* **36**(5), 2328–2342.

Toor, Saqib, Lasse Rosendahl, Jessica Hoffmann, Rudi P. Nielsen, Thomas Helmer Pedersen and Erik Gydesen Soegaard (2014), *Hydrothermal liquefaction of biomass: Application of hydrothermal reactions to biomass conversion*, Springer.

Toor, Saqib, Lasse Rosendahl, Mads Pagh Nielsen, Marianne Glasius, Andreas Rudolf and Steen Brummerstedt Iversen (2012), 'Continuous production of bio-oil by catalytic liquefaction from wet distillers grain with solubles (wdgs) from bioethanol production', *Biomass and Bioenergy* **36**, 327–332.

TOTSA (2006), *Crude Assay*. TOTSA Total Oil Trading SA.

VMG (2014), *Overview and Products*. Virtual Materials Group.

Wade, Jr. L.G. (2013), *Organic Chemistry Volume 1, 8th edition, Custom edition for the University of Alberta*, Pearson. ISBN-13:978-1-269-54513-6.

Wan, Dr. Hayley (2013), *Organic Chemistry, University of Alberta Laboratory Manual*, University of Alberta, Department of Chemistry.

Wildschut, Jelle (2009), Pyrolysis Oil Upgrading to Transportation Fuels by Catalytic Hydrotreatment, Technical report, Rijksuniversiteit Groningen. ISBN 978-90-367-4112-5.

Xu, Xingmin, Changsen Zhang, Yonggang Liu, Yunpu Zhai and Ruiqin Zhang (2013), 'Two-step catalytic hydrodeoxygenation of fast pyrolysis oil to hydrocarbon liquid fuels', *Chemosphere* **93**, 652–660.

Zhanabai, Saya (2014), *Properties of Atoms, Radicals and Bonds*. www.academia.edu/5364060/PROPERTIES _ OF _ ATOMS_R ADICALS_ AND_ BONDS.

Zheng, Ji-Lu and Qin Wei (2011), 'Improving the quality of fast pyrolysis bio-oil by reduced pressure distillation', *Biomass and Bioenergy* **35**, 1804–1810.